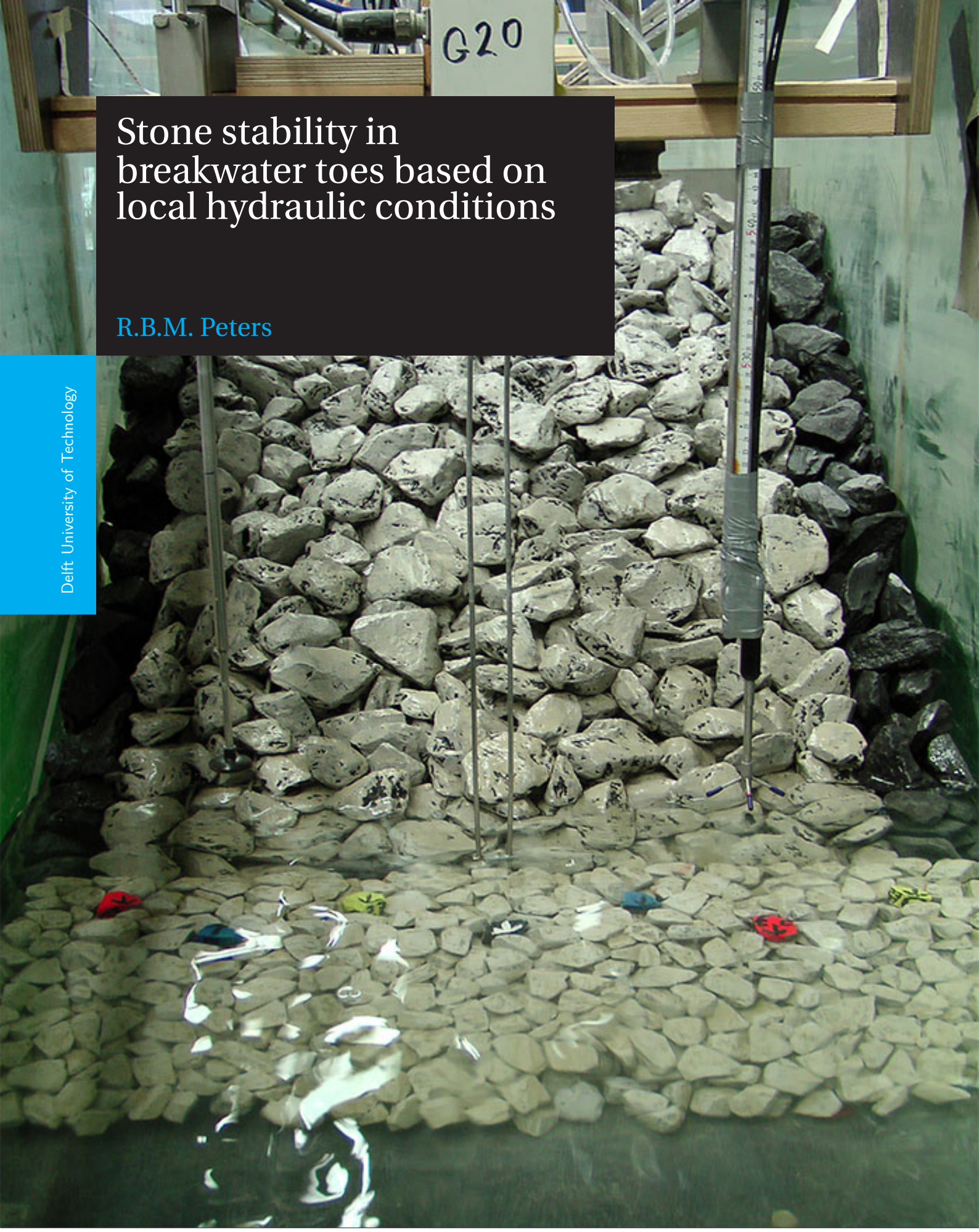

Stone stability in breakwater toes based on local hydraulic conditions

R.B.M. Peters

Delft University of Technology

TU Delft Delft University of Technology

Challenge the future

Master Thesis

Stone stability in breakwater toes based on local hydraulic conditions

Author:
R.B.M. (Ruben) Peters

Graduation committee:
Prof. dr. ir. W.S.J. (Wim) Uijttewaal
Delft University of Technology

Ir. H.J. (Henk Jan) Verhagen
Delft University of Technology

Ir. J.P. (Jeroen) Van den Bos
Delft University of Technology and Royal Boskalis Westminster N.V.

December 10, 2014

Preface

This report presents my study that was performed as the final stage of my study Hydraulic Engineering at Delft University of Technology. A lot of people have supported me during this period, for which I am thankful.

First of all I would like to thank my graduation committee members, Prof. dr. ir. Wim Uijttewaal, ir. Henk Jan Verhagen and ir. Jeroen van den Bos, for providing me with very useful input and enthusing me during the entire process.

I have spent a lot of time in the Fluid Mechanics Laboratory, where I have conducted my experiments. Thanks go to Sander de Vree, Jaap van Duin, Hans Tas and Frank Kalkman who have assisted me with the preparation of my experimental set-up. Constant van Heemst simultaneously performed his study on breakwaters in the wave flume and therefore the scale model was built in collaboration. I have enjoyed designing and building the breakwater together.

Furthermore I would like to thank my house mates, with whom I have shared wonderful times over the last few years. Moreover there was always someone I could consult on their specialities to help me further during my master thesis.

I would also like to thank my two sisters, who both have showed great interest and support in my graduation work. Last and utmost I would like to thank my parents who have enabled me to follow my studies in Delft. I am very grateful for the opportunity you gave me to become an engineer.

Ruben Peters
Delft December 10, 2014

Summary

Rubble mound breakwaters are widely used to shield the area behind it from the waves. To achieve this, the outfacing armour elements of a breakwater need to be large enough to withstand the wave forces. This armour layer cannot be placed directly on the bed, since scour around the armour elements will weaken the structural integrity of the armour layer. Toe structures are constructed to protect the armour layer against the effects of erosion.

Previous studies have resulted in empirical design formulas to determine the required stone size for toe structures. These formulas express the stability of the toe structure as a function of the wave height. Since the waves do not act directly upon the toe structure, these formulas lack some physical background. This thesis aims to find a more physically accurate relation between the toe stone stability and the local hydraulic parameters, like flow velocities and water pressures. If this can be achieved, more accurate design formulas can be developed.

Since this thesis deals with the stability of singular stones, it is focussed on the point of incipient motion of these individual stones. The forces acting upon a stone in a breakwater toe are identified and a stability criterion based on these forces is formed. The lift, drag and shear forces are the destabilising forces, whereas the weight of the stone is a stabilising force. The drag force and the shear force are functions of the flow velocity just above the toe and the lift force can be computed with the vertical pressure difference over the stone. With these forces the moment of force about the rotation point of the stone is computed (figure 1). When this moment of force becomes positive, the stone is expected to move.

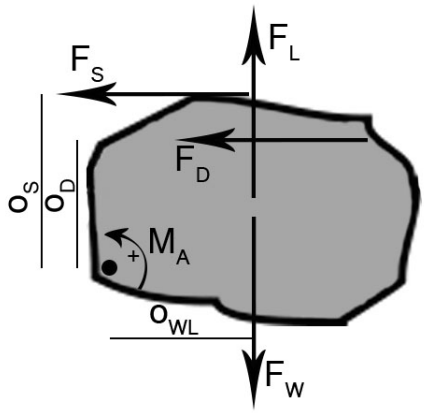

Figure 1: Moment of force on a stone in a breakwater toe

In order to verify this moment criterion, a wave flume experiment is designed. A scale model of a breakwater is constructed in which the stones of the armour layer and toe structure are all glued together. Seven cavities are equally spaced across the toe berm, three on the frontal edge of the toe and four in the middle. In these cavities the seven 'target stones' are placed, which are the only stones that can move during the experiments. Underneath each of the target stones a pressure sensor is placed. Furthermore, two velocity sensors and a wave gauge are located above the toe structure. Using this experimental arrangement, the local hydraulic properties at the toe structure can be measured. During the experiments the point of incipient motion is visually determined, so that the local hydraulic conditions around that point in time can be analysed. The majority of the 76 experiments are videoed, which gives a good impression of the behaviour of the target stones.

The performance of the moment criterion is initially analysed by visually inspecting the computed moments about the point of incipient motion for several experiment runs. The videos of the experiments are used during this analysis to get more insight in the characteristic behaviour of the stones. In the experiments in which movement occurred, the peak values of the computed moments are generally close to or higher than zero. However, at the point of incipient motion, the criterion is not always surpassed. It is found that the moment criterion is not always able to pinpoint the point of incipient motion, but it certainly serves as a good indicator of movement. The pressure difference over the stone are found to have the biggest influence on the moment of force (and therefore the stability) of a stone.

The master thesis of Baart (2008) has also proposed a criterion for movement in breakwater toes based on the local flow velocity. This criterion is evaluated as well and it is concluded that this criterion is too high. Even with the harshest wave conditions the Baart criterion is rarely surpassed, but stone movement did occur.

To analyse the performance of both criteria in a more objective manner, a binary classification test is used. This test uses the binary classifiers True Positive (TP), True Negative (TN), False Positive (FP) and False Negative (FN) to measure the performance of a predictor (in this case the moment and Baart criterion). Using these classifiers the Sensitivity and the Precision can be determined. The Sensitivity for the moment criterion is found to be 32%, meaning that in 32% of the cases a stone actually moved, this was predicted by the moment criterion. The Precision is determined to be 10%, which means that in only 10% of the times the moment criterion is surpassed, a stone had actually moved. The Baart criterion shows a Sensitivity of 1% and a Precision of 7%, thereby verifying that the criterion is too high. The criterion is adapted by changing the coefficient that accounts, amongst others, for the stone position. With this lowered criterion, a Sensitivity of 24% and a Precision of 27% is found.

From both analyses it can be concluded that both the moment criterion and the Baart criterion are not yet suitable for design practice. Which of the two criteria is better, is also inconclusive at this point. The adapted Baart criterion gives overall better results, but a coefficient had to be changed to achieve a better result. The appropriate value for this coefficient is therefore unknown, since a different situation may need a different value for the coefficient.

The moment criterion also needs to be improved. Several important parameters are not included in the current form of the criterion. The stone position and the effects of turbulence are the most important factors that are not accounted for in this study. It is recommended to investigate the effects of these two parameters, as they can improve the applicability of the moment criterion.

In conclusion, this study shows that it is possible to develop a design formula for breakwater toes that is based on local hydraulic parameters. The most important parameter appears to be the pressure difference over a stone.

Contents

List of Symbols

α	Slope of the breakwater (toe) $[rad]$
Δh	Vertical difference in trough level and run-up $[m]$
Δp	Pressure difference over a stone $[N/m^2]$
Δx	Horizontal distance between the middle of the toe and the highest 'wet point' on the breakwater by run-up $[m]$
Δ	Relative density of rock in water $[-]$
$\delta_{laminar}$	Laminar boundary layer thickness $[m]$
$\delta_{turbulent}$	Turbulent boundary layer thickness $[m]$
$\hat{u}_{bc}$	Critical flow velocity amplitude by Baart $[m/s]$
$\hat{u}_b$	Amplitude of the flow velocity at the toe bund $[m/s]$
ν	Kinematic viscosity of a fluid $[m^2 \cdot s^{-1}]$
ρ_s	Density of rock $[kg/m^3]$
ρ_w	Density of water $[kg/m^3]$
ξ	Irribarren number $[-]$
A_f	Frontal area of the stone influenced by drag $[m^2]$
A_L	Area affected by the lift force $[m^2]$
A_S	Area affected by the shear force $[m^2]$
c	Wave celerity $[m/s]$
C_D	Drag coefficient $[-]$
C_f	Shear force coefficient $[-]$
C_{PF}	Coefficient for porous flow $[-]$
C_S	Shear force on a stone $[N]$
D_{n50}	Nominal stone diameter [m]
F_D	Drag force $[N]$
F_L	Lift force on a stone $[N]$
F_{PF}	Porous outflow force $[N]$
g	Gravitational constant $[m/s^2]$
H	Wave height $[m]$
h	Water depth $[m]$
$H_{2\%}$	Wave height exceeded by 2% of the waves $[m]$
H_i	Incoming wave height $[m]$
h_m	Local still water depth at the structure $[m]$
H_s	Significant wave height $[m]$
h_t	Height of the toe $[m]$
h_t	Water depth above the toe (used in Gerding and Van der Meer) $[m]$

i	Hydraulic head gradient of piezometric level [−]
k	Wave number $[1/m]$
K_D	Dustbin factor in Hudson's formula [−]
L	Wave length [m]
L_{TA}	Horizontal distance from middle of the toe to the highest 'wet point' of the breakwater at still water level $[m]$
M_A	Moment of force on stone A about the rotation point $[Nm]$
m_{stone}	Mass of the stone $[kg]$
N	Number of displaced stones [-]
N_{od}	Damage parameter [-]
o_d	Arm for the drag force $[m]$
o_s	Arm for the shear force $[m]$
o_{wl}	Arm for the lift and the weight force $[m]$
p_{above}	Pressure above a stone $[N/m^2]$
p_{under}	Pressure under a stone $[N/m^2]$
R_u	Run-up level $[m]$
Re_x	Particle Reynolds number [−]
s	Wave steepness [−]
T	Wave period $[s]$
u	Flow velocity at 0.15 D_{n50} above the stone $[m/s]$
U_{max}	Maximum flow velocity over the toe by Nammuni-Krohn $[m/s]$
wl_{toe}	Water level at the toe $[m]$

List of Figures

List of Tables

Chapter 1

Introduction and problem description

1.1 The use of breakwaters

Breakwaters are used all over the world to shield the area behind it from waves. They are found at very large ports and small marinas to provide calm water for safe navigation and mooring in the port. They can also be used to protect the land area behind it from erosion.

Breakwaters come in different types although the two most common types are the monolithic breakwater and the rubble mound breakwater. The first type basically is a solid wall that is placed on a foundation on the bed. The rubble mound breakwater is a large heap of loose elements (gravel, rock) which is dumped on the bottom after which the stones are shaped into the form of the breakwater core. The outer layer of the breakwater has to be able to withstand the wave forces and therefore consists of very large rocks or concrete elements. An example of a rubble mound breakwater is shown in figure 1.1.

Figure 1.1: Rubble mound breakwaters at Zeebrugge, Belgium (http://www.kennisbank-waterbouw.nl)

A rubble mound breakwater is permeable, so it does not stop the water completely. Its function is to reduce the wave heights in the area behind the breakwater. A typical built-up of a rubble mound breakwater is shown in figure 1.2. This figure shows the different parts of a breakwater. As stated before, the core usually consists of gravel or smaller rocks but the armour layer (outer side) consists of the large elements that have to withstand the wave forces. A lot of research has been performed to determine how big these elements should be, if a certain wave height is present. The subject of this thesis is found at the bottom of the armour layer: the breakwater toe. The function of the toe is to support the large elements of the armour layer. If the armour elements were placed directly on the bed, the surrounding sand would erode and the elements would sink in these scour holes. The stones of the toe therefore are smaller than the armour elements, also because the hydraulic forces further from the water surface are smaller.

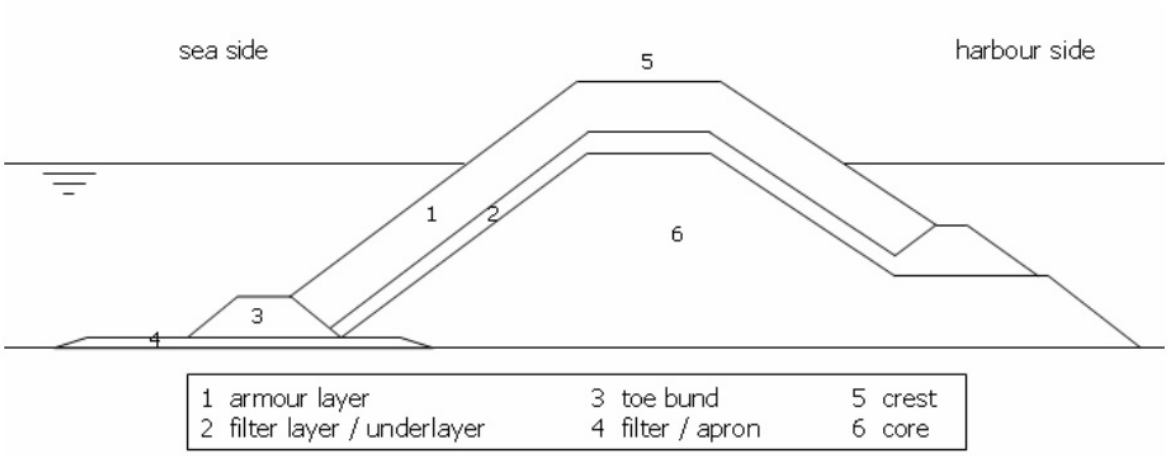

Figure 1.2: Typical cross-section of a rubble mound breakwater (Baart, 2008)

1.2 Research objective

Current design formulas for breakwater toes are based on empirical research, where the wave heights are usually coupled to the required stone size. This does, however, not describe what physically happens near the toe structure, since the waves do not act directly on the toe. The waves do cause the oscillatory flow over the toe structure which attacks the toe stones. This means that in the current design formulas there is a so-called 'black box' between the wave height and the required stone size. This study aims to find the local hydraulic conditions which cause a toe stone to start moving. The research objective is therefore:

To determine the point of incipient motion of stones in breakwater toes based on the local hydraulic conditions

In order to achieve this objective the following sub questions are defined:

- *Which local hydraulic parameters influence the stability of a stone?*
- *Can a relation be found which determines the point of incipient motion based on local hydraulic parameters?*

1.3 Research approach and report structure

First of all the previous research on breakwater toe stability will be reviewed, together with other research topics that are relevant to the present study. Chapter 2 summarises these topics and states the hypothesis for a stability criterion based on local hydraulic conditions. To verify this hypothesis chapter 3 presents the experimental arrangement for a flume experiment. The measurement data is analysed and processed in chapter 4, followed by the analysis of the experiments in chapter 5. Chapter 6 reviews the applicability of the criterion. Finally, chapter 7 summarises the conclusions of this study and gives recommendations for further research into this topic.

Chapter 2

Theory and criterion hypothesis

The aim of this thesis is to determine the point of incipient motion based on the local hydraulic parameters. The current design formulas for breakwater toes are based on external hydraulic parameters like the wave height. This chapter gives an overview of the previous research that is relevant to this thesis, and why these studies are relevant to this thesis. Thereafter an hypothesis for a criterion predicting the point of incipient motion is formed.

2.1 Previous research

2.1.1 Gerding (1993)

Summary of study

Gerding (1993) found that the knowledge on toe structure stability was limited and not based on systematic research. For these reasons he developed a new formula for the toe stability in rubble mound breakwaters which was both practically applicable and reasonably reliable. He performed scale model tests and introduced a damage parameter N_{od} which was defined as the number stones removed from a strip of 1 D_{n50} wide:

$$N_{od} \equiv \frac{N}{L/D_{n50}}, \tag{2.1}$$

where N is the number of displaced stones and L is the width of the strip in which the displaced elements are counted. Previously the damage was indicated in percentages, but according to Gerding this had the disadvantage that if the same number of stones is displaced from different toe structures (a higher or wider toe), the percentage changes but the amount of damage is actually the same. He does however state that the effect of a certain damage on a toe structure with a different shape may be different.

In the evaluation of the test results Gerding defines several damage levels for N_{od}, 0.5, 2 and 4 for hardly any damage, acceptable damage and unacceptable damage respectively. Furthermore he found which parameters have influence on the toe structure stability:

Nominal stone diameter	: D_{n50}
Significant wave height	: H_s
Stone mass density	: ρ_s
Water depth above the toe	: h_t
Damage level	: N_{od}

During these tests Gerding investigated two other parameters which had no significant influence on the stability:

Fictitious wave steepness	: s_{op}
Width of the toe	: b_t

After the tests an analysis was carried out in order to establish a formula describing the relation between the stability and the governing parameters. First of all Gerding proposed a power curve fits best through the measured points of H_s and N_{od}. Further analysis finally led to the newly formed relation:

$$\frac{H_s}{\Delta D_{n50}} = \left(0.24\frac{h_t}{D_{n50}} + 1.6\right) N_{od}^{0.15}. \tag{2.2}$$

This equation can be used if:

$3.0 < h_t/D_{n50} < 25$
and
$0.4 < h_t/h_m \quad < 0.9$

Relevance to this thesis

The formula derived by Gerding is widely used nowadays to determine the required stone sizes for the toe structure. This relation has the significant wave height H_s as its most important parameter. In this thesis a criterion will be derived that is not based on the significant wave height, but on the local hydraulic parameters. The experimental set-up that Gerding used, may serve as an example for the experiments that will be carried out in this study.

2.1.2 Van der Meer (1998)

Summary of study

The work of Gerding (1993) was a big improvement in determining the toe stability. However, Van der Meer (1998) found a problem in equation 2.2 by Gerding. As D_{n50} appears in both the toe depth h_t/D_{n50} and in the stability number $H_s/\Delta D_{n50}$ it was found that for low toe structures unrealistic and even negative toe diameters could be calculated. Van der Meer therefore re-analysed the work of Gerding and proposed a new formula:

$$\frac{H_s}{\Delta D_{n50}} = \left(2 + 6.2(h_t/h_m)^{2.7}\right) N_{od}^{0.15}. \tag{2.3}$$

Relevance to this thesis

Since the newly formed toe stability formula is an improvement of the work by Gerding, this study is very relevant to this thesis. The improved formula can compared to the criterion that will be developed in this study.

2.1.3 Hofland (2005)

Summary of study

The study of Hofland (2005) is not in the field of breakwaters, but focusses on the stability of stones in non-uniform flow. In his study Hofland aimed to determine what flow events and forces remove a stone from the bed. In his first experiment series he used pressure and velocity sensors to monitor these local hydraulic properties on a small scale. The focus of these measurements was on a cubical block, which represented a normal stone on a bed. In this cube several pressure sensors were incorporated, so the pressures surrounding the cube could be measured.

An important part of the study is aimed at determining the forces that are acting on singular stones, especially the lift and drag forces. Hofland argued that there are two origins for the fluctuating forces on the stones: the quasi-steady forces (no accelerations on small time scales) and forces induced directly by turbulent flow. He computes the quasi-steady drag force using:

$$F_D = \frac{1}{2} C_D \cdot \rho_w \cdot A_f \cdot u \cdot |u|. \tag{2.4}$$

He argued that, for the computation of the quasi-steady forces, it seems best to use the flow velocity at 0.15 times the particle size above the bed. The drag coefficient C_D at that height then usually ranges from 0.23-0.30 for all protrusions.

For high protruding stones Hofland found that the quasi-steady model performed well, but for stones with little to no protrusion the effects turbulence become larger. He argued that the forces induced by turbulence are relatively small and will only lead to the rocking of stones, but they have a significant contribution to the movement of (shielded) stones.

Relevance to this thesis

Although the study of Hofland (2005) is not in the field of breakwaters, parts of his study can be used as guidelines on how to conduct research on stone stability of individual stones. Moreover the determination of the quasi-steady forces and influence of the turbulence are very relevant for this research.

2.1.4 Baart (2008)

Summary of study

Baart (2008) tried to find a relation for toe stone stability that was based on the local conditions rather than the external boundary conditions, such as the wave height and water depth. Since local conditions were not measured during earlier experiments, Baart computes them theoretically and then checks whether the toe elements are stable under these conditions. This is the two-steps concept.

The first step is the determination of the local conditions at the toe. Baart distinguishes three driving sources for the water motions:

- Flow over the toe due to the incoming wave
- Flow over the toe due to down rush or the reflected wave
- Flow through the pores of the breakwater due to head differences

After the calculation of the velocity at the toe, the pore flow through the toe is considered. For the pore flow the head gradient i is the destabilizing force. The maximum head gradient occurs at the moment there is a wave trough above the toe and the run-up is at its highest point on the breakwater. Baart assumes that no outflow occurs through the armour layer, so the maximum head gradient is the difference in water level divided by the horizontal distance. This process is also shown in figure 2.1.

$$i = \frac{\Delta h}{\Delta x} = \frac{{}^{H}/_{2} + R_u}{L_{TA} + {}^{R_u}/_{\tan\alpha}}, \tag{2.5}$$

where L_{TA} is the horizontal distance between the toe and the breakwater at still water level and R_u is the run-up which can be determined using Hunt's formula:

$$R_u = 0.5 \cdot H \cdot \xi. \tag{2.6}$$

The factor 0.5 is a correction that should be applied for rip-rap structures and ξ is the Irribarren number:

$$\xi = \frac{\tan\alpha}{\sqrt{H/L_0}}. \tag{2.7}$$

Figure 2.1: Porous outflow through the toe (Baart, 2008)

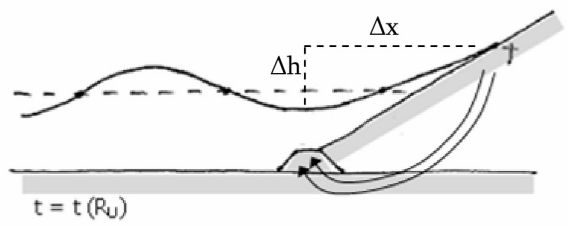

Now that the local physical processes are determined (Step 1), the relation between those processes and the stability of the rock is determined (Step 2). First he identifies the flow forces on the rock, which are drag, lift, shear forces and forces caused by porous outflow. The stabilizing elements are the weight and the interaction with other elements. The drag, lift and shear forces all influenced by the flow speed with the same proportionality:

$$F_{D,L,S} \propto C_{D,L,S} \cdot \rho_w u^2 D_{n50}^2. \tag{2.8}$$

The force exerted by the porous flow is determined as:

$$F_{PF} = C_{PF} \cdot \rho_w g i D_{n50}^3, \tag{2.9}$$

where C_{PF} is a coefficient that accounts, amongst others, for the shape and orientation of the rock.

After identifying the forces and their directions, Baart determined the equilibrium point for these forces, i.e. the point where the element is *just* stable, as:

$$\frac{\hat{u}_b^2}{(\Delta - C_{PF} \cdot i) g D_{n50}} = C. \tag{2.10}$$

Further derivation, using the Rance/Warren stability criterion combined with the porous flow, yields an equation for the critical value for the velocity:

$$(\hat{u}_{bc})^{2.5} = 0.46\sqrt{T} \cdot ((\Delta - C_{PF} \cdot i)g)^{1.5} \cdot D_{n50}. \tag{2.11}$$

If the local velocity $\hat{u}_b$ is higher than the critical velocity $\hat{u}_{bc}$, the stone(s) should start to move. The value for the porous flow coefficient C_{PF} was found by fitting his criterion to the dataset of Gerding (1993) and he found that $C_{PF} = 0.40$ gave the best results.

Relevance to this thesis

Baart has developed a toe stability criterion which is based on local hydraulic conditions. He has achieved this by using the data obtained by previous studies on toe stability. Since these studies did not actually measure the local hydraulic conditions Baart had to estimate these conditions. The present study will measure these local conditions and can therefore be used to verify the criterion developed by Baart. It is interesting to compare the performance of the Baart criterion with the criterion that will be developed in this study.

2.1.5 Nammuni-Krohn (2009)

Summary of study

As part of a minor research project Nammuni-Krohn (2009) aimed to complement the work performed by Baart by accurately measuring the flow velocities near the breakwater toe. She performed her measurements with several water heights, toe heights and stone sizes. Velocity measurements were performed at several locations above the toe. By curve fitting her data she found an empirical formulation for the maximum horizontal flow velocity occurring above a toe:

$$U_{max} = U_0 \cdot (m\xi \frac{h_t}{h_m} + a), \tag{2.12}$$

where m and a are linear fit coefficients. In her study she determined that for $D_{n50} = 0.025$, $m = 0.015$ and $a = 1.034$ should be used. U_0 is defined as:

$$U_0 = \frac{\pi H}{T} \frac{1}{\sinh(k(h_m - h_t))}. \tag{2.13}$$

It should be noted that here h_t represents the toe height rather than the water height above toe, as is used in the research of Gerding and Van der Meer.

Relevance to this thesis

By developing a formula for the calculation of the flow velocity near a breakwater toe based on the wave conditions, Nammuni-Krohn (2009) made a step in making design formulas for breakwater toes based on local hydraulic conditions more generally applicable. If the local conditions can be reliably approximated by empirical formulas, there is less need to perform experiments or apply numerical models to determine these conditions.

2.2 Forces and moments on a stone

Based on the previous research, it seems that the point of incipient motion based on local hydraulic parameters can be best determined when the behaviour of singular stones are researched. Especially the study by Hofland (2005) is a good example of how this can be performed. Since the focus lies on individual stones, it is logical to look at forces acting on those stones. These forces can be approximated if the local hydraulic parameters like flow velocity and water pressures are known. This section therefore presents the forces acting on a stone and how they can be approximated when the local hydraulic parameters are known.

2.2.1 Forces acting on a stone

Stones in toes of breakwaters are subjected to oscillating flows caused by the incoming waves that break on the slope of the breakwater and are then reflected. For stones in a flow there are several forces that play an important role for their stability. The destabilising forces are the lift, drag and shear force (F_L, F_D, F_S respectively). The stabilising force is the weight of the stone F_W. These forces are depicted schematically in figure 2.2. The origin of these forces and the way they can be determined are treated in the next sections.

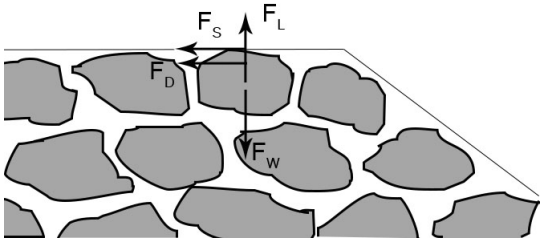

Figure 2.2: Forces on a stone in a breakwater toe

Weight of the stone

F_W is the force that accounts for the underwater weight of the stone, which can be determined by:

$$F_W = (\rho_s - \rho_w) \cdot D_{n50}^3 \cdot g. \tag{2.14}$$

Since this force has a downwards direction, it is a stabilising force.

Lift force

The other vertical force is the lift force F_L. It originates from the pressure difference between the top and the bottom of the stone. If the pressure underneath the stone is higher than the pressure above the stone, the net lift force will be directed upwards and thus destabilises the stone. When this pressure difference is multiplied by the area of the stone it acts upon, the lift force can be calculated using:

$$F_L = (p_{under} - p_{above}) \cdot A_L. \tag{2.15}$$

Drag force

The drag force F_D originates from the water flow on the frontal area of the stone. It can be determined by:

$$F_D = \frac{1}{2} C_D \cdot \rho_w \cdot A_f \cdot u \cdot |u|. \tag{2.16}$$

The velocity u is the velocity at $0.15 D_{n,50}$ above the surface, for which Hofland (2005) concluded the drag coefficient was rather constant for different protrusion values ranging from 0.23-0.3.

Shear force

When a fluid flows over an object it exerts a shear force on this object, which can be determined by:

$$F_S = C_f \cdot \frac{1}{2} \cdot \rho_w \cdot u \cdot |u| \cdot A_S, \tag{2.17}$$

where $A_S \approx D_{n,50}^2$ is the top area of the stone over which the water flows.

The determination of the shear coefficient C_f is a bit more complicated and no approximate value for C_f was found in the literature. It is therefore approximated using the aerodynamics theory for incompressible turbulent flow over a flat plate (Anderson, 2007)

$$C_f = \frac{0.074}{Re_x^{0.2}}, \tag{2.18}$$

where the particle Reynolds number is computed as:

$$Re_x = \frac{u \cdot D_{n,50}}{\nu}. \tag{2.19}$$

It should be noted that this method is not very representative for this case, since the method was developed for air flowing over a flat plate. Moreover the theory is developed for fully developed boundary layers, which is very different from oscillating water flows in which the boundary layers will probably not fully develop during one wave period. Nonetheless, since no other method was found to describe this case, the theory described by Anderson (2007) is used as an approximation to determine the order of magnitude of the shear force. If these forces are very small, the shear force may be omitted from further analysis.

Turbulence induced forces

As was found in the study of Hofland (2005), the turbulence induced forces play a role in the movement of stones. Since these forces are relatively small, they only cause the rocking of stones. However, they still have a significant influence especially for low protruding stones. The determination of these turbulence forces is a study on its own and therefore beyond the scope of this thesis. It should be kept in mind that the results of this thesis do not account for turbulence. The computed forces on the stones will probably be lower than would be the case if the turbulence induced forces were incorporated in this study.

In his study Hofland made an estimation of the magnitude of the turbulence induced forces on a sphere and a cylinder (diameter of 2 cm) in an open channel flow with a flow velocity of 2 m/s. For this case he found forces of roughly 0.01 N as an order of magnitude.

2.2.2 Moment of force on a stone

When observing stones in breakwater toes it can be seen that they usually roll out of their place. It is therefore logical to determine the moment of force about a certain point on the stone. Figure 2.3 shows the forces acting on the stone and their arm to the point about which the stones are assumed to roll. When the resulting moment of force becomes positive, the stone should start to roll out.

$$M_A = F_L \cdot o_{wl} - F_W \cdot o_{wl} + F_D \cdot o_d + F_S \cdot o_s. \tag{2.20}$$

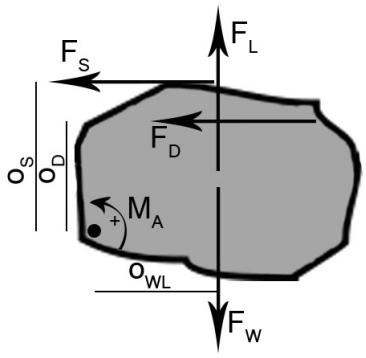

Figure 2.3: Moment of force on a stone in a breakwater toe

In order to verify this criterion, the local hydraulic conditions at the point of incipient motion need to be known. Since previous research on breakwater toes has focussed on the external wave parameters, this data is not yet available. During the experiments of Gerding (1993) only wave gauges were used to determine the wave parameters. Research of Nammuni-Krohn (2009) added velocity sensors to the experimental set-up, but pressures under the stones of breakwater toes have not been measured before. During this study an experiment will be performed in which the wave conditions, flow velocities and pressures under the stones will be measured in order to verify the moment criterion.

Chapter 3

Experimental arrangement

As described in chapter 2.2, the focus of this study lies on the forces acting on single stones. To be able to calculate these forces, the local hydraulic parameters need to be known. Therefore an experiment is designed which will be able to provide the pressures and the velocities in the vicinity of the toe stones.

3.1 Experimental configuration

3.1.1 Geometry

The experiment is performed in the wave flume of the Fluid Mechanics Laboratory at Delft University of Technology. The wave flume has a length of 42 m, a width of 0.8 m and a height of 1 m. Within this flume a wave generator with automatic reflection compensation is present. The desired waves can be generated by creating an input file for the wave generator in which the wave height, wave period and duration of the experiment are defined.

At the end of the wave flume a rubble mound breakwater is constructed from natural stones. This breakwater consists of a core, armour layer, crown wall and toe. The crown wall is not required for this study, but this breakwater is also used for a study by Van Heemst (2014), concerning the forces on crown walls. Therefore a breakwater that suits both studies is designed and built in collaboration.

The breakwater has a scale of roughly 1:30, resulting in a breakwater with a crest height of 0.72 m. A slope of 1:1.5 is chosen, which is often used in breakwaters. All the relevant dimensions of the breakwater can be seen in figure 3.3. The model differs from a realistic situation by the lack of a foreshore. The reason for the absence of a foreshore is twofold. Firstly, there are the dimensional constraints of the wave flume. The introduction of a foreshore would raise the ground level of the breakwater with about 0.20 m. This results in less possible variations in water height, as the flume is only 1 m high. Secondly, a foreshore is not necessary for the creation of representative local hydraulic conditions, it would only complicate the analysis of the results.

Stone sizes of the breakwater

The stone size of the armour layer is determined by using the Hudson formula (equation 3.1). The Hudson formula is used because it is a simple formula for which very few parameters are required. This is sufficient for present study, as the armour layer is not a critical part of this study. It is only used to design a representative breakwater.

$$\frac{H_s}{\Delta D_{n50}} = \sqrt[3]{K_D \cot \alpha}, \tag{3.1}$$

where K_D is a dustbin factor which ranges from 3-4 for natural rock and α is the slope of the breakwater.

The slope of this breakwater is 1:1.5 and a wave height of 0.15 m is chosen as design wave. This wave height is about the median of the wave heights that will be used during this study. Consequently the chosen stone size will be too small in some experiments and too large in others. However, in section 3.1.2 it will be explained why this will cause no problems. Using the aforementioned values, the required stone size (D_{n50}) of the armour layer is about 0.05 m. Stones of approximately this size were ordered and after a sample of about 200 stones was weighed, it was found that the nominal diameter of the armour stones was 0.044 m.

The core consists of natural rock with a nominal diameter of 0.022 m. These stones were readily available in the lab and their size is also appropriately in relation to the stones of the armour layer, which are twice as big.

The toe of the breakwater is 0.12 m high and has a slope of 1:1.5. The stones have a nominal diameter of 0.025 m.

The grading curves of the stones used in the experiment are shown in appendix A.

Target stones

During the pre-tests, several sizes for the target stones were tested for different wave conditions. These pre-tests were designed using Gerding's formula (equation 2.2), in which several wave and water height combinations were used to find the required sizes of the stones for a damage parameter of $N_{od} = 0.5$, indicating some damage. Note that the value of H_s does not represent the highest wave, but since this study uses regular waves, every wave should theoretically be the highest wave. The Gerding formula is only used as a first approximation to determine the wave conditions for which a stone of a certain size would start to move. The results of this computation are shown in table 3.1. In this table 'xx' means that either the waves are larger than the water depth above the toe, or the stone size was too small to be taken into consideration. Using these results, it was decided to do pre-tests with waves ranging from 0.12 m to 0.22 m and stones from 0.020 m to 0.035 m in order to check what stones could be moved during which wave conditions.

It was found that target stones of 0.023 m started to move with a lot of different hydraulic conditions. Stones of 0.025 m could only be moved with the highest possible wave conditions, but since the waves became distorted during these conditions, they are not included in the final testing schedule. Stones bigger than 0.025 m would not move at all. Stones with a size of 0.020 m were a bit too small for the cavities that were made for the target stones. These stones had little to no contact with the other stones of the toe, which is not representative of the real situation. It was therefore decided to perform all the tests with target stones of 0.023 m. The detailed characteristics of the target stones can be found in appendix A.2.

Table 3.1: Required stone sizes in meters according to Gerding

$H_s[m]$	0.1	0.12	0.14	0.16	0.18	0.20	0.22
$h_t[m]$							
0.18	0.015	0.023	0.032	0.040	0.049	xx	xx
0.28	xx	0.008	0.017	0.025	0.034	0.042	0.050
0.38	xx	xx	xx	0.010	0.018	0.027	0.035
0.48	xx	xx	xx	xx	xx	0.012	0.020

3.1.2 Construction

The goal of the experiment is to determine the point of incipient motion of stones in a breakwater toe based on the local hydraulic parameters. It is therefore important that the initial movement of individual stones can be spotted easily. To achieve this, the stones of both the armour layer and the toe are glued together with the exception of a seven 'target stones' on the toe. The core of the breakwater is simply 'dumped' into the the flume, after which it is shaped. This results in a breakwater that does not deform during the experiment, since all of the outfacing elements of the breakwater are fixed. Photos of the breakwater construction are shown in figure 3.2.

Construction of the armour layer

The armour layer used in this study consists of a solid (reinforced) plate of glued stones. The stones are coated with a two component epoxy-coating called Poly-Pox GT625 using a concrete-mixer. Thereafter they are cast into a mould in two layers with a concrete mesh in the middle. The concrete mesh is added to ensure the solid plate does not break during the transport of the plate. After the mould is removed, the plate is simply placed on top of the breakwater core.

Construction of the breakwater toe

The breakwater toe is also constructed using Poly-Pox GT625, but the moulding process is a bit different since the toe has more features. The most important feature is that there are seven cavities on top of the toe. In these cavities the 'target stones' are placed during the experiments, which are the only stones in the toe that can move.

Since the purpose of this experiment is to determine the local hydraulic parameters at the point of incipient motion, pressure meters will be placed underneath the stones. Therefore room for the tubes and cables is reserved in the moulding process and afterwards holes are drilled at the locations of the target stones. The locations of the target stones are evenly spread over the berm of the toe and are shown in figure 3.1.

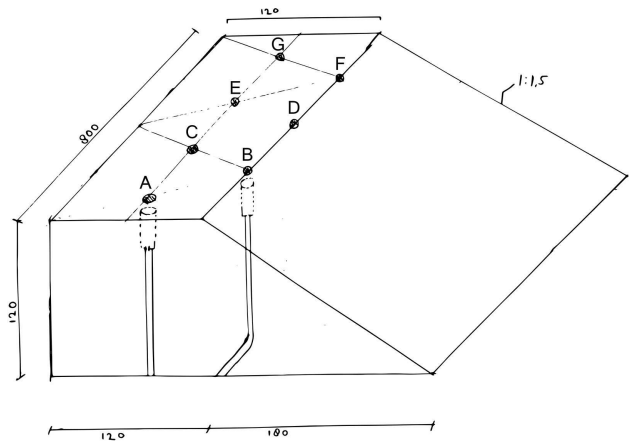

Figure 3.1: Toe cross-section and location of pressure meters (distances in mm)

Figure 3.2: Breakwater construction

3.1.3 Instrumental configuration

Three parameters are measured during the experiments: the water levels, the flow velocities above the toe and the pressure under the target stones. The instrumentation and their location in the flume will be presented in this section.

Instrumentation

The water levels are measured with standard wave gauges. These gauges consist of two rods through which a current is sent, at the water level the current travels through the water to the other rod. The higher the water level, the lower the resistance. With this simple principle the water level can be measured.

The pressures are measured using a modified Honeywell pressure sensor. This small sensor measures the pressure differential using a small diaphragm. The standard sensor is modified so that it fits in a plastic tube with a diameter of 20 mm. One side of the sensor is open to the water and the other side is connected to the atmosphere by means of a tube.

The velocities above the toe are measured by two Electro Magnetic velocity Sensors (EMS). Initially it was planned to use one EMS and one Acoustic Doppler Velocimeter (ADV), since the ADV is more accurate and is able to measure turbulence better. The ADV, however, requires suspended sediment in the water to measure the flow velocities. It was found that such a large amount of sediment was required for reliable results, that the toe structure would hardly be visible. Since this experiment depends heavily on visual observations, the ADV could not be used for the main experiments. Instead it is used afterwards to verify whether the velocities measured by the EMS are accurate and to get a better insight in the turbulent properties during the experiments.

During the experiments a button is pressed to mark the moment of incipient motion by visual observation. If a stone comes out of its cavity the button is pressed, resulting in peak in the dataset. This way it is easy to find the moment of incipient motion in the dataset. The real moment of incipient motion, however, will be a little earlier than the moment the button is pressed, since the reaction time of the observer plays a role.

Most of the performed tests are recorded using a standard camera, placed next to the glass wall of the wave flume. The purpose of this camera is to find links between the obtained data and visual observation. Moreover the footage can be used to determine the point of incipient motion more accurately.

Instrumental set-up

Figure 3.3 shows the experimental set-up for this study.

Three wave gauges (WG1, WG2, WG3) are placed 6 meters in front of the breakwater. These wave gauges can be used to separate the incoming wave from the wave paddle and the reflected wave from the breakwater.

Another wave gauge is placed at the breakwater (WG_toe) to measure the water level above the middle of the toe, which is 6 cm from the edge of the toe and 6 cm from the armour layer. To the left and and the right of this wave gauge two EMS's are placed at 5 cm above the toe, one behind stone B and one behind stone F (EMS B, EMS F). The reason they are placed relatively high is that the EMS is almost as big as the stones of the toe. If they are placed too close to the structure they will interfere with the flow. From measurment R064 on EMS F is replaced by an ADV for more accurate velocity measurements.

The seven pressure meters are placed under the target stones of the toe (pA-pG). Pressure meters pB, pD and pF are located on the edge of the toe and pA, pC, pE and pG on the middle of the toe (6 cm from the edge). The tubes and cables of the sensors are taped to the inner wall of flume, so that they affect the flow as little as possible.

Calibration and recordings

The signal of all the instruments are amplified and recorded using Dasylab at a frequency of 500 Hz. Prior to the measurement campaign the wave gauges and pressure meters are statically calibrated in order to determine the calibration factor for each of these sensors. The calibration factor of the EMS-velocity sensors are known.

Firstly, the wave gauges are calibrated by lowering them into the water and defining this position as the base level. Thereafter, they are moved 10 cm upwards and downwards from the base level. By dividing the voltage difference by the height difference, the calibration factor can be determined. The calibration for the pressure meters follows a similar method, but in this case the sensors were fixed, so the water level was changed during

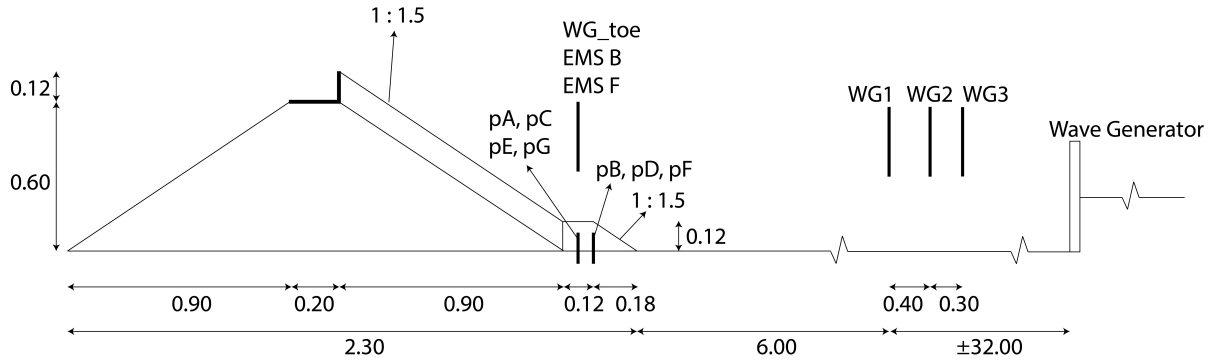

Figure 3.3: Experimental set-up with the relevant distances [m] and slopes

the calibration process. This procedure is repeated several times and the average of the calibration factors is taken. Table 3.2 shows the structure of the dataset and the calibration factors.

Table 3.2: Structure of the dataset

Column	Description	Calibration factor
1	Time	1 [s]
2	Pressure A	-0.0811 [v/mwc]
3	Pressure B	-0.0806 [v/mwc]
4	Pressure C	-0.0745 [v/mwc]
5	Pressure D	-0.0815 [v/mwc]
6	Pressure E	-0.0830 [v/mwc]
7	Pressure F	-0.0873 [v/mwc]
8	Pressure G	-0.0870 [v/mwc]
9	Button	-
10	EMS X at F	0.1 [v/(m/s)]
11	EMS Y at F	0.1 [v/(m/s)]
12	EMS X at B	0.1 [v/(m/s)]
13	EMS Y at B	0.1 [v/(m/s)]
14	Wave Gauge toe	0.0242 [v/mwc]
15	Wave Gauge 1	0.0240 [v/mwc]
16	Wave Gauge 2	0.0248 [v/mwc]
17	Wave Gauge 3	0.0268 [v/mwc]

3.2 Measurement campaign

Now that the experimental configuration has been introduced, the measurement campaign will be presented. First, the hydraulic conditions will be shown followed by the measurement campaign. Finally, the testing procedure will be introduced.

3.2.1 Hydraulic conditions

A regular wave field is used for this study, meaning there are no significant differences in wave height and wave period within one test run. In most research on breakwaters irregular waves are used, which represent the reality better. These studies, however, were aimed at finding an empirical relation between the wave characteristics and the damage to the breakwater (toe). The present study is interested in the local hydraulic conditions at the moment of incipient motion. It is not very relevant how these local conditions are formed, as long as they represent the same process, being wave-structure interaction. By using regular waves, the analysis will be much easier.

Another advantage of regular wave characteristics is that the duration of each experiment run can be drastically shortened. In an irregular wave field only the highest waves will cause critical damage and therefore a lot of waves need to be generated to at least have a few of these high waves. Usually, this results in experiments with a duration of about a 1000 waves (30 minutes if the wave period is 2 seconds). With regular waves every wave will, in theory, be the highest wave and therefore the experiment runs can be a lot shorter. The runs are

therefore set to last 4 minutes. If a stone is not out of its cavity by then, it will most likely not go out thereafter.

The wave heights used during the experiments are in the same order of magnitude as the waves used during the studies of Gerding (1993) and Nammuni-Krohn (2009). A lot of different wave conditions were tested during the pre-tests to check whether the target stones would move during these conditions and to check whether the wave generator was capable of creating these waves. Based on these tests, wave heights between 0.12 and 0.24 m are chosen for the experiments. Waves lower than 0.12 m are not relevant for this study, since the chosen stones are stable under those circumstances. The upper limit of 0.24 m is a limitation of the wave flume. Higher waves would break shortly after they were generated.

Aside from the wave height, the wave period should also be determined. For this experiment the wave steepness is used to determine the periods, which is a widely used method to determine wave periods:

$$s = \frac{2\pi \cdot H}{g \cdot T^2}. \tag{3.2}$$

The wave steepness used is either 0.02, 0.03 or 0.04. Although Gerding (1993) concluded there was no significant influence of the wave steepness on the stone stability, Ebbens (2009) found that in shallow water there is an influence. For deeper water the influence appeared to be smaller.

In this experiment the water depths range from 0.30 to 0.50 m. The lower limit is 0.30 m, because the velocity sensors need to be submerged at all times. The toe is 0.12 m high, so the water height above the toe is equal to 0.18 m. This may result in non-submerged velocity sensors with the larger wave heights.

3.2.2 Measurement campaign

Not all combinations of hydraulic conditions can be tested in the wave flume, because the larger waves break just after they are generated. Moreover, it is important that the hydraulic conditions are harsh enough, to start the movement of the target stones. Therefore a lot of hydraulic combinations were tested, to see if they were achievable in the flume and if they resulted in movement of stones. If this was the case, that combination would be used in the measurement campaign. During the measurement campaign, interesting hydraulic conditions are performed multiple times. Measurements R001-R014 were used to verify the equipment and to make the last alterations in the testing schedule and procedure. From test R020 onwards the tests were videoed, and from test R039 onwards the video time could be accurately linked to the time used in the dataset. Finally in tests R064-R076 the EMS at location F was replaced by an ADV. The complete measurement campaign is presented in table 3.3. The wave lengths for the different are also computed using the equation for transitional water depth (equation 3.3). After the computation it was verified that all the measurements in this study are in the transitional water depth ($\frac{1}{20} < \frac{h}{L} < \frac{1}{2}$).

$$L = \frac{gT^2}{2\pi} \tanh(kh) \tag{3.3}$$

Table 3.3: Measurement campaign

Measurement	$h_m[m]$	$H[m]$	$s[-]$	$T[s]$	$L[m]$
R001	0.30	0.12	0.04	1.39	2.13
R002	0.30	0.14	0.04	1.50	2.34
R003	0.30	0.12	0.02	1.96	3.18
R004	0.30	0.14	0.02	2.12	3.47
R005	0.30	0.16	0.04	1.60	2.52
R006	0.35	0.16	0.04	1.60	2.69
R007	0.35	0.16	0.02	2.26	3.99
R008	0.35	0.18	0.04	1.70	2.89
R009	0.30	0.14	0.04	1.50	2.34
R010	0.30	0.12	0.02	1.96	3.18
R011	0.30	0.12	0.02	1.96	3.18
R012	0.30	0.12	0.02	1.96	3.18
R013	0.30	0.14	0.02	2.12	3.47
R014	0.30	0.16	0.04	1.60	2.52

Continued on next page

Table 3.3 – continued from previous page

Measurement	$h_m[m]$	$H[m]$	$s[-]$	$T[s]$	$L[m]$
R015	0.30	0.14	0.02	2.12	3.47
R016	0.35	0.16	0.04	1.60	2.69
R017	0.35	0.16	0.02	2.26	3.99
R018	0.35	0.18	0.04	1.70	2.89
R019	0.35	0.18	0.04	1.70	2.89
R020	0.38	0.15	0.02	2.19	4.00
R021	0.38	0.17	0.02	2.33	4.29
R022	0.38	0.17	0.03	1.91	3.43
R023	0.38	0.19	0.03	2.01	3.63
R024	0.38	0.18	0.04	1.70	2.99
R025	0.38	0.20	0.04	1.79	3.17
R026	0.40	0.16	0.04	1.60	2.84
R027	0.40	0.18	0.04	1.70	3.05
R028	0.40	0.18	0.04	1.70	3.05
R029	0.40	0.20	0.04	1.79	3.25
R030	0.40	0.21	0.04	1.83	3.33
R031	0.40	0.18	0.03	1.96	3.61
R032	0.40	0.20	0.03	2.07	3.84
R033	0.45	0.20	0.04	1.79	3.41
R034	0.45	0.22	0.04	1.88	3.61
R035	0.45	0.20	0.02	2.53	5.06
R036	0.45	0.22	0.03	2.17	4.27
R037	0.45	0.22	0.03	2.17	4.27
R038	0.45	0.22	0.04	1.88	3.61
R039	0.35	0.18	0.04	1.70	2.89
R040	0.35	0.16	0.04	1.60	2.69
R041	0.35	0.16	0.02	2.26	3.99
R042	0.35	0.18	0.04	1.70	2.89
R043	0.30	0.14	0.04	1.50	2.34
R044	0.30	0.14	0.02	2.12	3.47
R045	0.30	0.16	0.04	1.60	2.52
R046	0.30	0.16	0.04	1.60	2.52
R047	0.38	0.17	0.02	2.33	4.29
R048	0.38	0.19	0.03	2.01	3.63
R049	0.38	0.18	0.04	1.70	2.99
R050	0.38	0.20	0.04	1.79	3.17
R051	0.40	0.18	0.04	1.70	3.05
R052	0.40	0.20	0.04	1.79	3.25
R053	0.40	0.21	0.04	1.83	3.33
R054	0.40	0.18	0.03	1.96	3.61
R055	0.40	0.20	0.03	2.07	3.84
R056	0.45	0.20	0.04	1.79	3.41
R057	0.45	0.22	0.04	1.88	3.61
R058	0.45	0.20	0.02	2.53	5.06
R059	0.45	0.22	0.03	2.17	4.27
R060	0.50	0.20	0.04	1.79	3.55
R061	0.50	0.20	0.02	2.53	5.31
R062	0.50	0.22	0.04	1.88	3.77
R063	0.50	0.24	0.04	1.96	3.96
R064	0.40	0.18	0.04	1.70	3.05
R065	0.40	0.18	0.03	1.96	3.61
R066	0.40	0.20	0.04	1.79	3.25
R067	0.40	0.20	0.03	2.07	3.84
R068	0.40	0.20	0.03	2.07	3.84
R069	0.38	0.17	0.02	2.33	4.29
R070	0.38	0.18	0.04	1.70	2.99

Continued on next page

Table 3.3 – continued from previous page

Measurement	$h_m[m]$	$H[m]$	$s[-]$	$T[s]$	$L[m]$
R071	0.38	0.19	0.03	2.01	3.63
R072	0.35	0.20	0.04	1.79	3.07
R073	0.35	0.16	0.04	1.60	2.69
R074	0.35	0.16	0.02	2.26	3.99
R075	0.35	0.18	0.04	1.70	2.89
R076	0.30	0.14	0.04	1.50	2.34

Testing procedure

In order to be able to compare the different tests, they need to be performed in a similar way. To this purpose a procedure is followed during each test to satisfy this requirement.

Before the test starts, the target stones are (re)placed into their cavities, their position and orientation are the same during all the tests to ensure the similarity. After the equipment is checked, and zero-drifts of the equipment (if any) are corrected, the test can start.

During the test the target stones are observed and if movement occurs a button is pressed to mark this point in the dataset. Since the reaction time of the observer plays a role in this procedure, the marked point will probably a bit off. From R039 on, a stopwatch is shown in the video which makes the determination of the moment of incipient motion more accurate. Attention is also paid to the wave conditions, to check whether waves are breaking or if they become oblique during the tests. The wave generator stops after 4 minutes and the recording is saved. After the measurement a quick log of the experiment is written, which describes the main events, observations and abnormalities of the test. These logs can be found in Appendix D.

Chapter 4

Measured data analysis

This section presents the data obtained during the measurements and notable observations will be discussed. A first remark is that the measured water levels and velocities above the toe (which are measured in the middle of the toe) are assumed to be the same on the edge of the toe (which is 6 cm from the center) at that moment. To check whether this is acceptable, the wave celerity will be determined for transitional water depth $\left(\frac{1}{20} < \frac{h}{L} < \frac{1}{2}\right)$ using:

$$c = \sqrt{\frac{gL}{2\pi} \tanh\left(2\pi \frac{h}{L}\right)}. \tag{4.1}$$

For the hydraulic conditions used in this study, this yields a wave celerity of roughly 2 m/s, meaning that the the 6 cm difference will be covered in 0.03 seconds. This is such a small difference, that the previously mentioned assumption is well within limits.

4.1 Wave gauges

A total of four wave gauges were used during the experiments: one above the toe and three about 6 meters from the toe structure. As was described in section 3.1.3, the three wave gauges can be used to identify the incoming wave from the reflected wave. The wave gauge at the toe was used in the computation of the pressures above the toe.

To determine the incoming wave heights (H_i), `Refreg` is used. This MATLAB program was written for the Laboratory of Fluid Mechanics at DUT and uses the method described by Goda and Suzuki (1976). The wave records of two wave gauges, which should be positioned roughly $L/4$ from each other, are used as input to separate the incoming from the reflected wave. For this a stable wave record should be used, which is representative for the measurement. Figure 4.1 shows a typical wave record for wave gauge 3 (wave generator side), whereas figure 4.2 shows the record for the wave gauge at the toe. From these figure it can be seen that there is a spin-up time for the waves to fully develop into their 'stable' wave height. After 50 seconds the waves are stabilised and for the other measurements very similar spin-up times were observed. A conservative spin-up time of 60 seconds is therefore chosen. Near the end of the measurements there are also irregularities, because at that point the wave generator already stopped. Moreover, no stone movement occurred past the 180 seconds mark. A period of 100 seconds, from 60-160 seconds, is therefore used to determine the incoming wave height with `Refreg`. The results are presented in table B.1. The `Refreg` analysis indicates that the actual incoming waves are on average 10-20% lower than the waves that were asked from the wave generator.

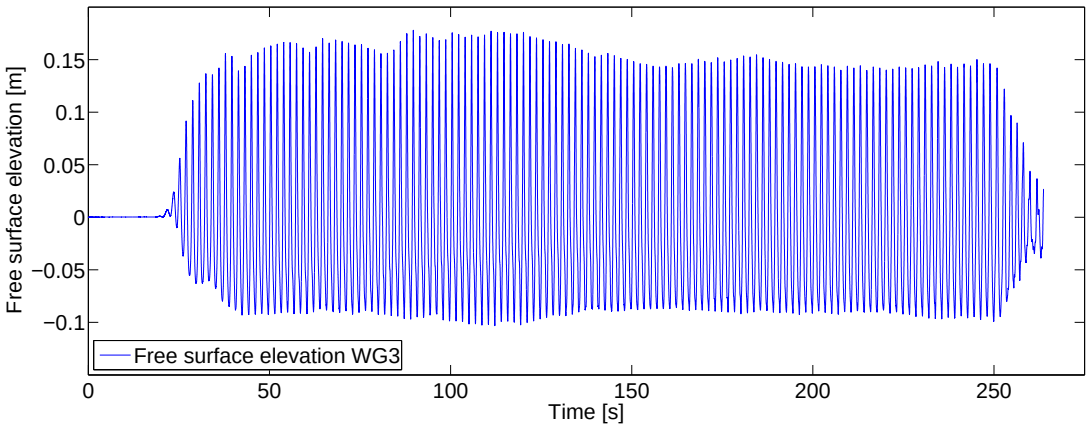

Figure 4.1: Typical free surface elevation of the wave gauge 6 meters in front of the breakwater (WG3 during R033)

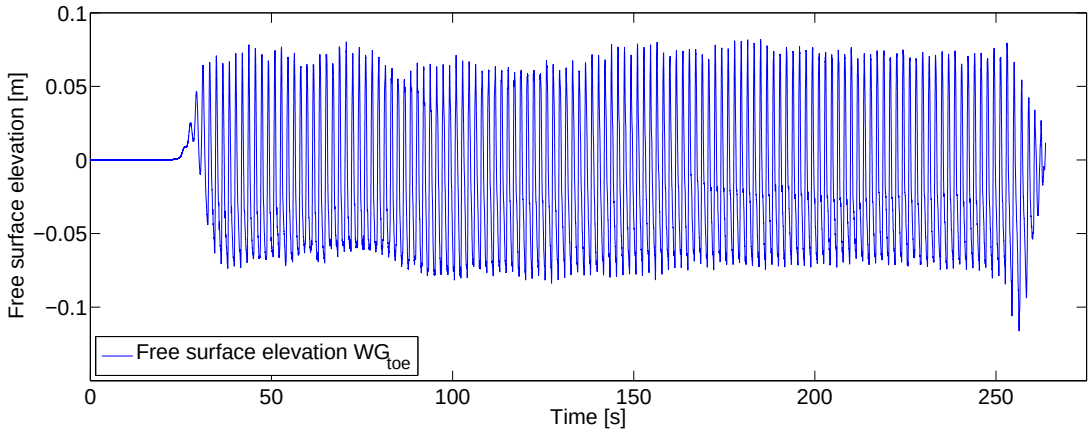

Figure 4.2: Typical free surface record of wave gauge at the toe (R033)

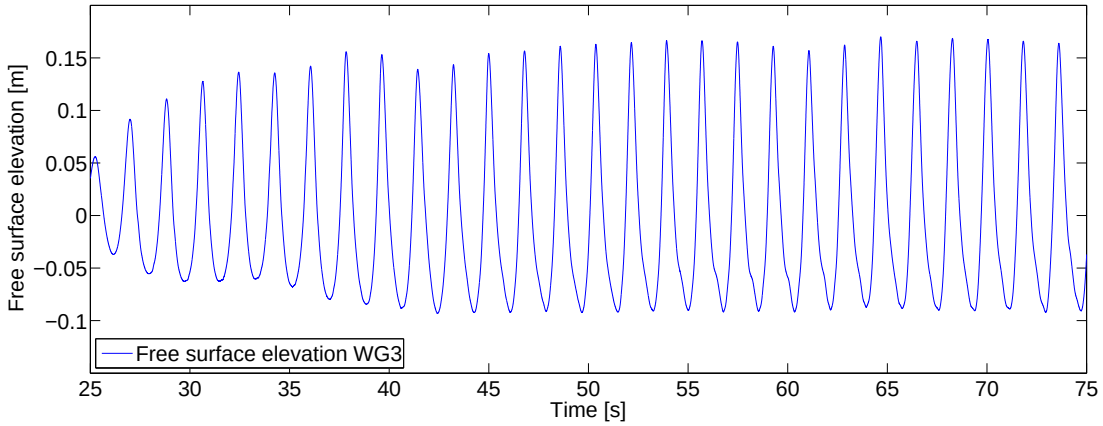

Figure 4.3: Detailed view of the free surface elevation record of the wave gauge 6 meters in front of the breakwater (WG3 during R033)

A possible explanation for the results of the `Refreg` analysis, is that the program computes the amplitude of symmetric wave (peak height and trough depth are the same), but the wave record of figure 4.1 clearly shows that the peaks are higher than the troughs are deep and that the waves are asymmetric. Moreover, `Refreg` requires the two wave gauges to be about $^L/_4$ apart from each other, which is not always the case and thus leading to errors. Another analysis is therefore performed, which determines the values for the peaks and troughs in the 'stable' period of the measurements, after which the root mean squared value is determined using equation 4.2. In this equation N is the total number of peaks. This yields a characteristic value for the wave peaks and troughs for each measurement, after which the wave height is determined as $H = a_{peak} + a_{trough}$. This does not account for reflection at the breakwater. `Refreg` computed typical reflection values of 30%, which is in line of what is to be expected with breakwaters. A paper on wave reflection from coastal structures by Zanuttigh and Van der Meer (2006) also shows that typical reflection values for permeable rock lie around 30%. This reflection coefficient is applied to the wave heights found by the peak-trough analysis.

$$a_{rms} = \sqrt{\frac{1}{N}\sum_{i=1}^{N} a_i^2}. \tag{4.2}$$

Table B.1 shows the results of the peak-trough analysis next to the `Refreg` analysis. From this table it can be seen that both analyses show mixed results. An example of this is R047, where a wave input of 0.17 m was asked from the wave generator. `Refreg` gives an incoming wave height of 0.07 m which is far too low, whereas the peak trough analysis gives a wave height of 0.19 m which is too big. This measurement shows an extreme case of the errors, but these apparent errors are seen in more cases. Although for some measurements it is questionable which method gives the best answer, it is chosen to use the incoming wave heights as computed by `Refreg`, since this has a more solid theoretical background.

4.2 Velocity data

During the majority of the experiments the velocity was measured using two EMS velocity meters. As described in section 3.1.3, they were placed just behind stones B and F. A typical EMS velocity measurement is shown in figure 4.4. It can be seen that the EMS at B usually measures a lower velocity compared to the EMS at F. This is only the case in the positive x-direction (incoming waves), the down rush velocities are very comparable. This phenomenon is seen in almost all the tests, which means that there are two possibilities: either the velocities near stone B are actually lower, or one of the EMS's has a deviation in the positive x-direction.

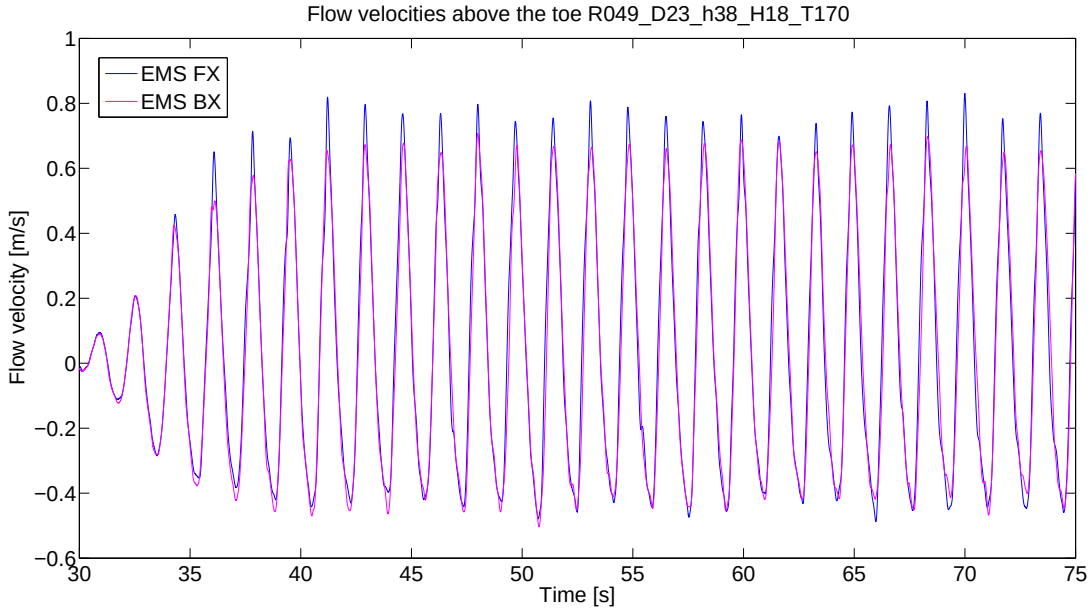

Figure 4.4: Flow velocities measured with the EMS at the toe

The last series of measurements were performed with an ADV near stone F. The ADV should give a more accurate velocity profile and more turbulence information. Some turbulence could be seen on the recording screen during the measurements. Unfortunately, the data that was written to the file had a frequency of 100 Hz, instead of the intended 500 Hz, which was shown on the recording screen. The frequency of 100 Hz was too low to determine the turbulent properties of the flow. The data can, however, be used to validate the velocities measured by the EMS velocity meters. Figure 4.5 shows the measured velocity with the ADV under the same wave conditions as the measured velocities in figure 4.4. It can be seen that these velocities are very comparable for this case, which was also observed for the other cases. It therefore seems that the EMS velocity sensors provide the correct velocity profile.

As was explained in section 3.1.3, the velocity sensors could not be placed too close to the bottom because they would interfere with the flow above the stones. The measured velocities do therefore not represent the local flow velocity directly above the toe. Previous research by Hofland (2005) argued that the velocity at $0.15 \cdot D_{n50}$ could best be used when computing the (quasi-steady) forces on a stone. For this study that means that the velocity at $0.15 \cdot 0.023 = 3.5 \cdot 10^{-3}$ m above the bed should be considered.

In order to determine the velocity at 3.5 mm above the bed, the velocity profile near the bed needs to be known. Since we are very close to the bed, this point probably lies within the boundary layer and it is therefore not straightforward to determine the velocity. To this purpose the boundary layer theory in oscillatory flow by Jonsson (1980) is used. Figure 4.6 shows a typical velocity profile for oscillating flow over a rough wall. The geometry in the current study is much more complicated, as this study deals with a breakwater toe and armour layer which influence the flow. Moreover, the waves are breaking on the armour layer, resulting in a more complex flow pattern. However, from the different methods that were reviewed, the research of Jonsson best resembled the flow over a breakwater toe and is therefore chosen as the best option.

As can be seen in figure 4.6, the boundary layer thickness δ needs to be known to determine the velocity at a certain point z. The calculation for this thickness is developed in the same study by Jonsson, for oscillating flow over a rough wall. Still, this method can be used to get an idea of the thickness of the boundary layer.

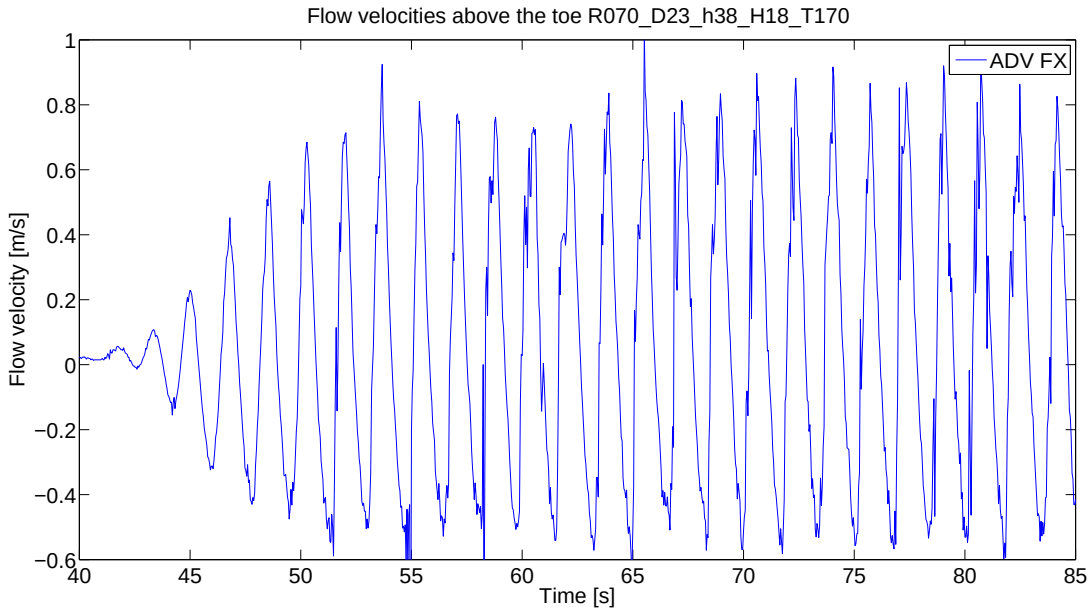

Figure 4.5: Flow velocity measured with the ADV at the toe

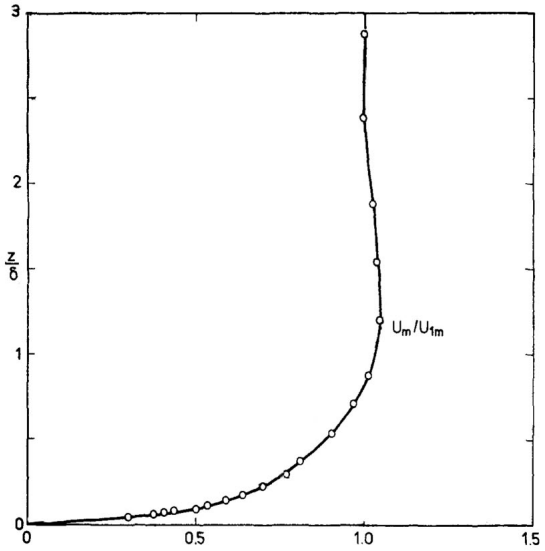

Figure 4.6: Dimensionless velocity in over a rough wall for an oscillatory boundary layer by Jonsson (1980)

The laminar boundary layer thickness δ can be determined by:

$$\delta_{laminar} = \sqrt{\frac{\pi}{4}} \cdot \sqrt{\nu \cdot T}. \tag{4.3}$$

In this study the wave periods varied from 1.50 - 2.53 s and therefore the laminar boundary layer thickness would have varied from 1.24 - 1.61 mm respectively, which would mean that the velocity at 3.5 mm above the bed is equal to the free stream velocity.

Since some turbulence was observed during the measurements, the boundary layer for turbulent oscillating flow is determined using:

$$\delta_{turbulent} \approx 0.072(a_{1m}^3 \cdot k)^{1/4}, \tag{4.4}$$

where a_{1m} is the free stream particle amplitude:

$$a_{1m} = \frac{U_{1m}}{\omega} = \frac{0.8}{\omega} \tag{4.5}$$

and k is the Nikuradse roughness, which is estimated to be $0.5D_{n50}$. The value for U_{1m} is taken as 0.8 m/s, as this is a typical velocity observed during the experiments. ω is determined with the previously mentioned wave periods, varying from 1.50 - 2.53 s. This yields a turbulent boundary layer thickness of about 10 mm, meaning that the point of interest lies within the boundary layer. At a height of 3.5 mm above the bed the velocity then is roughly 80% of the free stream velocity, as can be deducted from figure 4.6 ($\frac{z}{\delta} = 0.35$).

Since it is hard to determine the velocity using the theory of Jonsson (1980), another approach is to look at studies which have measured velocities at breakwater toes at multiple heights. The research of Nammuni-Krohn (2009) is such a study, where the velocity was measured at 1, 3, and 5 cm above the bed. From her measurements it can be seen that there are hardly any deviations between the velocities in vertical direction. It can be seen, however, that the velocities at 1 cm from the bed are generally a little higher than those at 3 and 5 cm. Therefore it is assumed that at 1 cm the velocity is in the start of the 'bulge' of figure 4.6. When plotting this point together with the velocity profile by Jonsson, it can be argued that the velocity at 3.5 mm ($u_{0.15}$) above the stones is about $0.9 \cdot U_{1m}$, as can be seen in figure 4.7. Therefore the measured velocities at 5 cm, which can be considered as the free stream velocity, are multiplied by 0.9 to approximate the velocity at 3.5 mm above the bed. From this point on, if the velocity u is mentioned, this is the velocity at 3.5 mm above the stones.

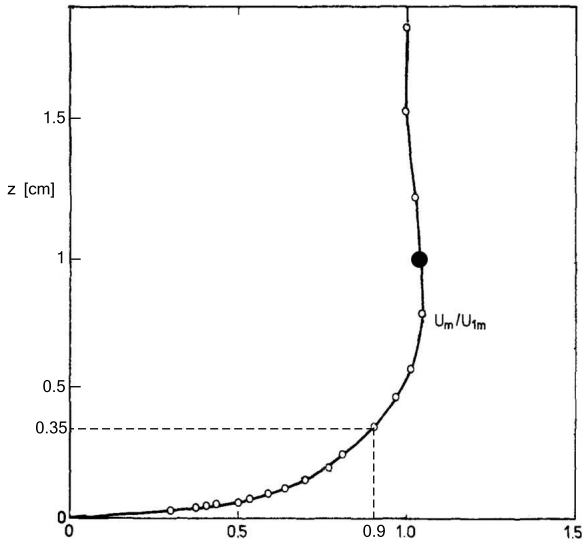

Figure 4.7: Velocity profile of Jonsson (1980) combined with observations from the study of Nammuni-Krohn (2009) to approximate the velocity at 3.5 mm above the bed

It is acknowledged that there is an uncertainty in the determination of the velocity just above the stones. It is, however, assumed that the velocity at 3.5 mm is within the boundary layer, but not so close to the bed that the velocity is greatly diminished. It is reasonable to assume that the velocity at 3.5 mm is between 60% and 100% of the free stream velocity. If the velocity at 3.5 mm would turn out to be 60% of the free stream velocity, this means that the computed drag forces in this study will be bigger that they should have been. These effects will be analysed in the quantification of the forces in section 5.1.1.

4.3 Pressure data

The most important measurements of this experiment were the pressure measurements underneath the stones, since this was data that has not been acquired by earlier studies. The pressures were measured under the seven target stones, but only two of those stones have shown movement during the test conditions: stone B and stone F. The pressure differences, or deviations, from the starting position underneath stone F during test R045 are presented in figure 4.8.

The measured deviations appear to be in line with expectation that the pressure deviation should be about the same as the wave height. The pressure deviation for stone F appears to have a amplitude of 5 cm, in a test where a wave height of 16 cm was asked from the wave generator. Section 4.1 made clear that the actual wave heights are lower than the asked wave heights, so these results are very plausible.

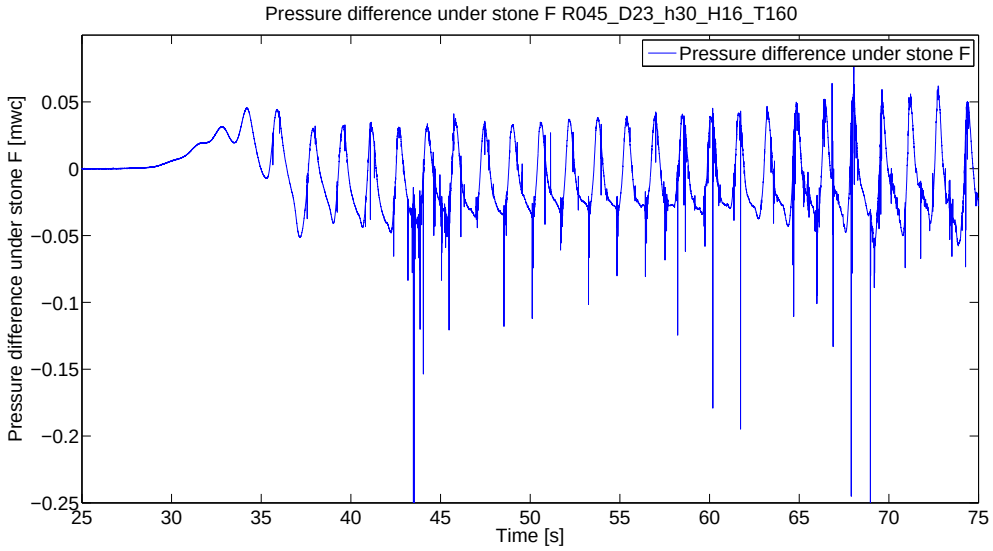

Figure 4.8: Unfiltered pressure signal under stone F during R045

Another important observation is the occurrence of spikes in the pressure data set. These spikes are not instrument noise, as might be expected, but they are the result of the stones that are rocking in their holes and thereby tapping the pressure sensors. Figure 4.9 shows the pressure deviations underneath stone F. During this test in still water, the stone was moved by hand to simulate the rocking behaviour during the tests with waves. It can be seen that pressure deviations are in the same order of magnitude as the spikes in figure 4.8, so it can be safely assumed that the spikes originate from the rocking of stones. This can be verified by the video of the tests, during the periods that the spikes are present the stone is rocking. Moreover in figure 4.8 the spikes are no longer present after the stone is out of its cavity.

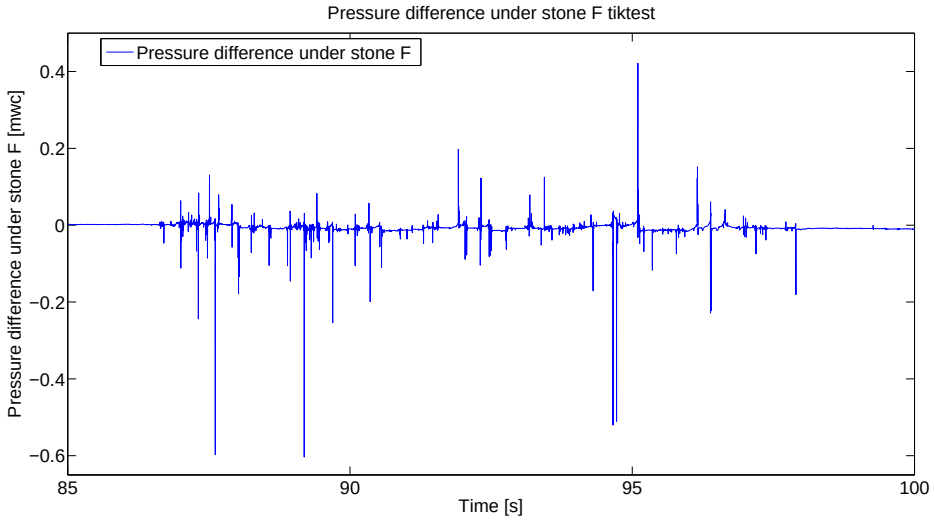

Figure 4.9: Pressure signal due to stone rocking

Since it is established that the spikes in the dataset originate from the rocking of the stones, some filtering is applied to make the graphs more readable. To this purpose a moving average filter is implemented, which averages over a period of 0.1 s (five data points). A longer filter period would result in too much smoothing of the peaks, thus altering the data in an undesirable way. The result of the filter is shown in figure 4.10. It can be seen that the 'noise' has been drastically reduced, however there are still some spikes present. As mentioned before, these spikes can be eliminated by applying a harsher filter, but this would result in too much alteration of real data.

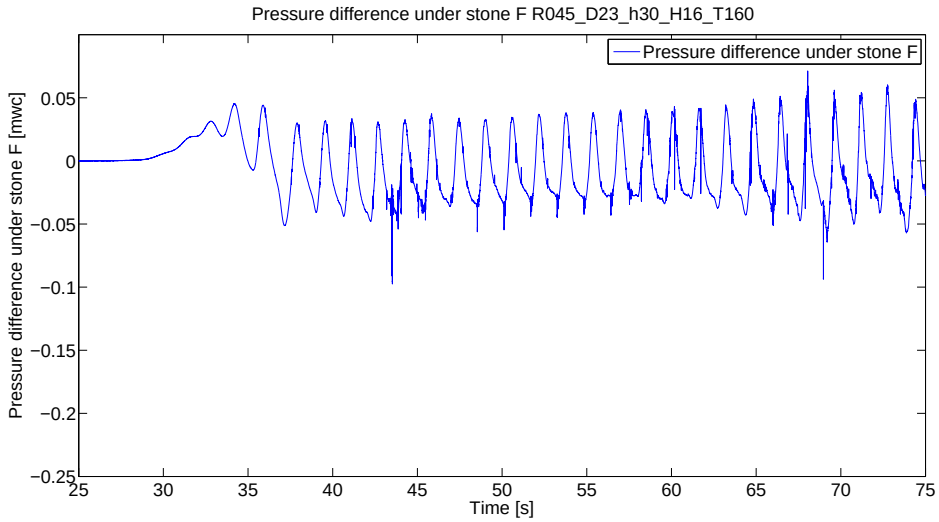

Figure 4.10: Filtered pressure signal under stone F during R045

With the pressures under the stone measured, the last parameter that needs to be determined is the pressure above the stone. These pressures are calculated using Bernoulli's principle, using the water level and flow velocity above the toe:

$$p_{above} = wl_{toe} + \frac{u^2}{2g}. \tag{4.6}$$

The water level is measured in the middle of the toe and the velocity at two points near stone B and F. The exact pressure above each stone is therefore not exactly known. During the tests, however, the spatial difference along the transverse axis was observed to be little, rendering this an acceptable approximation. For stones A, B, C and D the velocity from EMS at B is used, and for stones E, F and G the EMS at F.

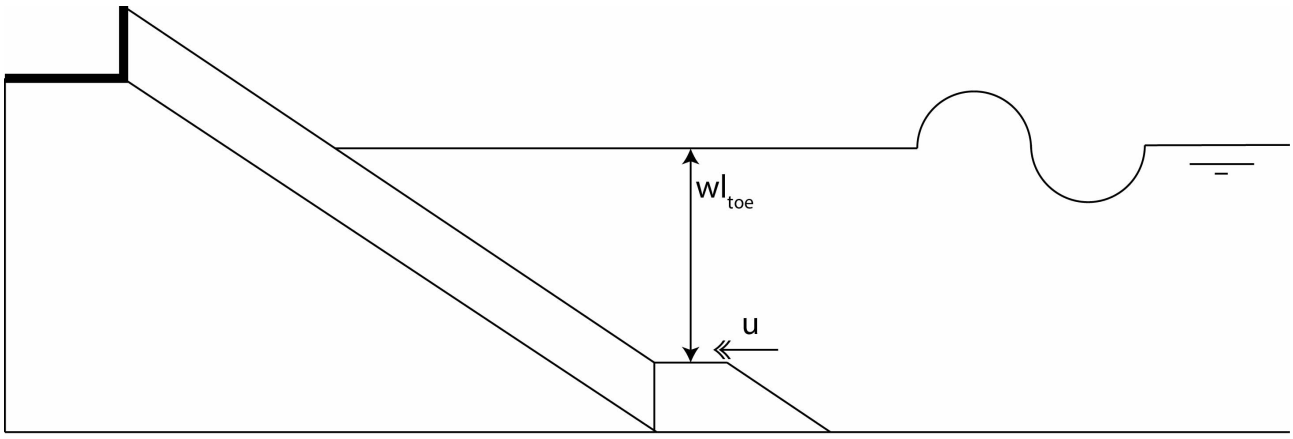

Figure 4.11: Definition sketch for the computation of the pressure above the stones

Chapter 5

Analysis of the experiments

The data obtained during the measurement was intended to verify the hypothesis that the point of incipient motion of stones in breakwater toes could be predicted by the moment criterion presented in chapter 2.2. This chapter presents the analysis of the experiment data and the observations that were made during the measurements.

5.1 Forces and moments on the stone

In chapter 2.2 the proposed model for toe stone stability was introduced. This section aims to verify this model and quantify the forces, using the local hydraulic parameters that were determined in section 4. This is done for test R045, since this was a test in which a lot of movement occurred. In section 5.3 a more detailed description of the tests will be given, also by using the video material that was obtained during the tests.

5.1.1 Quantified forces on the stone

Weight of the stone

The first force that was introduced was the stabilising underwater weight force F_W. Since the weight of the individual stones is known, the underwater weight can be determined by equation 5.1 rather than by the more generic equation 2.14.

$$F_W = (m_{stone} - D_{n50}^3 \cdot \rho_w) \cdot g. \tag{5.1}$$

Lift force

The lift force was assumed to be the determining force for the stability of the the toe stones, which could be calculated with the pressures. The pressures were previously shown in mwc, but will be shown in the SI-unit N/m^2 from now on. The lift force F_L can then be computed with:

$$F_L = (p_{under} - p_{above}) \cdot D_{n50}^2. \tag{5.2}$$

For stone B during measurement R045, this results in the forces as presented in figure 5.1. The maximum lift forces on stone B range from roughly 0.1 - 0.2 N. In figure 5.2 the pressures under and above the stone are presented. It can be seen that the pressure above the stone has a higher amplitude than the pressure under the stone. From the plot it becomes clear, that when the wave crest is above the toe, the net force is directed downwards and during the wave trough the lift force becomes positive, destabilising the stone. The lift force has at its maximum in between the wave trough and crest, as can be seen in figure 5.3. This can also be deducted from figure 5.4, where the difference between the pressure under the stone (blue) and above the stone (red) is plotted.

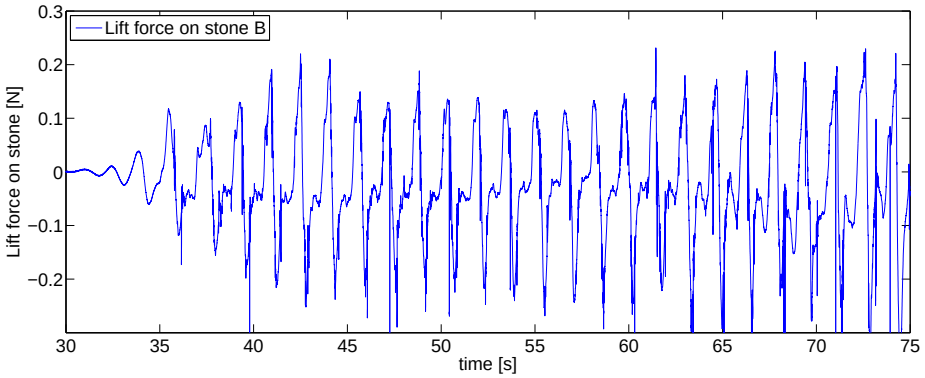

Figure 5.1: Computed lift force on stone B during R045

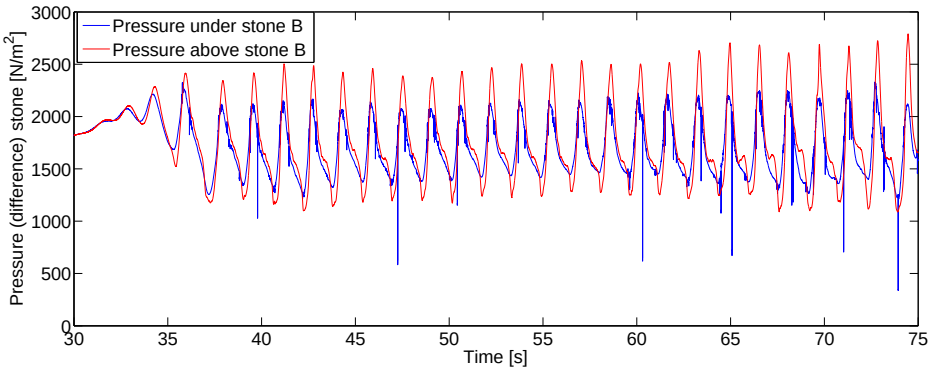

Figure 5.2: Pressure under and above stone B during R045

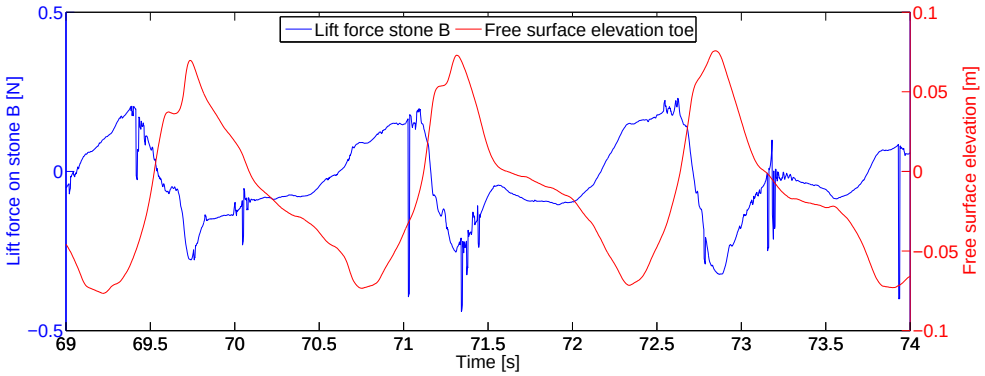

Figure 5.3: Detail of computed lift force and water level difference at stone B during R045

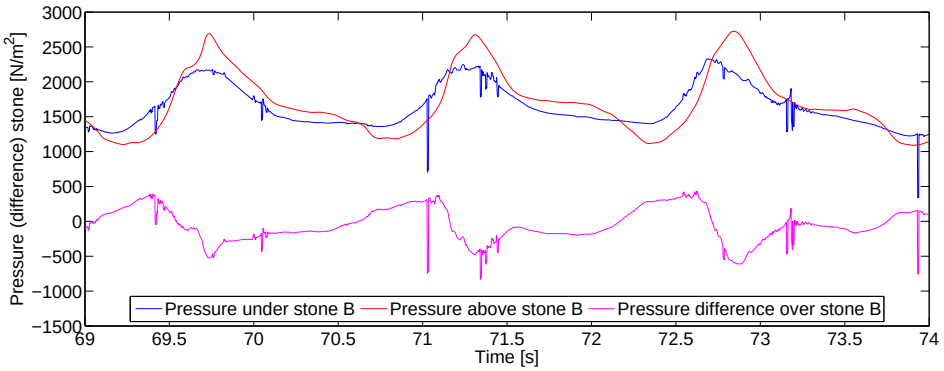

Figure 5.4: Detail of pressure under and above stone B during R045

An interesting phenomenon is the difference in lift force between the stones on the edge of the toe (B, D, F) and the stones on the middle of the toe (A, C, E, G). The pressure differences and thus the lift forces of the stones near the edge are larger than the lift forces in the middle of the toe. Figures 5.5 and 5.6 show the lift forces on stone A, B, C, D and E, F, G respectively and it can be seen that stone B and D are subjected to larger lift forces than A and C. The same holds for stone F compared to stones E and G. Since all the forces start at the same point and there is no zero-drift, it can thus be argued that the lift force amplitudes for the stones on the edge of the toe are larger than those in the middle of the toe.

The origin of this difference must lie in the pressures under the stones, since the pressures above stones A, B, C and D (and E, F, G) are computed using the same parameters (EMS B and EMS F respectively, combined with the wave gauge at the toe). The pressures under stones B, D and F therefore must have higher peaks than stones A, C, E and G. An explanation for this phenomenon is that near the edge of the toe the water can easier flow into the toe (i.e. between the stones of the toe) than it can in the middle of the toe. This causes a bigger pressure built-up under the stones near the edge of the toe, resulting in a higher lift force. This finding may explain why only stone B and F moved out of their cavities during the measurements. It was observed that stone D was also rocking heavily, but was obstructed by the stones around it and therefore did not move out.

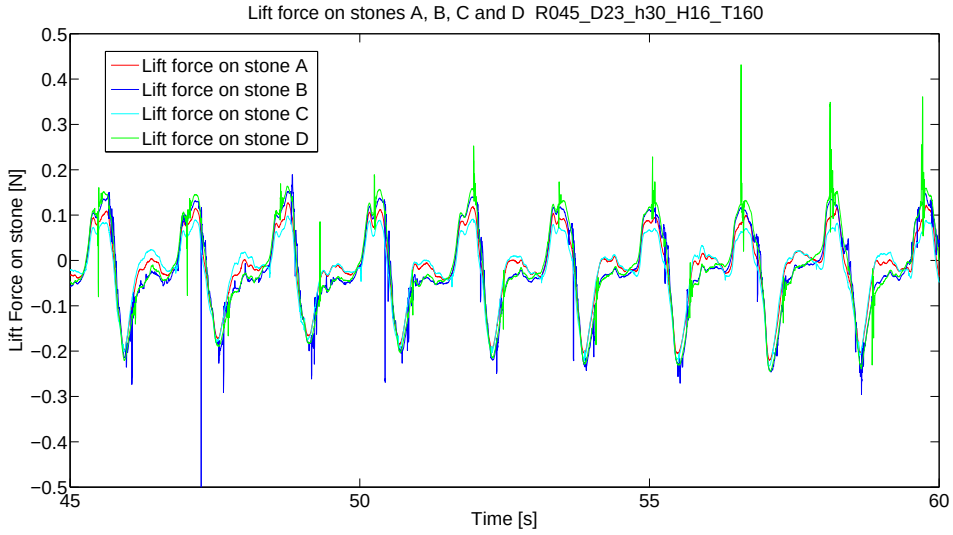

Figure 5.5: Computed lift force on stone A, B, C and D during R045

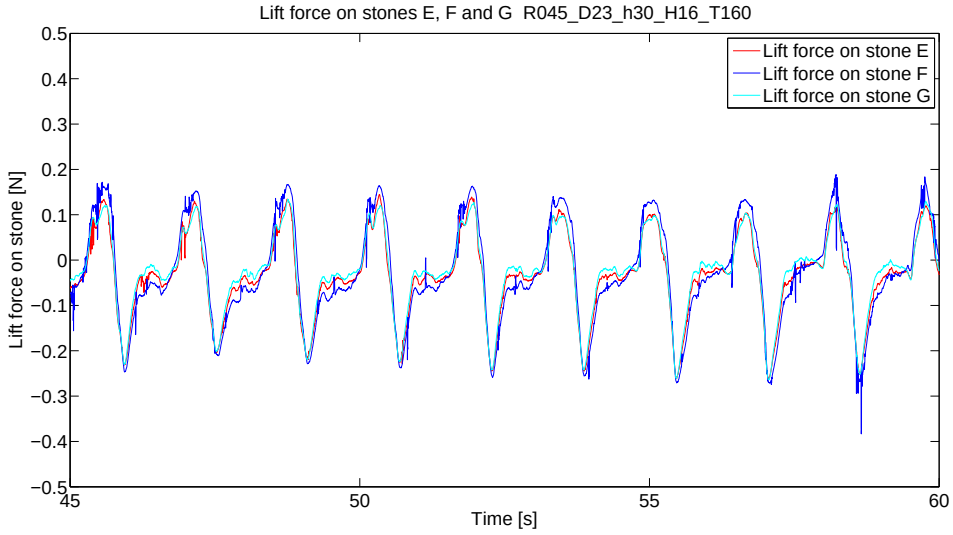

Figure 5.6: Computed lift force on stone E, F and G during R045

Drag force

The drag force is to be determined using:

$$F_D = \frac{1}{2} C_D \cdot \rho_w \cdot A_f \cdot u \cdot |u|. \tag{5.3}$$

Since the flow velocity is the only parameter involved in the calculation of the drag force, they are in phase with each other. This also means that it is in phase with the waves. The maximum drag thus occurs as the wave crest is above the toe, and the velocity is at its top.

The velocity u is the velocity at $0.15 \cdot D_{n50}$, which was approximated in section 4.2 as 0.9 times the free stream velocity that was measured. Hofland (2005) concluded that the drag coefficient at $0.15 \cdot D_{n50}$ above the bed was rather constant for different protrusion values, ranging from 0.23-0.3. The assumed value of $C_D \approx 0.23$ is corresponding with stones which have a low protrusion. The stones in this study, however, had very low protrusion, so the actual drag force might be lower than the drag force that is calculated. The frontal area A_f differs from stone to stone. For each target stone the frontal area is aprroximated as a percentage of the nominal stone diameter (for example $0.5 \cdot D_{n50}^2$ for stone B). The values for the other stones can be found in table A.2. Using these values, the drag force for stone B during R045 is determined and presented in figure 5.7a. With maximum forces of about 0.01 N, the drag force is about 10 to 20 times lower than the lift force.

As was discussed in section 4.2, there is some uncertainty in the determination of the flow velocity just above the

toe. In the current analysis it is assumed that this velocity is 90% of the free stream velocity ($u = 0.9 \cdot u_{1m}$). It was assumed that the velocity would be no lower than $u = 0.6 \cdot u_{1m}$ and therefore the drag force is also computed with this value and presented in figure 5.7b. The drag force is 2-3 times lower than the force computed with $u = 0.9 \cdot u_{1m}$. However, since the drag force is already relatively small when compared to the lift force, this has a minor effect on the moment of force that acts on the stones.

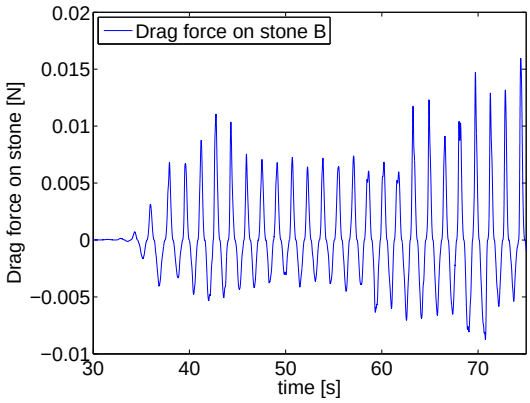

(a) Computed drag force on stone B during R045 with $u = 0.9 \cdot u_{1m}$

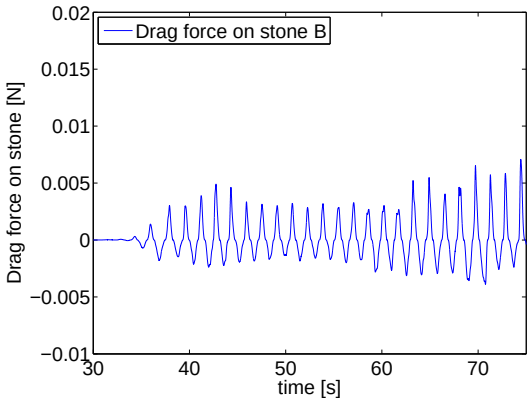

(b) Computed drag force on stone B during R045 with $u = 0.6 \cdot u_{1m}$

Figure 5.7: Computed drag force on stone B during R045

Shear force

In section 2.2.1 it was stated that the shear force will be computed using:

$$F_s = C_f \cdot \frac{1}{2} \cdot \rho_w \cdot u \cdot |u| \cdot A_s, \tag{5.4}$$

in which

$$C_f = \frac{0.074}{Re_x^{0.2}} \tag{5.5}$$

and the particle Reynolds number is:

$$Re_x = \frac{u \cdot D_{n50}}{\nu}. \tag{5.6}$$

From the initial data analysis of the velocities it is known that the order of magnitude of the velocity is about 1 m/s, which yields to an approximate value of $C_f \approx 0.01$.

As was stated in section 2.2.1, the theory for the computation of the shear force has its origins in aerodynamics and is therefore not very representative for the use in breakwater toes. A more suitable computation however could not be found.

Using the above mentioned values, an approximation of the shear force is made and shown in figure 5.8. With maximum values of only 0.002 N the shear force is so small compared to the lift and drag force, that it will be neglected in the analysis from now on.

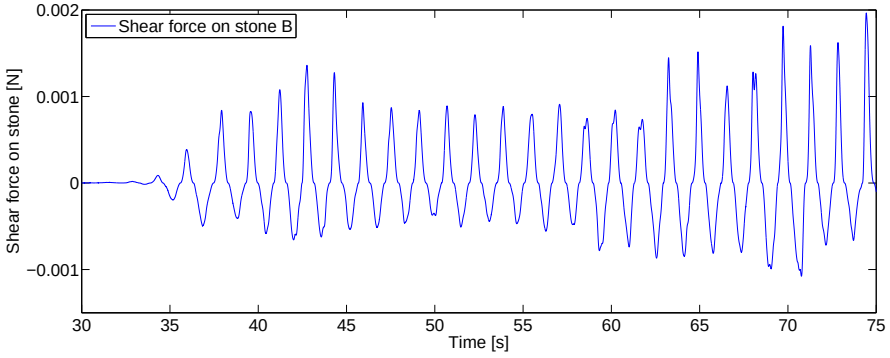

Figure 5.8: Computed shear force on stone B during R045

Turbulence induced forces

As was discussed in section section 2.2.1, the determination of turbulence induced forces is outside the scope of this study. Moreover, since the measurements of the ADV had a frequency that was too low to inspect the turbulent properties of the flow, it is not possible estimate the influence.

Hofland (2005) made an estimation of the magnitude of the turbulent forces and found that they were in the order of 0.01 N (for both the drag and the lift force). This estimation was performed for a particle size of 2 cm and a flow velocity of 2 m/s. The particle size is almost the same as the nominal diameter of the target stones in this study (2.3 cm), but the flow velocity is roughly 2 times higher than the highest measured flow velocity. Although the turbulence induced forces for this study will probably be lower, this is the best approximation that was found.

An increase of 0.01 N due of turbulent forces, does not have a very big influence on the lift force. In measurement R045 the highest lift forces are roughly 0.15 N, so the added turbulence does not have a big influence. This is different for the drag force, where the computed (quasi-steady) drag force is of the same order of magnitude as the turbulent drag force. However, as was noted in the discussion of the drag force earlier in this section, the total drag force is still small compared to the lift force. Therefore the influence on the computation of the moment of force is relatively small.

Taking this all in consideration, it seems reasonable to disregard the turbulence induced forces for the purpose of this study. It should, however, be noted that the actual forces (and therefore the moment of force) may be a little higher in reality.

5.1.2 Moment of force on a stone

With the forces known and the shear force neglected, the moment of force on the stone can be determined using the schematic representation of the forces in figure 5.9. The length of the two arms for the forces are measured for the seven target stones. The point around which the stone rotates is determined by looking at the video footage that was obtained during the tests. The lift force is acting on the center of gravity, together with the weight of the stone. The arm of the drag force is approximated by looking at the protrusion of the stones during the tests. As the stones were replaced in the same position and orientation after each test, these values are the same for all the performed tests. The properties of each of the target stones are presented in appendix A.2.

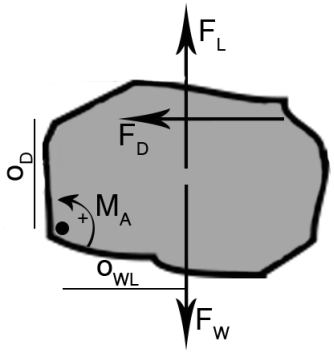

Figure 5.9: Moment of force on a stone in a breakwater toe

Using the stone properties and the forces that have been calculated, the moment of force on the stone (in this case stone B) can be determined by applying equation 5.7. The resulting graph is presented in figure 5.11.

$$M_B = F_L \cdot o_{wl} - F_W \cdot o_{wl} + F_D \cdot o_d. \tag{5.7}$$

The vertical red dashed line in figure 5.11 is the point the stone was deposited landwards (towards the breakwater). It can be seen that this happens just after the point that the moment of force becomes positive. During the period, depicted in figure 5.11, the moment of force on stone B is often close to crossing the critical value. In a few occasions positive moments were computed, even though no stone movement occurred. However, from the video it can be seen that at these points the stone was rocking heavily.

Note: from this point on the moment of force is simply denoted as moment for brevity's sake

Figure 5.10: Initial position and orientation of the target stones

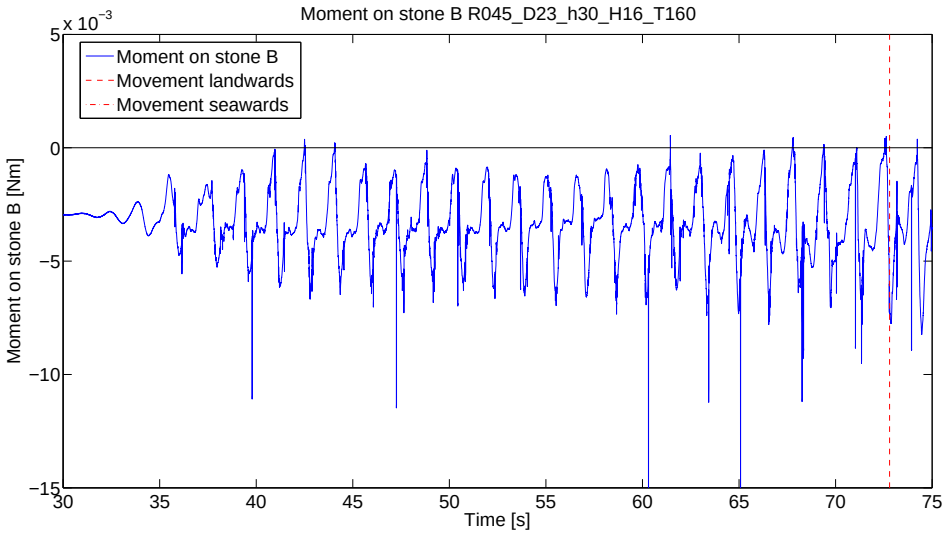

Figure 5.11: Computed moment of force on stone B during R045

5.2 Velocity criterion of Stephan Baart

In his study Baart (2008) also developed a criterion which can be used to determine movement of stones in breakwater toes as was discussed in 2.1.4. His criterion states that there is a critical flow velocity above which movement of stones will occur. This criterion reads:

$$(\hat{u}_{bc})^{2.5} = 0.46\sqrt{T} \cdot ((\Delta - C_{PF} \cdot i)g)^{1.5} \cdot D_{n50}, \tag{5.8}$$

where $C_{PF} = 0.4$ and i is the maximum hydraulic gradient between the highest "wet point" on the breakwater and the toe given by:

$$i_{max} = \frac{\Delta h}{\Delta x} = \frac{H/2 + R_u}{L_{TA} + R_u/\tan\alpha}. \tag{5.9}$$

5.2.1 Computation of the critical velocity

To test the performance of the Baart criterion, it will be applied on the experiments that were performed in this study. This means the parameters of equation 5.8 need to be determined for the experiments. This section

will show the calculation of the critical velocity for measurement R045 ($h_m = 0.30m$, $H = 0.16m$, $T = 1.60s$, $L = 2.52m$).

First, the Iribarren number ξ is determined by dividing the slope of the breakwater by the square-root of the wave steepness or:

$$\xi = \frac{\tan\alpha}{\sqrt{H/L_0}} = \frac{1.5}{\sqrt{0.16/2.52}} = 5.95. \tag{5.10}$$

The run-up can then be determined by:

$$R_u = 0.5 \cdot H \cdot \xi = 0.5 \cdot 0.16 \cdot 5.95 = 0.48m \tag{5.11}$$

and L_{TA} by

$$L_{TA} = 0.06 + (h_m - h_t) \cdot \tan\alpha = 0.06 + (0.3 - 0.12) \cdot 1.5 = 0.33m, \tag{5.12}$$

in which 0.06 m is the horizontal distance from the middle of the toe to the breakwater slope. Now the maximal hydraulic gradient over the stones, as defined by Baart, can be computed as:

$$i_{max} = \frac{H/2 + R_u}{L_{TA} + R_u/\tan\alpha}, = 0.86 \tag{5.13}$$

which leads to a critical velocity of:

$$\hat{u}_{bc} = (0.46\sqrt{T} \cdot ((\Delta - C_{PF} \cdot i)g)^{1.5} \cdot D_{n50})^{1/2.5} = 0.83m/s. \tag{5.14}$$

Figure 5.12 shows this critical velocity together with the flow velocities above the toe during R045.

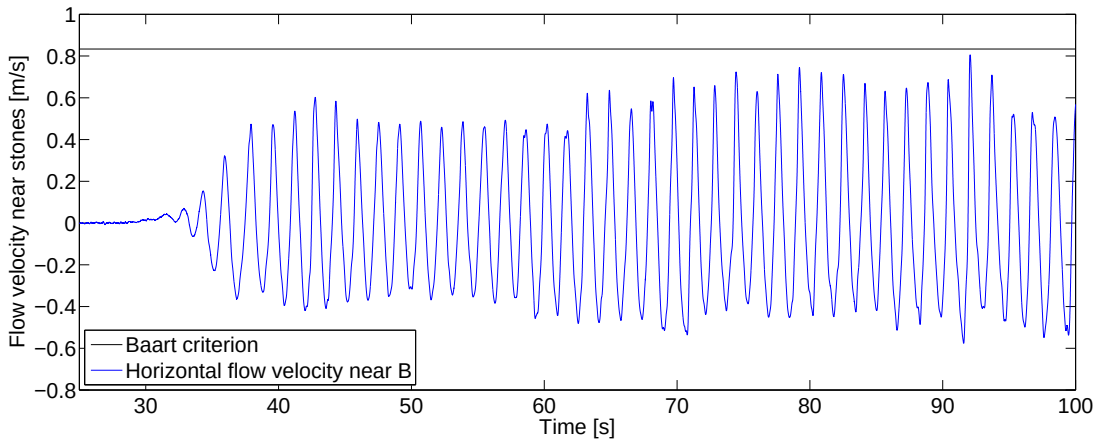

Figure 5.12: Horizontal flow velocity record just above the toe near stone B during R045

5.3 Detailed experiment analysis

This section will give a detailed description of several characteristic tests. In this description the links between the data and the video material will be pointed out, along with remarks on the local hydraulic parameters around the point of incipient motion. Also, a qualitative description of the test will be given, which tries to explain what mechanisms cause a stone to move. It should be noted that the interpretations in this section rely heavily on the videos of the measurements and the experience that was gained during the measurements. Some distinctive patterns were observed during the measurements, which are hard to express in words. It is therefore very useful for the reader to watch the videos, so that the results can be interpreted better. The videos and the dataset can be acquired through *this link*. (doi:10.4121/uuid:4eb8d0ae-53e6-4914-b241-7b53a04169ea)

Even though a lot of measurements with different wave parameters were performed, some repeating behaviour has been observed. This section will therefore zoom in on a few measurements and show this characteristic behaviour by using the measurement videos as well as the data obtained during those measurements. Since only stone B and F moved during the experiments, the focus lies on these stones. For additional information of the measurements, the reader is referred to the experiment logs in appendix D.

5.3.1 R041

Measurement R041 is chosen as example, because it had only one movement seawards. During the majority of the measurements the first movement, if any, was directed landwards. Moreover, the moment criterion is defined for landwards movement, so it is interesting to check how it performs for seawards movement.

Table 5.1: Hydraulic properties and movement during R041

Measurement	$H[m]$	$h_m[m]$	$s[-]$	$T[s]$	Movement B [s]	Movement F [s]
R041	0.16	0.35	0.02	2.26	-	66.300 sw

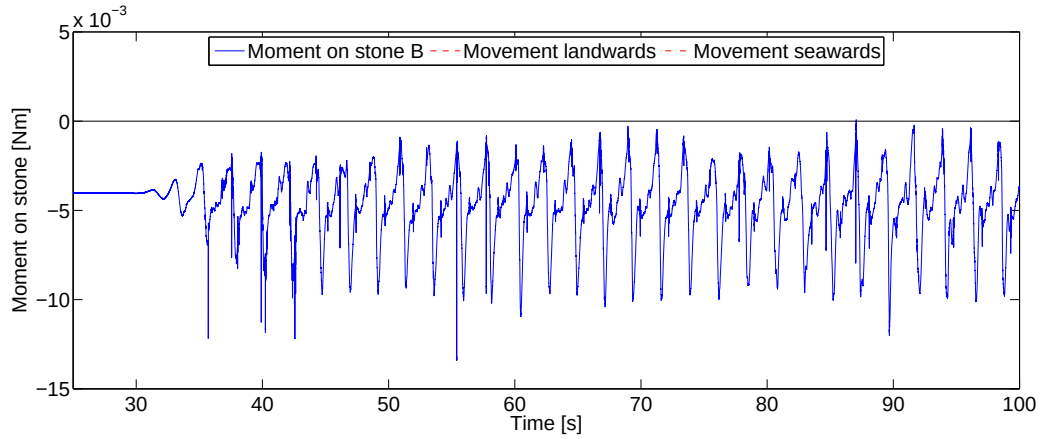

(a) Computed moment on stone B during R041

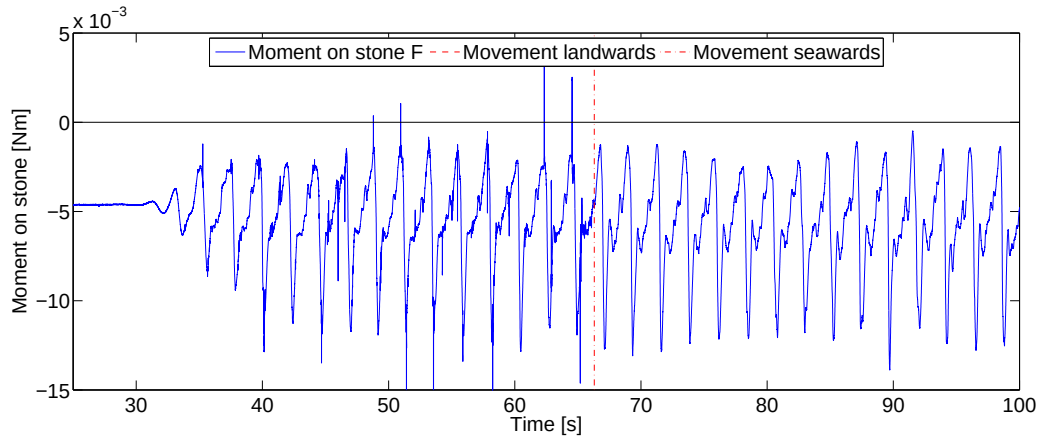

(b) Computed moment on stone F during R041

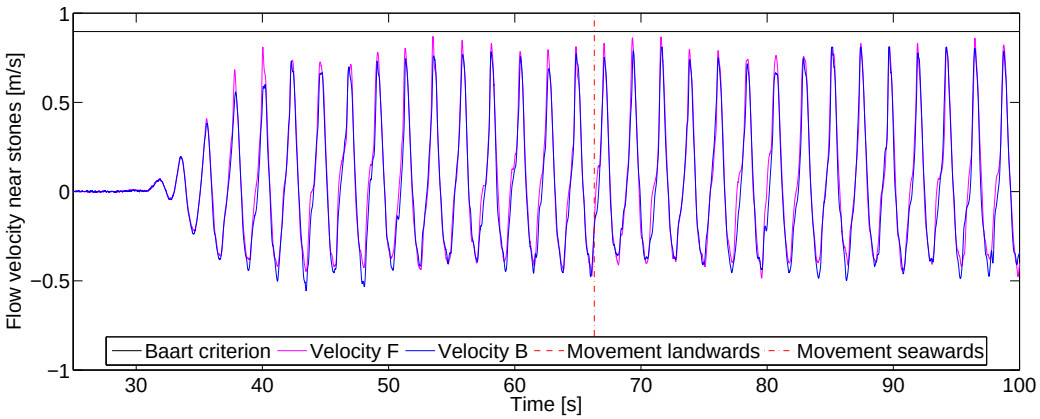

(c) Velocity near the stones during R041

Figure 5.13: Moment and Baart criterion during R041

From the moment graphs it can be observed that the computed moment on the stone never surpasses the zero line (with the exception of the spikes). It therefore seems that the moment criterion does not work well in this case. The Baart criterion seems to perform a little better here, although the peaks do not pass the critical value. From figure 5.14b it can be seen that the stone moves in between two velocity peaks that have not reached critical value and just after the return flow peak.

In the video of the measurement it can be seen that stone F is rocking slightly in its hole and just before it rolls out towards the sea, it was lifted landwards. It therefore seems that the stone is destabilised by the incoming flow and is more vulnerable for the return flow. This is because the stone gets slightly lifted, thus increasing the area affected by the flow velocity (drag force).

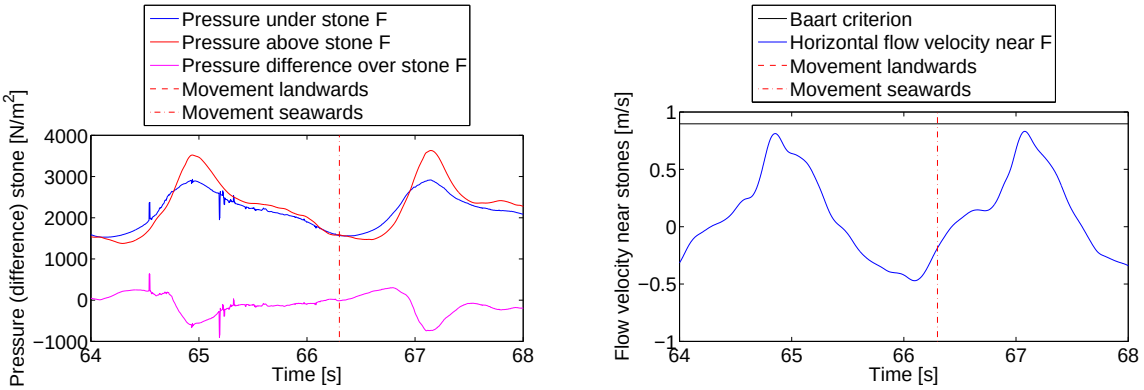

(a) Pressures near stone F during R041

(b) Velocity near stone F during R041

Figure 5.14: Local hydraulic conditions about the time of incipient motion

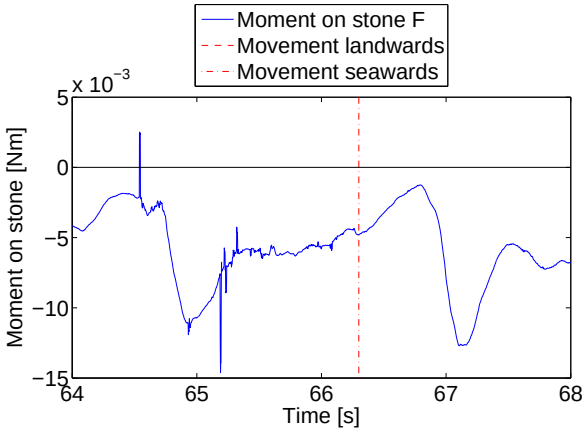

Figure 5.15: Moment on stone F about the time of incipient motion during R041

5.3.2 R044

During R044 no movement occurred, which also makes it an interesting experiment to look into. Figure 5.16 shows that the computed moments on the stones only sporadically come close to the criterion of zero, but the spikes in the moment figures indicate that the stones were rocking a bit. The Baart criterion also is not passed, although it came close a few times. During the experiments it was observed that the front stones were rocking slightly, but much less than in tests with higher waves, which is in line with the found moments and velocities.

Table 5.2: Hydraulic properties and movement during R044

Measurement	$H[m]$	$h_m[m]$	$s[-]$	$T[s]$	Movement B [s]	Movement F [s]
R044	0.14	0.30	0.02	2.12	-	-

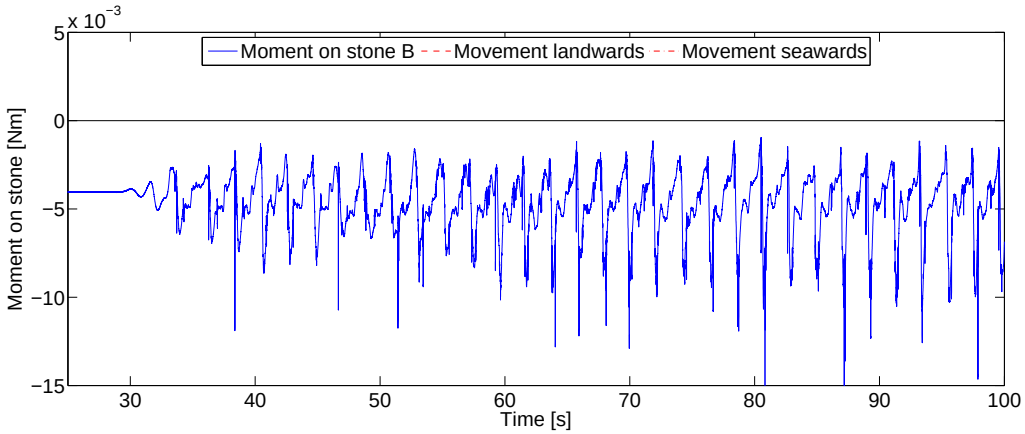

(a) Computed moment on stone B during R044

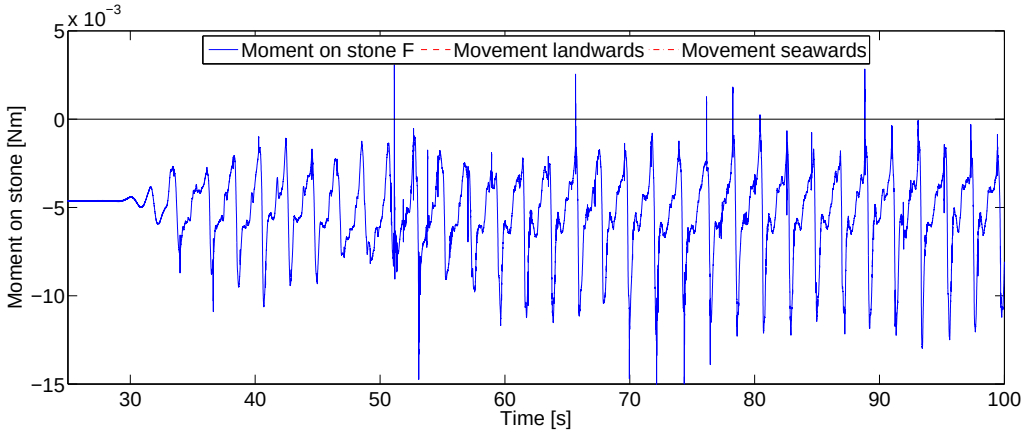

(b) Computed moment on stone F during R044

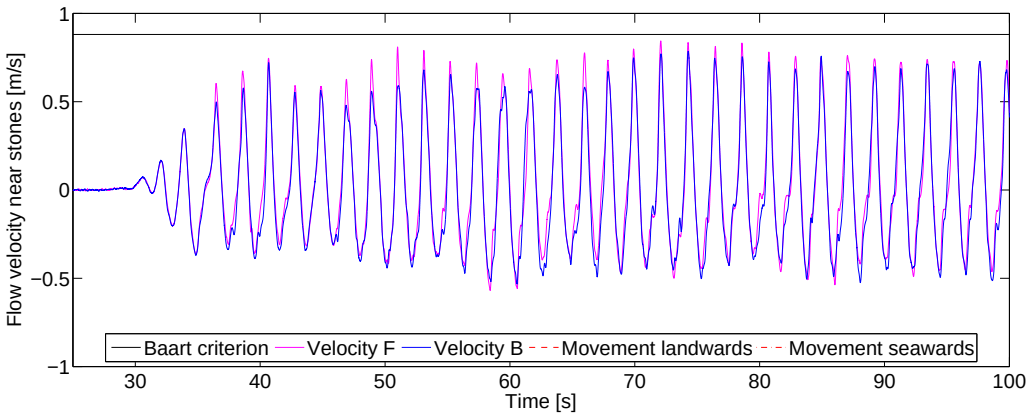

(c) Velocity near the stones during R044

Figure 5.16: Moment and Baart criterion during R044

5.3.3 R045

Measurement R045 was chosen, because a lot of movement occurred during this run. In table 5.3 the relevant information of this experiment is presented. Figure 5.17 gives an overview of the two criteria during this measurement. Figure 5.18 shows the local hydraulic conditions at the points of incipient motion.

Table 5.3: Hydraulic properties and movement during R045

Measurement	$H[m]$	$h_m[m]$	$s[-]$	$T[s]$	Movement B [s]	Movement F [s]
R045	0.16	0.30	0.04	1.60	72.800 lw 92.000 lw	42.840 lw 81.600 sw

Figures 5.17a and 5.17b show the moment graphs for R045. It can be seen that the moment criterion holds pretty well for stone B, at the time of movement the moment is positive. For stone F the performance is somewhat lower, as both movements occur at a time where the moment is less zero. The first (landwards) movement happens during a period were the moment peaks are close to zero, thereafter a period of lower moments appears. During this period the stone more or less stands in its cavity. About 60 seconds into the test, the stone starts to rock, which explains the spikes in 5.17b near that time. At 81.600 s the stone finally rolls out to the seaside and the spikes stop.

The Baart criterion shows mixed results. In figure 5.17c it can be seen that the velocity measured near F shows higher amplitudes than B and also passes the critical value, which is not the case for the velocity near B. The stones do, however, move out at the local maxima for the velocity.

Figure 5.18 shows the local conditions about the time of incipient motion for the four occurrences in this measurement. The first time stone F moves out at the point where the velocity is the highest, but still below the Baart criterion. In the video it can be seen that the stone lies relatively still and then suddenly moves out. Thereafter the stone moves back into its hole, but is positioned upright and therefore the drag has more influence on the stone. In between the first and second time stone F moves out, it is rocking in its hole until it finally is dragged out seawards. As can be seen in figure 5.18f the stone moves out even before the maximum return flow occurs.

Stone B corresponds pretty well with the moment criterion, at the point where the stone moves out the criterion is (just) met. Moreover, the criterion is quite precise for this measurement, meaning that the criterion is not surpassed if the stone did not move out. From figures 5.18d and 5.18h it can be seen that the stone moves out at the point where the velocity is the highest. It therefore seems that the mechanism that causes a stone to move landwards, consists of two steps: First there is the pressure peak, which greatly diminishes the stabilising weight force of the stone and quickly thereafter the incoming flow velocity moves the stone out of its cavity. At the first movement of B the velocity was much lower than the critical velocity and at the second movement just below it. The Baart criterion therefore does not seem to work very well here.

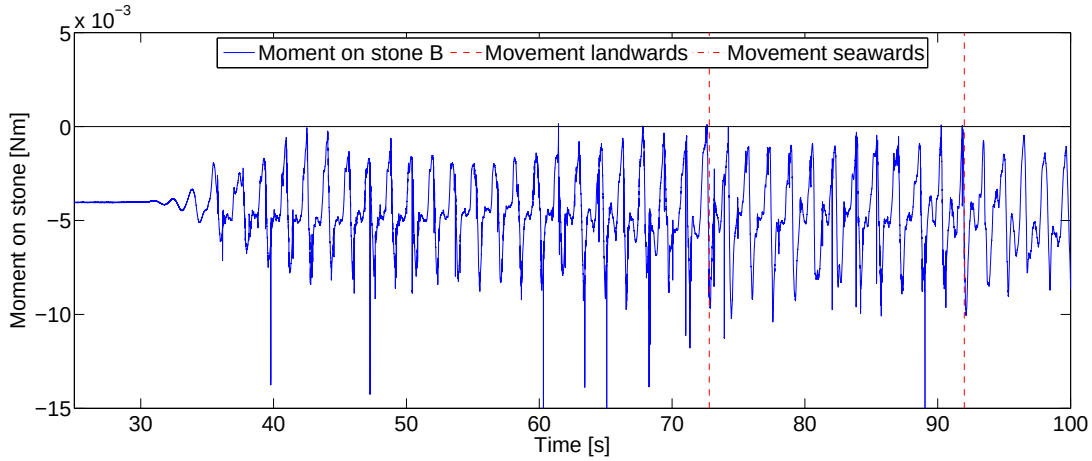

(a) Computed moment on stone B during R045

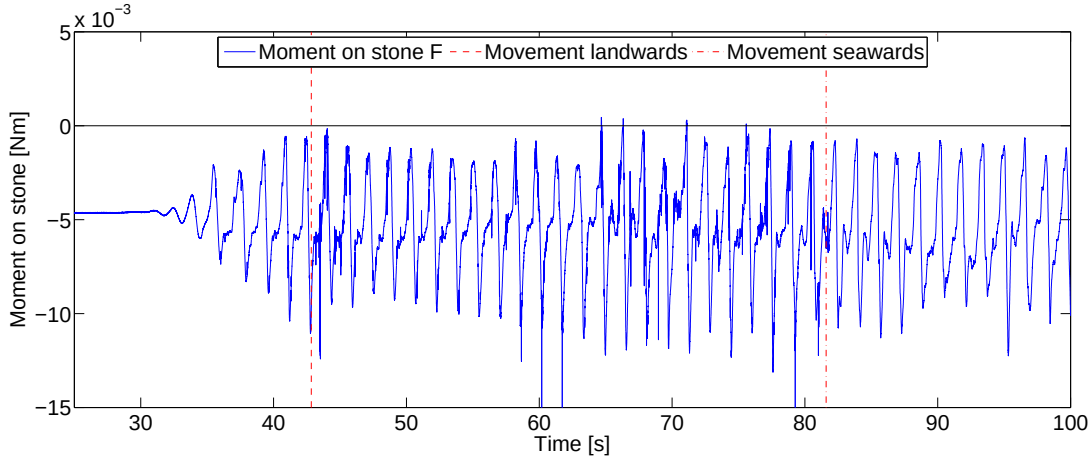

(b) Computed moment on stone F during R045

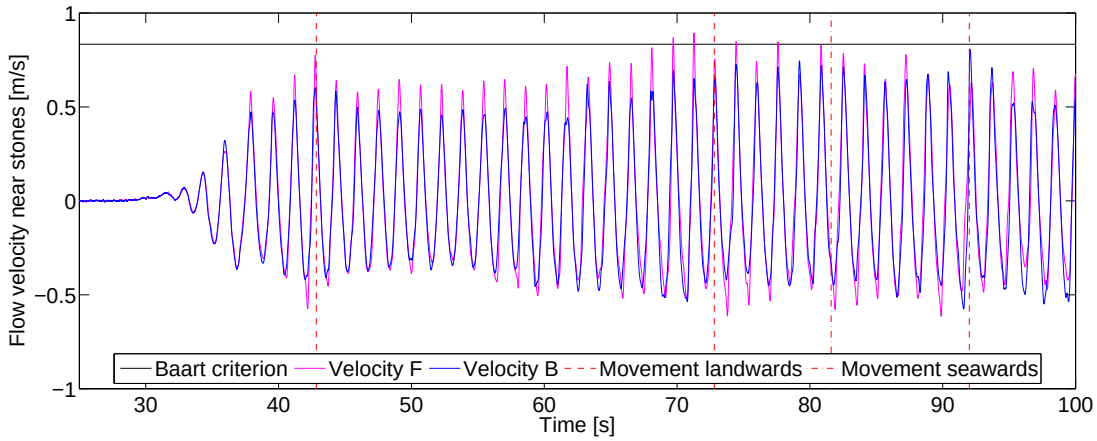

(c) Velocity near the stones during R045

Figure 5.17: Moment and Baart criterion during R045

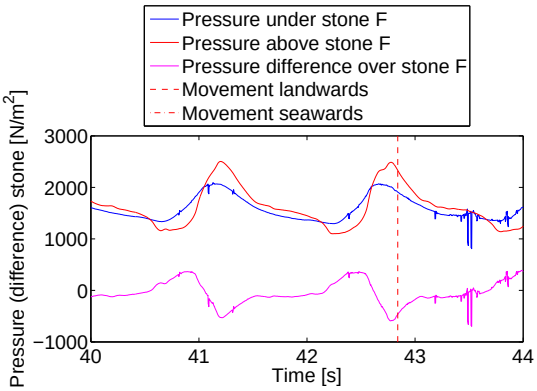

(a) *Pressures near stone F during R045*

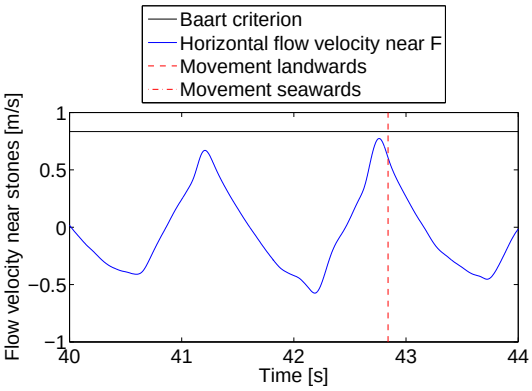

(b) *Velocity near stone F during R045*

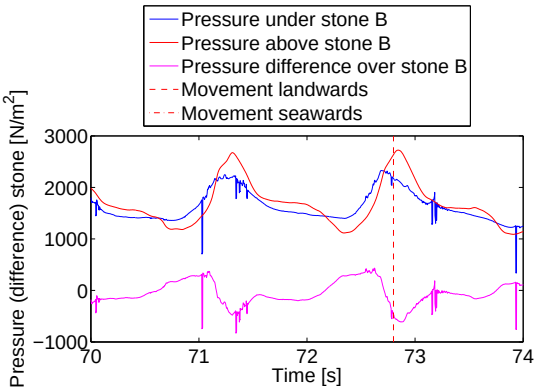

(c) *Pressures near stone B during R045*

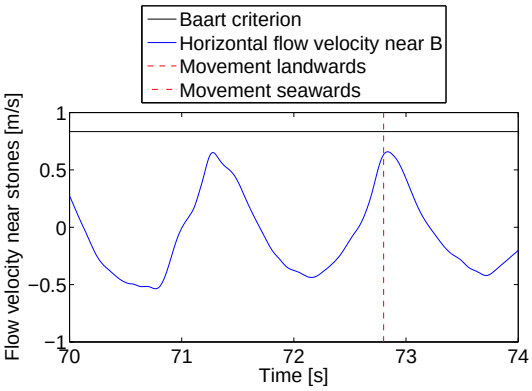

(d) *Velocity near stone B during R045*

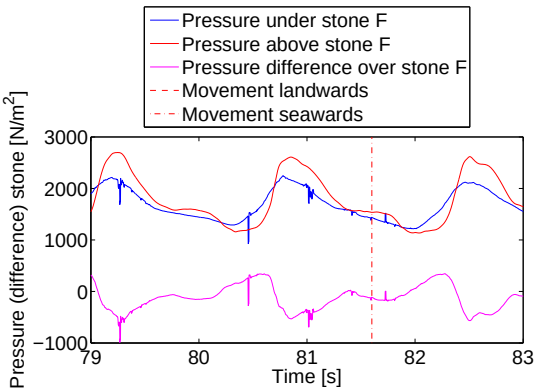

(e) *Pressures near stone F during R045*

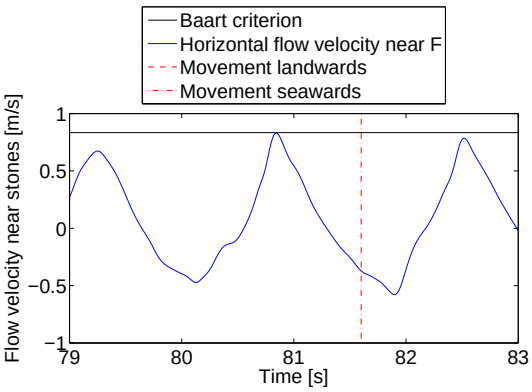

(f) *Velocity near stone F during R045*

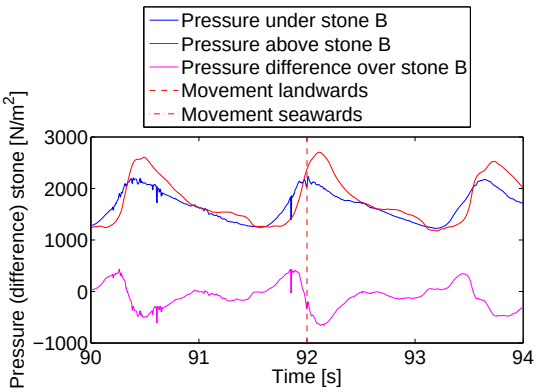

(g) *Pressures near stone B during R045*

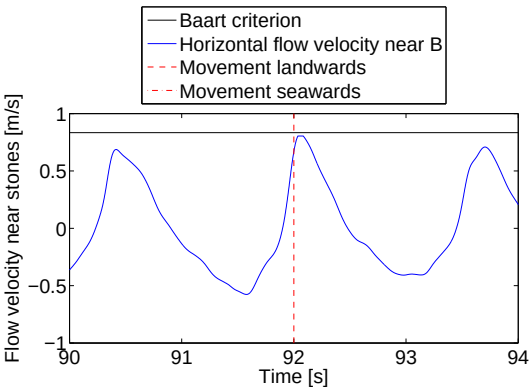

(h) *Velocity near stone B during R045*

Figure 5.18: Local hydraulic conditions about the time of incipient motion

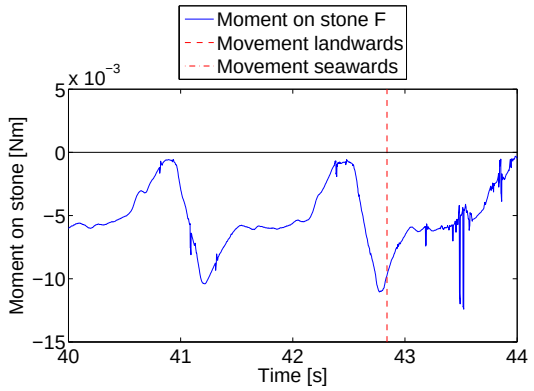

(a) Computed moment on stone F during R045

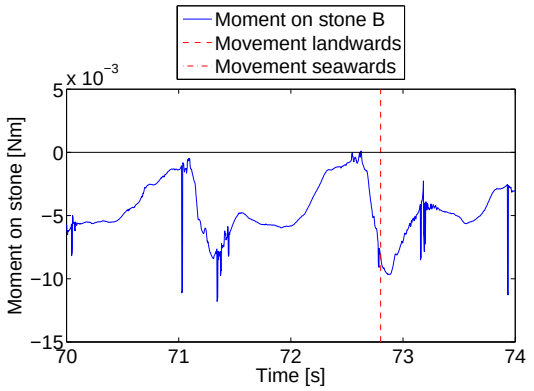

(b) Computed moment on stone B during R045

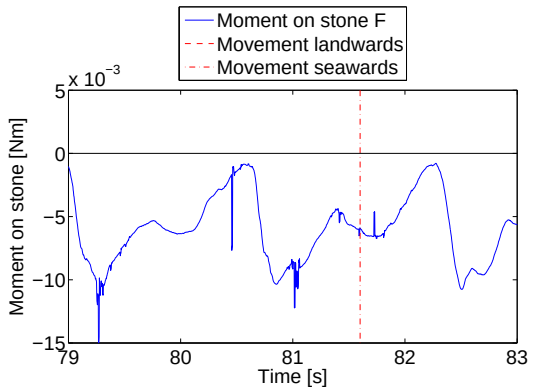

(c) Computed moment on stone F during R045

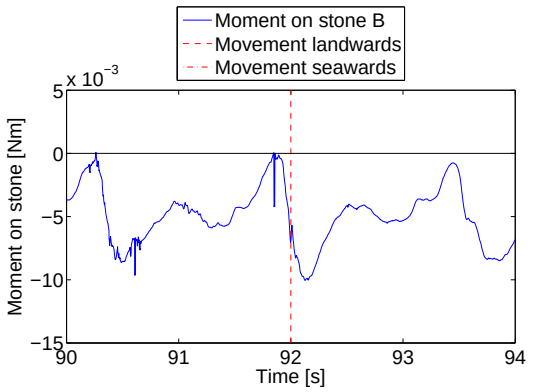

(d) Computed moment on stone B during R045

Figure 5.19: Computed moments on the stone about the time of incipient motion

5.3.4 R057

R057 is chosen because it is an experiment with one of the highest wave heights that was tested during the measurement campaign.

Table 5.4: Hydraulic properties and movement during R057

Measurement	$H[m]$	$h_m[m]$	$s[-]$	$T[s]$	Movement B [s]	Movement F [s]
R045	0.22	0.45	0.04	1.88	40.440 lw 97.760 sw	40.440 lw

From the moments overview in figure 5.21 it can be seen that the computed moments are close to or higher than the critical value from the start on. The Baart criterion is only surpassed once in the first 100 seconds. After only a few waves, both stones B and F roll out of their holes towards the breakwater. From figures 5.20a and 5.20b it can be seen that this happens only just after the moment criterion is surpassed.

After the stones have moved out, stone F is lying on top of the toe for some time, until it is dragged seawards after a few seconds. Stone B falls back in its cavity, but in a different position and appears to be stuck. After roughly a minute it is suddenly destabilised and tilts landwards, but eventually moves out seawards. In figure 5.21a it can be seen that prior to the second movement the moments on the stone are quite high compared to the period before. Interestingly enough the flow velocity near B is more or less the same or somewhat lower prior to the second movement. This indicates that the pressure difference over the stones was increased, while the flow velocities remained more or less the same.

Since the waves during this measurement were so high, some of the stones on the second row were also rocking quite a bit. Especially stone E was rocking heavily, whereas stone C showed no movement at all. The moment graphs in figure 5.23 confirm this, since the moment graph of stone C has a small amplitude and does not really come close to the critical value of zero. Stone E, however, shows very large amplitudes, indicating large pressure variations. Moreover the criterion is even surpassed a couple of times, even though the stone did not move out.

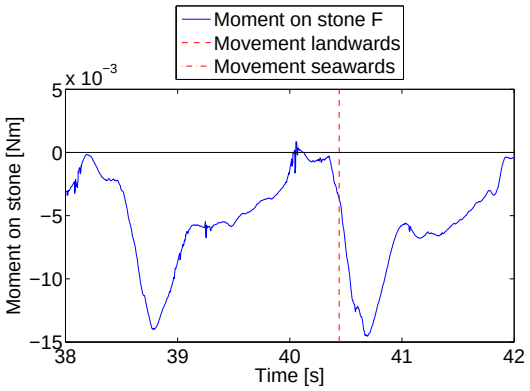

(a) Computed moment on stone F during R057

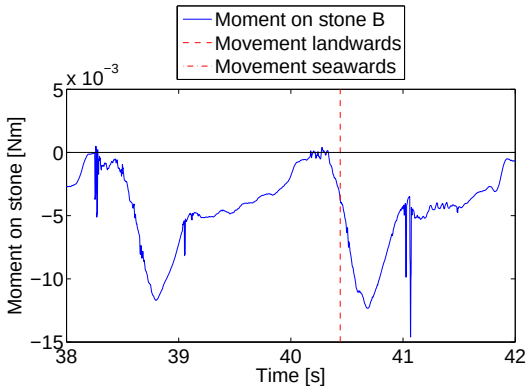

(b) Computed moment on stone B during R057

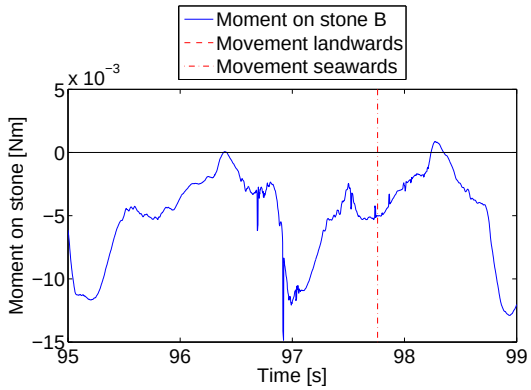

(c) Computed moment on stone B during R057

Figure 5.20: Computed moments on the stone about the time of incipient motion

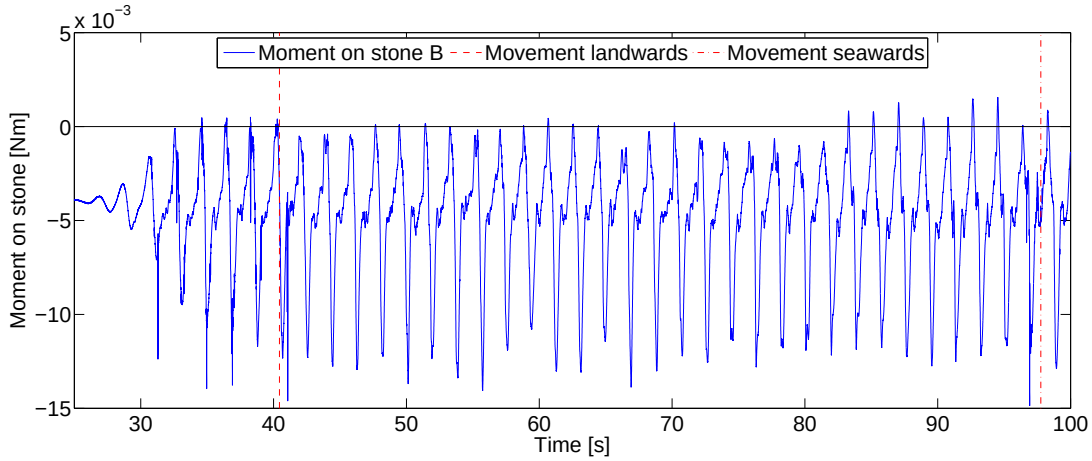

(a) Computed moment on stone B during R057

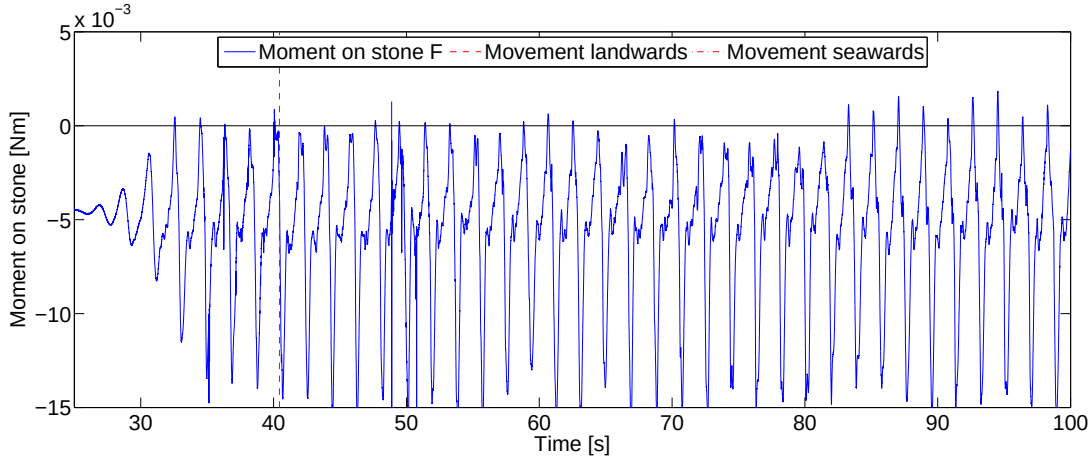

(b) Computed moment on stone F during R057

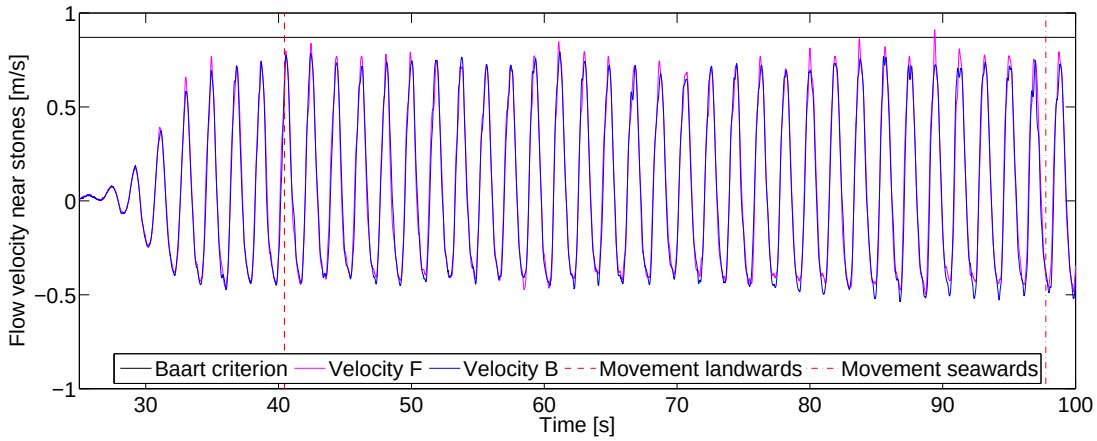

(c) Velocity near the stones during R057

Figure 5.21: Moment and Baart criterion during R057

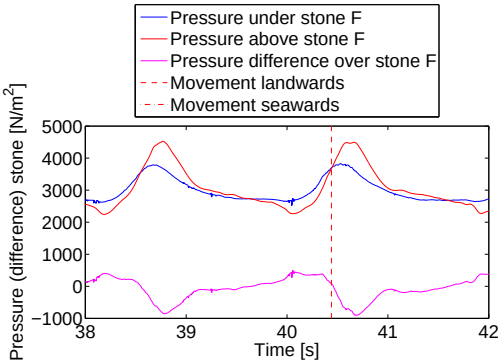

(a) Pressures near stone F during R057

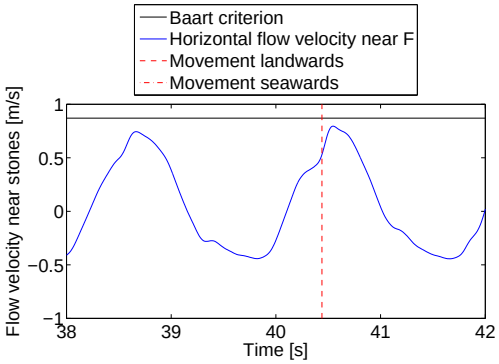

(b) Velocity near stone F during R057

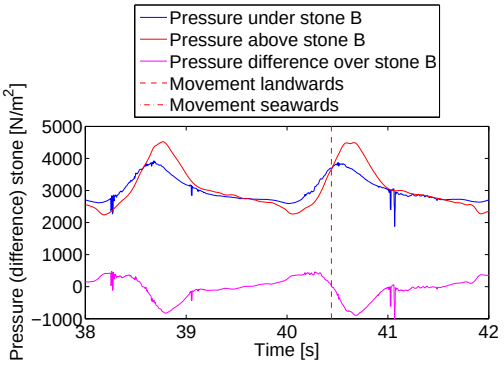

(c) Pressures near stone B during R057

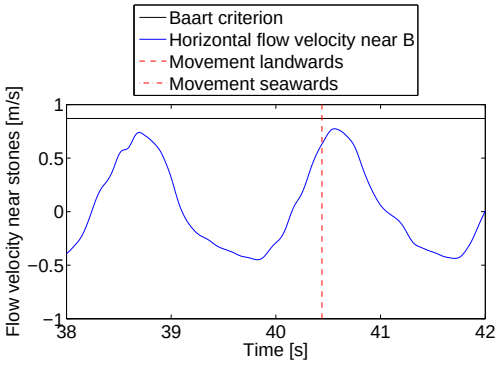

(d) Velocity near stone B during R057

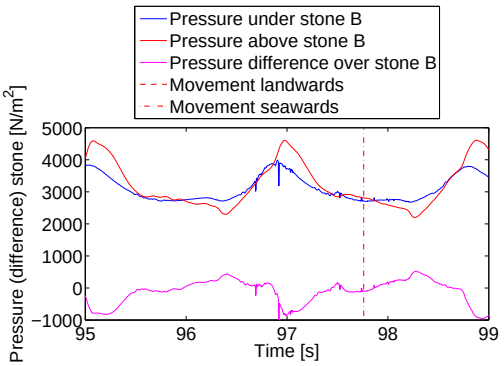

(e) Pressures near stone B during R057

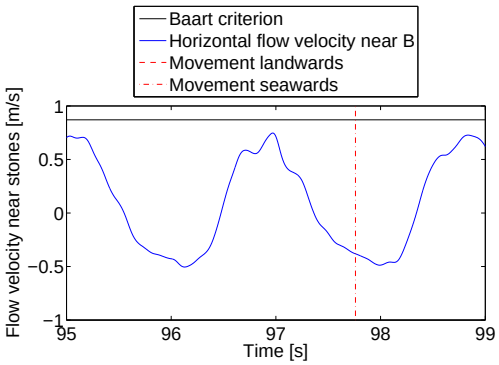

(f) Velocity near stone B during R057

Figure 5.22: Local hydraulic conditions about the time of incipient motion

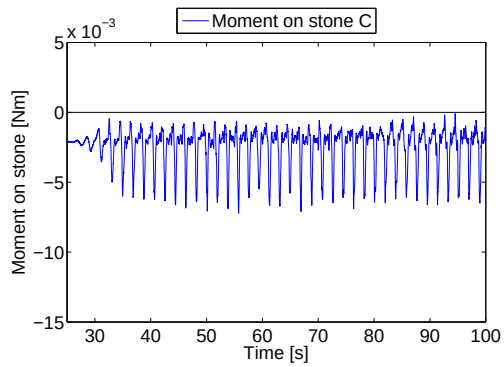

(a) Computed moment on stone C during R057

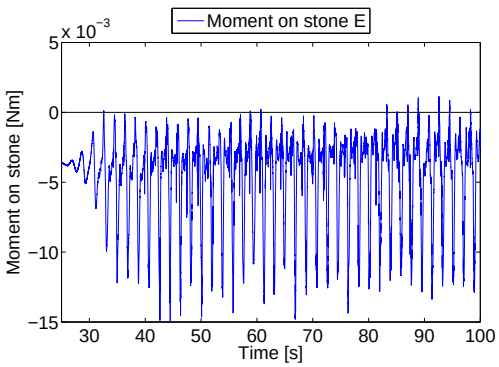

(b) Computed moment on stone E during R057

Figure 5.23: Computed moments on stone C and E during R057

5.3.5 R062

Measurement R062 was also a measurement with very high waves, during which only landwards movement occurred.

Table 5.5: Hydraulic properties and movement during R062

Measurement	$H[m]$	$h_m[m]$	$s[-]$	$T[s]$	Movement B [s]	Movement F [s]
R045	0.22	0.50	0.04	1.88	64.600 lw 87.200 lw	42.040 lw

The overview for the moments on stones B and F in figure 5.25 show that the criterion is surpassed regularly, for stone F it even appears that there is no moment peak below the criterion (the beginning of the wave series ignored). Surprisingly, the measured velocities are lower than in R057 and never come close to the critical value.

Zooming in on the time of incipient motion, it can be seen that in all of the three cases the moment criterion was passed, but the Baart criterion was not. The stones do, however, move out at the point where the incoming flow velocity is the highest. This seems in compliance with the earlier mentioned assumption that the pressure difference peak, which causes the moment peak, destabilises the stone after which the incoming wave rolls the stone out of its cavity.

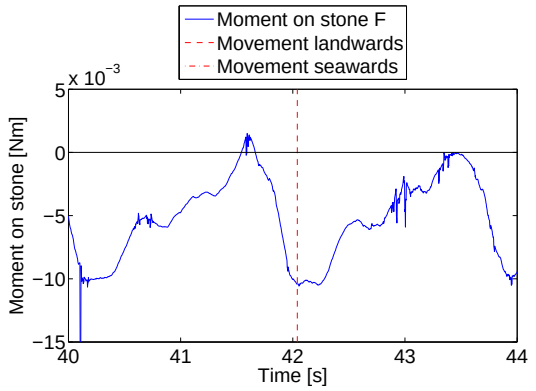

(a) Computed moment on stone F during R062

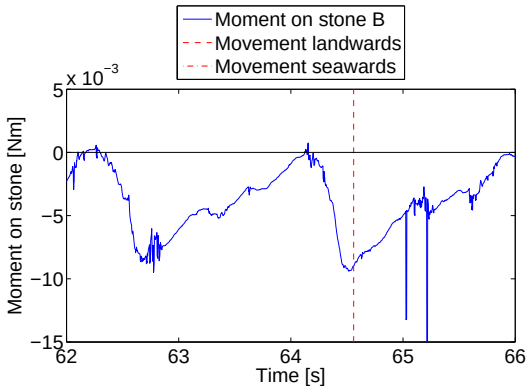

(b) Computed moment on stone B during R062

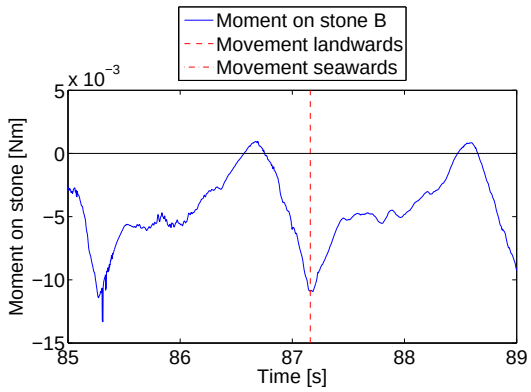

(c) Computed moment on stone B during R062

Figure 5.24: Computed moments on the stone about the time of incipient motion

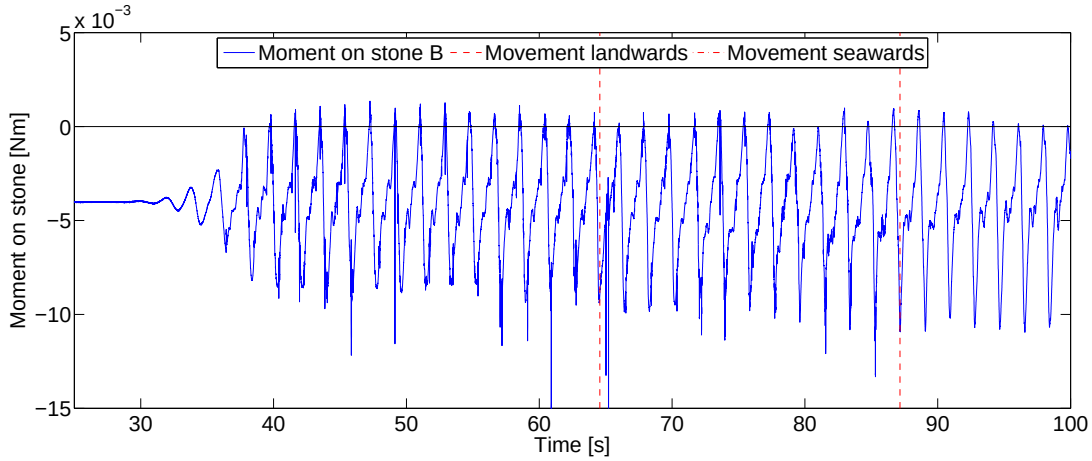

(a) Computed moment on stone B during R062

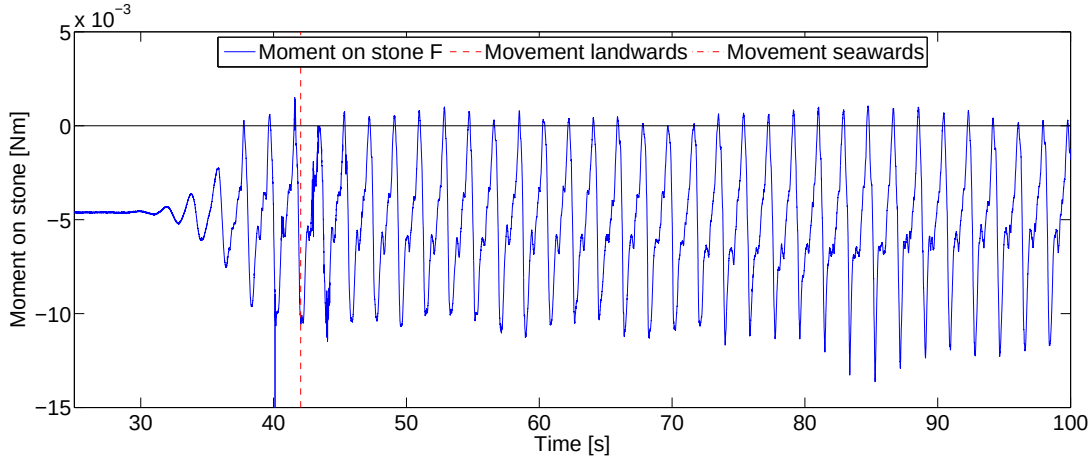

(b) Computed moment on stone F during R062

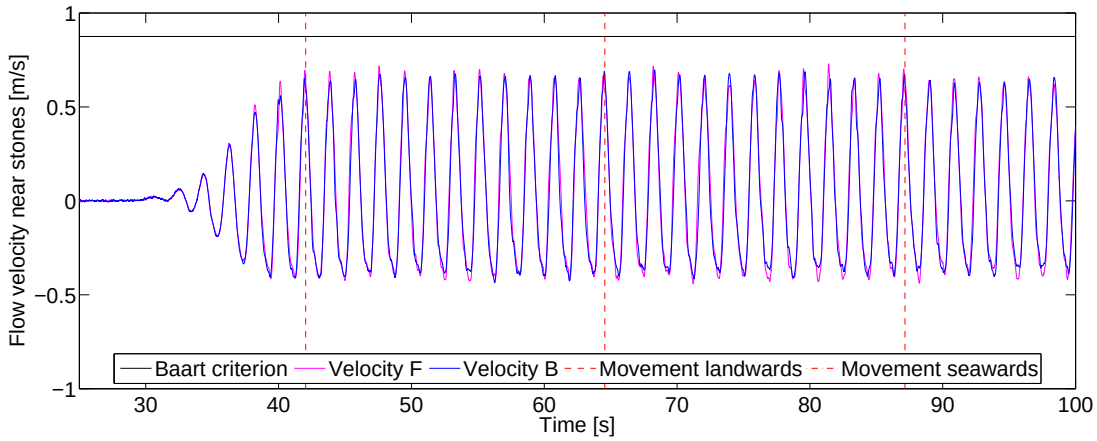

(c) Velocity near the stones during R062

Figure 5.25: Moment and Baart criterion during R062

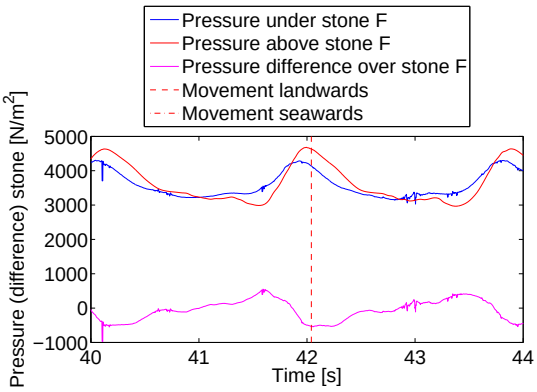

(a) *Pressures near stone F during R062*

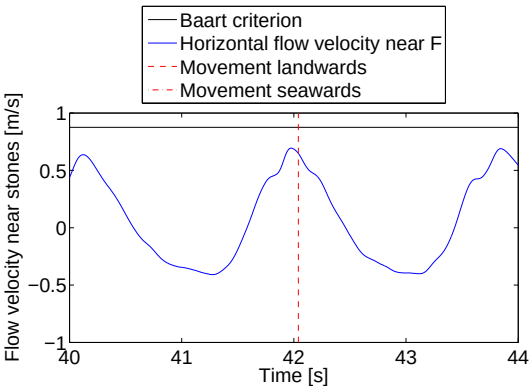

(b) *Velocity near stone F during R062*

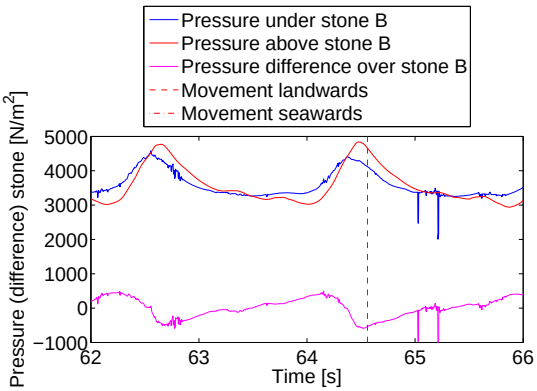

(c) *Pressures near stone B during R062*

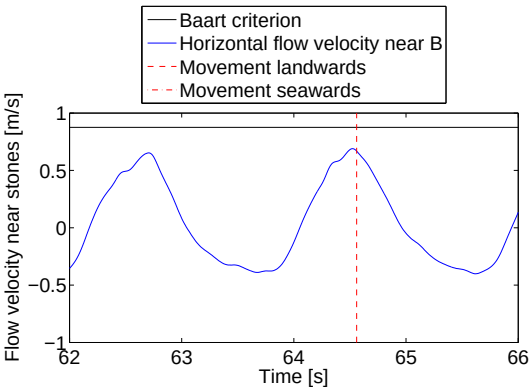

(d) *Velocity near stone B during R062*

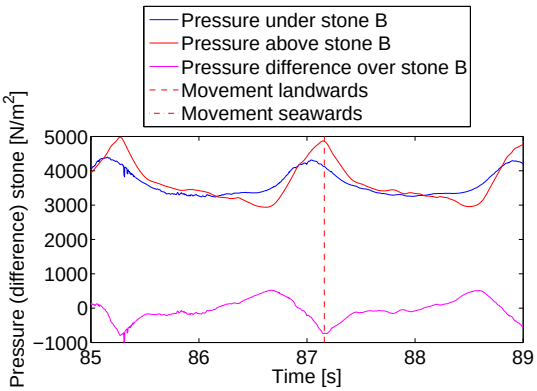

(e) *Pressures near stone B during R062*

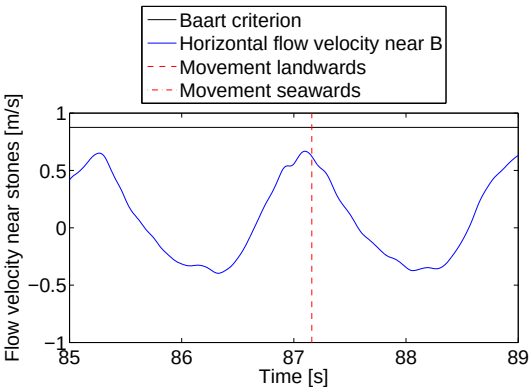

(f) *Velocity near stone B during R062*

Figure 5.26: Local hydraulic conditions about the time of incipient motion

5.3.6 Concluding remarks

The measurements that were treated in previous section, were only a selection of the measurements that were analysed in this visual manner. Based on all the measurements that were visually analysed, several concluding remarks can be made.

Although the moment criterion is not always able to pinpoint the point of incipient motion, it seems to be a good indicator to predict if there will be movement during a certain measurement. In other words, if a lot of peak values are close to or higher than the critical value, stone movement usually occurred during that measurement.

The Baart criterion seems to be too high to predict stone movement. Even with the highest wave series the critical value is rarely surpassed, which makes it somewhat unreliable. It should be investigated if the Baart criterion can be adapted to achieve better results with it, since it is observed that stones are likely to go out during local maxima in flow velocity.

The videos are also very useful in determining the mechanisms behind individual stone movement. Moreover, they can help to understand why a certain stone did not move out while the criterion was passed or the other way around. Sometimes stones got jammed in their cavities, or were repositioned in such a way that they were more vulnerable for the flow. Stones D and F are good examples of this. Stone D experienced the same pressures and velocities as stone B and F (which were also located near the edge of the toe), but never moved out of its cavity. This was because the stone was obstructed by its surrounding stones and therefore stone D could not roll out. Stone F was often repositioned during the measurements, which usually led to it being more vulnerable for the return flow. This mechanism was also observed for stone B for the seawards motions.

For the landwards motion a mechanism can also be observed. First there is a moment peak, after which the incoming flow picks the stone up and moves it out. The moment peak is primarily caused by the pressure difference over the stone and is located just before the velocity peak. This two-step action causes stones to move out landwards.

The positioning of the stone is a very important factor that has not been accounted for in the moment criterion. To be able to do this, more experiments with more loose stones could be performed. This could lead to a more probabilistic approach of the moment criterion, to account for differences in placement of stones. Another option to deal with this factor, could be the introduction of a damage parameter in the moment criterion.

A final remark about the moment criterion is that it assumes that a stone is immediately out of its cavity when the critical value of zero is surpassed. This is not physically correct, as some time is required to get the stone moving (mass acceleration). However in the current study the moment criterion is used as a predictor for stone movement and it seems to perform reasonably well at that task.

5.4 Criterion performance

Although the more or less visual analysis of section 5.3 is very useful to get an idea of the performance of the moment criterion, the method is not very useful to evaluate large number of experiments. Another method is therefore used to determine the performance of the moment criterion. The same comparison method is used for the Baart criterion to check the difference in performance.

5.4.1 Comparison method

The binary classification test will be used to evaluate the results of the measurements. Binary classification can be used to test a predictor, if the actual condition is known. A typical application of this method is found in medical testing, where a blood test can indicate if a person has a certain disease or not. There are four possible outcomes for this test:

1. *True Positive*: The blood test is positive and the patient actually has the disease.
2. *True Negative*: The blood test is negative and the patient does not have the disease.
3. *False Positive*: The blood test is positive, but the patient does not actually have the disease.
4. *False Negative*: The blood test is negative, but the patient does have the disease.

This method can also be used for the criteria that have been developed to predict stone movement in breakwater toes. The Baart criterion and the moment criterion, that has been proposed in this study, both give a critical

value for the flow velocity and the moment on a stone respectively. If this value is exceeded, it is expected that movement of the stones occurs. Since during the experiments the point of incipient motion was observed, the binary classification definitions can be rewritten as:

1. *True Positive*: The critical value is exceeded and the stone has moved in the experiment.
2. *True Negative*: The critical value is not exceeded and the stone has not moved in the experiment.
3. *False Positive*: The critical value is exceeded, but the stone has not moved in the experiment.
4. *False Negative*: The critical value is not exceeded, but the stone has moved in the experiment.

The first task is to determine for the experiments how many True Positives (TP's), True Negatives (TN's), False Positives (FP's) and False Negatives (FN's) have occurred. Not all experiments can be used in this analysis and will therefore be excluded. These experiments are listed in appendix D, together with an explanation why they were not used. For the other measurements all the peak values for the moments and the flow velocities are determined using the `findpeaks` function of MATLAB. Since the velocity signal shows a smooth sinusoidal pattern, the peaks can be found quite easily. The moment graph shows a more distorted signal and although the peaks above M=0 are easily determined, peaks below M=0 are harder to identify. The TN values are therefore not determined in this analysis.

The TP values are determined by identifying all the locations in the dataset where the critical value for M or u is exceeded and saving the corresponding times. These times are then compared to the times at which the stones were actually moved. If within a band of half a wave period of the saved time (Test outcome positive) the stone actually has moved (Condition positive), this is counted as a TP. If the stone did not move, this is counted as FP. A FN can be determined by checking if within half a wave period of a stone actually moving out, a positive test outcome was found. If this is not the case the test failed to identify a positive condition, which is counted as a FN.

The parameters for TP, FP, FN can be used to determine several performance indicators for the criterion under consideration. Table 5.6 shows the definitions for the parameters and performance indicators that are used in the binary specification test.

Table 5.6: Definition table for the binary classification test

		Condition (Measurement)		
		Condition positive	Condition negative	
Test outcome (criterion)	Test outcome positive	True Positive	False Positive (Type I error)	Positive predictive value (PPV,Precision) = (ΣTrue Positive) / (ΣTest outcome positive)
	Test outcome negative	False Negative (Type II error)	True Negative	
		True positive rate (TPR, Sensitivity) = (ΣTrue Positive) / (Σ Condition positive)		
		False negative rate (FNR) = (ΣFalse Negative) / (ΣCondition positive)		

The True Positive Rate (or Sensitivity) is used to determine if the test is capable of determining the condition correctly. It is computed by dividing the total number of TP's and dividing them by the total number of positive conditions (movements). The Sensitivity thus gives the probability of a positive test outcome, given that the stone moves out. The Positive Predictive Value (or Precision) gives an indication of how often the test gives a positive outcome and the stone does actually move out. In other words: the probability that a stone will actually move out, if the test gives a positive result. The False Negative Rate (FNR) is the number of times the test did not identify an actual movement (FN), divided by the total number of movements, which is the same as 1-TPR.

The complete results of the binary classification test are presented in appendix C. In these tables all the required parameters are listed that can be used to determine the performance of both the moment criterion and the Baart criterion.

5.4.2 Results of the binary classification test

Tables C.1 and C.2 show the complete results of the binary classification test. Since this is a very big and detailed table, it is summarised in table 5.7 and some extra performance indicators are added. For the Sensitivity and Precision the 95% Confidence Interval is added, giving an indication of the spread. The parameter FP here indicates the average number of False Positives before movement occurred per measurement. Using this table some remarks can be made about the performance of the two criteria.

Table 5.7: Summary of the binary classification test results

	Moment	Baart
Sensitivity	0.32 (95% CI ±0.13)	0.01 (95% CI ±0.03)
FNR	0.68 (95% CI ±0.13)	0.99 (95% CI ±0.03)
Precision	0.10 (95% CI ±0.06)	0.07 (95% CI ±0.06)
Sensitivity B	0.29 (95% CI ±0.14)	0.00 (95% CI -)
Sensitivity F	0.35 (95% CI ±0.15)	0.02 (95% CI ±0.03)
Precision B	0.06 (95% CI ±0.06)	0.00 (95% CI -)
Precision F	0.25 (95% CI ±0.11)	0.07 (95% CI ±0.06)
FP A	6.23	0.00
FP B	7.58	0.00
FP C	0.38	0.00
FP D	84.50	0.00
FP E	15.70	5.80
FP F	1.78	0.45
FP G	18.20	5.80

Moment criterion

The moment criterion shows a Sensitivity of 32% and an overall Precision of 10%, which means that in 32% of the times a stone moved, the moment criterion was exceeded and 10% of the times the criterion was exceeded a stone actually moved. Although these results seem very low, they are an indication that the correct parameters are considered, since the performance is too good to be originated from random noise. There is, of course, room for improvement and therefore the possible limitations for the moment criterion are analysed.

A very important factor which is not taken into account in the moment criterion, is the placement of the stone. A perfect example of this is stone D. This stone experienced the highest loads during the experiments, but was never moved out of its cavity. This explains the very high count of False Positives for this stone. When the experiment videos are analysed, it can be seen that stone D is blocked from rolling out by its surrounding stones.

Another observation is that the moment criterion seems to work better for stone F than for stone B. The Sensitivity of the stones is more or less equal, but Stone B shows a lot more FP's per measurement, causing the precision to be very low. A possible explanation for this is that stone F is generally faster out of its cavity than Stone B. In the measurements where Stone F was moved the average time was roughly 51 seconds, whereas for stone B this was 82 seconds. This means that, with an average wave period of 2 seconds, about 30 more waves pass over the toe before the stone moves out. The chance for a FP is therefore bigger for stone B, causing the Precision to drop.

Baart criterion

It can immediately be seen that the Baart criterion does not perform well according to this analysis. Out of a total of 65 movements, only 1 was predicted with the Baart criterion, leading to a Sensitivity of only 1%. Based on the analysis in section 5.3, however, this was expected as the critical flow velocity was almost never exceeded. It therefore seems that the current Baart criterion is too high to predict individual stone movement.

An origin of error might be the constants that are used in the formula for the critical velocity. The most obvious choice is C_{PF}, as this is the porous flow coefficient that accounted for several factors including the shape and orientation of the rock. In his study Baart found that $C_{PF} = 0.40$ gave the best results for the datasets that he used. It should be noted that the data sets used in the research of Baart did not focus on movement of individual stones, but measured movement in damage parameter N_{od}. Baart then used a classification for the damage parameters to indicate what damage is acceptable. This means that movement of individual stones is allowed in his criterion and thus explains why the threshold lies too high for the present study. Although lowering the threshold increases the True Positives, it also increases the False Positives. An

optimum should be found, which is achieved by increasing the value C_{PF} and checking the influence on the results of the binary classification test. The results are presented in table 5.8. From this table it can be seen that by increasing C_{PF} the Sensitivity increases rapidly, however the FP's also increase, thus decreasing the Precision. The optimum value for the current application appears to be $C_{PF} = 0.65$, where the Sensitivity is 24% with a Precision of 27%. This means that 24% of the times a stone moved out, the criterion was also exceeded and 27% of the times the criterion is exceeded the stones actually moved in the experiment. Figures 5.27 through 5.31 show the measured velocities with the adapted Baart criterion.

Table 5.8: Baart criterion with different values for C_{PF}

	C_{PF} 0.40	$C_{PF} = 0.50$	$C_{PF} = 0.60$	$C_{PF} = 0.65$
Sensitivity	0.01 (CI ±0.03)	0.03 (CI ±0.04)	0.12 (CI ±0.08)	0.24 (CI ±0.11)
FNR	0.99 (CI ±0.03)	0.97 (CI ±0.04)	0.88 (CI ±0.08)	0.76 (CI ±0.11)
Precision	0.07 (CI ±0.06)	0.06 (CI ±0.04)	0.19 (CI ±0.10)	0.27 (CI ±0.12)
Sensitivity B	0.00 (CI -)	0.02 (CI ±0.03)	0.07 (CI ±0.07)	0.12 (CI ±0.10)
Sensitivity F	0.02 (CI ±0.03)	0.03 (CI ±0.04)	0.19 (CI ±0.12)	0.33 (CI ±0.15)
Precision B	0.00 (CI -)	0.33 (CI ±0.18)	0.18 (CI ±0.13)	0.13 (CI ±0.10)
Precision F	0.07 (CI ±0.06)	0.07 (CI ±0.05)	0.28 (CI ±0.11)	0.41 (CI ±0.13)
FP A	0.00	0.15	1.15	2.93
FP B	0.00	0.10	0.80	1.63
FP C	0.00	0.15	1.15	2.93
FP D	0.00	0.15	1.05	2.93
FP E	5.80	13.43	25.48	32.25
FP F	0.45	0.68	1.00	1.23
FP G	5.80	13.43	25.48	32.25

	$C_{PF} = 0.70$	$C_{PF} = 0.75$	$C_{PF} = 0.80$	
Sensitivity	0.26 (CI ±0.11)	0.33 (CI ±0.12)	0.37 (CI ±0.11)	
FNR	0.74 (CI ±0.11)	0.67 (CI ±0.12)	0.63 (CI ±0.11)	
Precision	0.23 (CI ±0.12)	0.17 (CI ±0.08)	0.16 (CI ±0.12)	
Sensitivity B	0.12 (CI ±0.10)	0.19 (CI ±0.11)	0.33 (CI ±0.10)	
Sensitivity F	0.40 (CI ±0.15)	0.45 (CI ±0.16)	0.45 (CI ±0.15)	
Precision B	0.07 (CI ±0.05)	0.07 (CI ±0.05)	0.10 (CI ±0.05)	
Precision F	0.36 (CI ±0.13)	0.30 (CI ±0.11)	0.26 (CI ±0.13)	
FP A	7.63	13.43	20.70	
FP B	3.45	5.78	8.95	
FP C	7.63	13.43	20.70	
FP D	7.63	13.43	20.70	
FP E	39.83	47.45	55.33	
FP F	1.65	2.08	2.68	
FP G	39.83	47.45	55.33	

Medical example

It may be hard to get a feeling for the values of Sensitivity and Precision of a predictor test, so a brief medical example is given. Although the field of application is completely different, it can give more insight in the performance of the Baart and Moment criterion.

The medical example under consideration was described in an article by Allison et al. (2007), which focussed on faecal occult blood tests (stool samples) as a predictor for colorectal cancer. The analysed test is the recommended screening test by the United States Preventive Services Task Force and the Institute of Medicine, but it was deemed to have a relatively low sensitivity of 64.3% and it was therefore compared with another test. The result of this study, for which almost 6000 test subjects were evaluated, was that the new test had a sensitivity of 81.8% and that it may be useful as a replacement for the old test. The old test had a precision of 1.5% whereas the new test had a precision of 5.2%. Comparing these results to the results found for the predictors in current study, it can be seen that the Sensitivity for the Baart and Moment criterion are rather low. The Precisions are better for the present study, meaning that if a test is positive it is more likely that the condition is true. For medical research, however, it is more important to have a high Sensitivity, since it is better to get more False Positives during the screening period, than to miss a patient that actually has the disease. Follow-up tests, like a colonoscopy, can give a more definitive answer, but are not desirable as screening method since they may be more expensive and less accessible for patients.

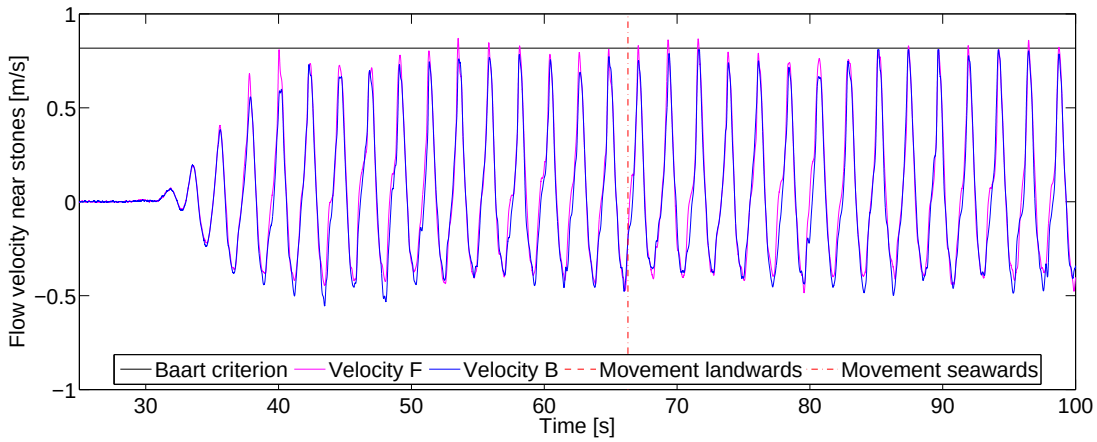

Figure 5.27: Adapted Baart criterion with $C_{PF} = 0.65$ for R041

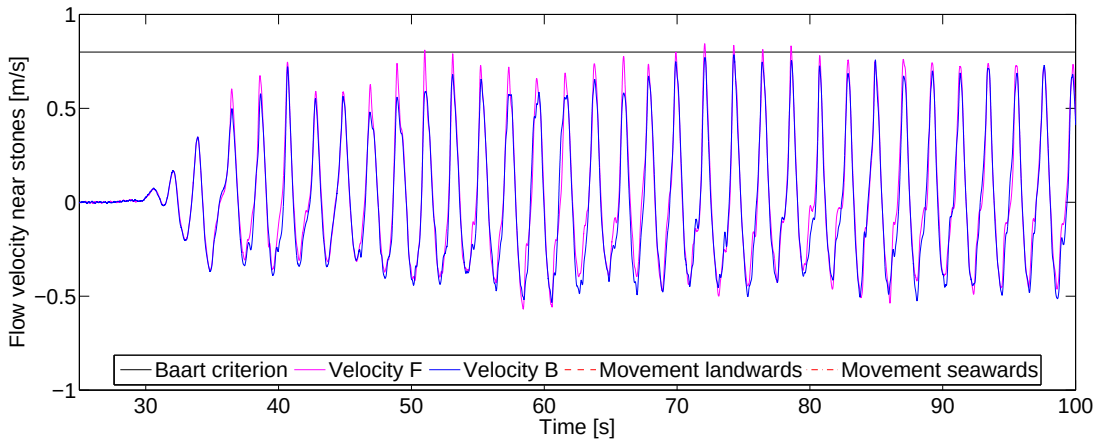

Figure 5.28: Adapted Baart criterion with $C_{PF} = 0.65$ for R044

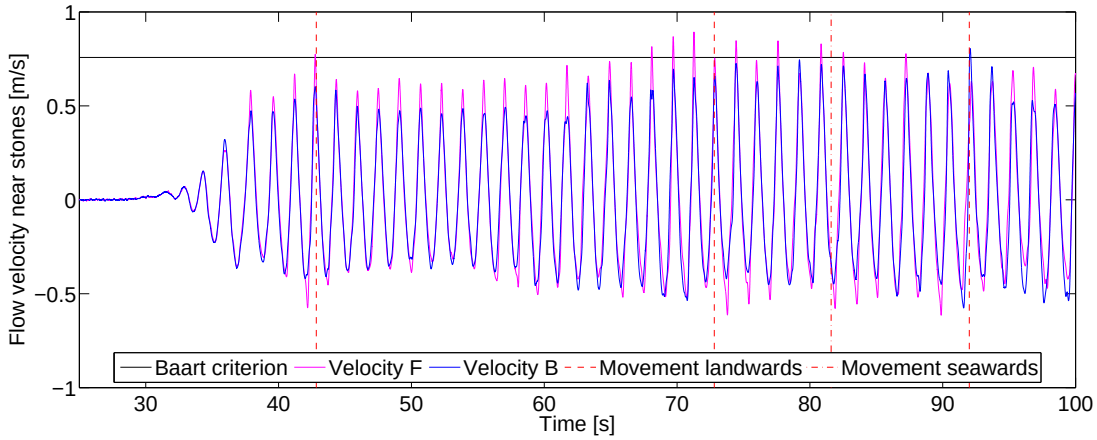

Figure 5.29: Adapted Baart criterion with $C_{PF} = 0.65$ for R045

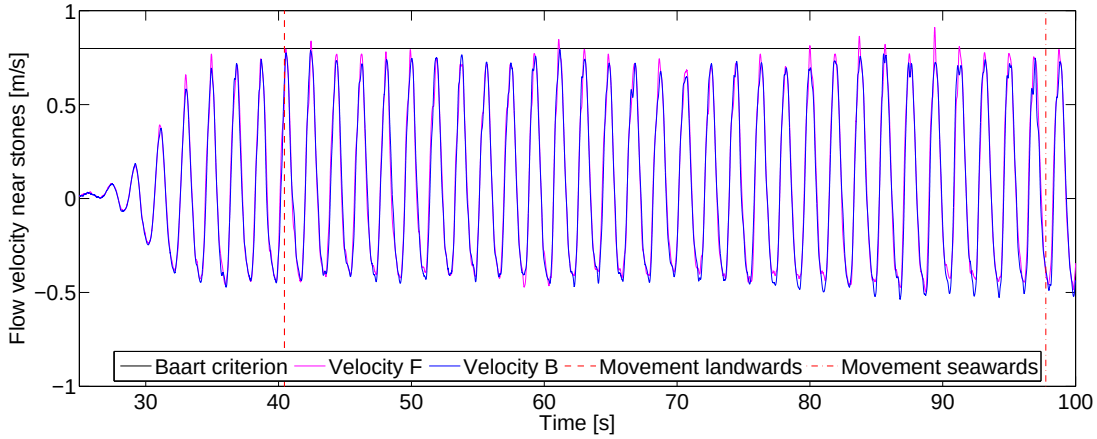

Figure 5.30: Adapted Baart criterion with $C_{PF} = 0.65$ for R057

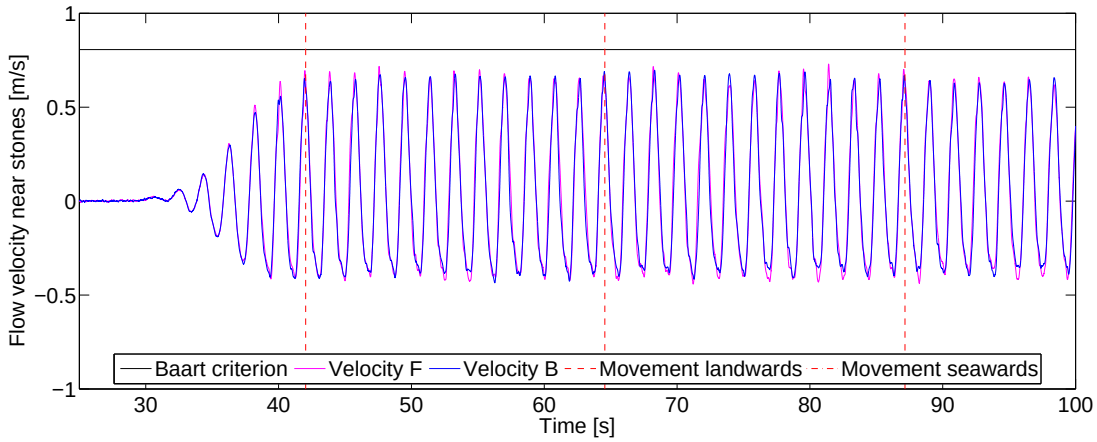

Figure 5.31: Adapted Baart criterion with $C_{PF} = 0.65$ for R062

5.4.3 Evaluation of the two criteria

Based on the results of the binary classification test it can be concluded that both the moment criterion and the (adapted) Baart criterion perform reasonably well in determining the point of incipient motion. The adapted version of the Baart criterion (with $C_{PF} = 0.65$) shows a high precision 27% compared to the 10% for the moment criterion. For the Sensitivity and the FNR the opposite is true: the Baart criterion performs less than the moment criterion, although the differences are small with Sensitivities of 24% (FNR 76%) and 32% (FNR 68%) respectively.

The question is whether the Precision or the Sensitivity is more important. A low Sensitivity means that there are more False Negatives (movement occurred but was not predicted), which leads to more unexpected stone movement. The Sensitivity may be increased by lowering the threshold, but this also leads to a lower precision. A low Precision means there are more False Positives (no movement occurred where it was predicted). There can be several reasons why a stone does not move, even though the critical value is surpassed. The biggest factor is probably the orientation of the stone, which is very varying in a rubble mound breakwater. If a stone is blocked by other stones it requires a bigger moment of force to move out. There must be a point where the moment is so big that a stone will move out, regardless of its position. Figure 5.32 shows this principle for 3 fictitious stones. Each line represents a stone that has a different orientation and therefore is more stable or less stable than the other stone. This principle can possibly be translated into the damage parameter N_{od}, leading to a better applicability for the moment criterion.

The Precision (False Positives) appears to be easier to account for than the Sensitivity, and therefore the Sensitivity is deemed to be more important at this point. Since both criteria have more or less the same Sensitivity (the moment criterion is slightly better), it seems that the Baart criterion with $C_{PF} = 0.65$ is overall better, because its Precision is higher. However, it is questionable how well the adapted Baart criterion with $C_{PF} = 0.65$ will work for another dataset, or if the coefficient needs to be fitted again to achieve good results. The moment criterion has a more solid physical background, but at the moment it lacks in general applicability. Which of the two criteria is best for future design use is therefore inconclusive at this point.

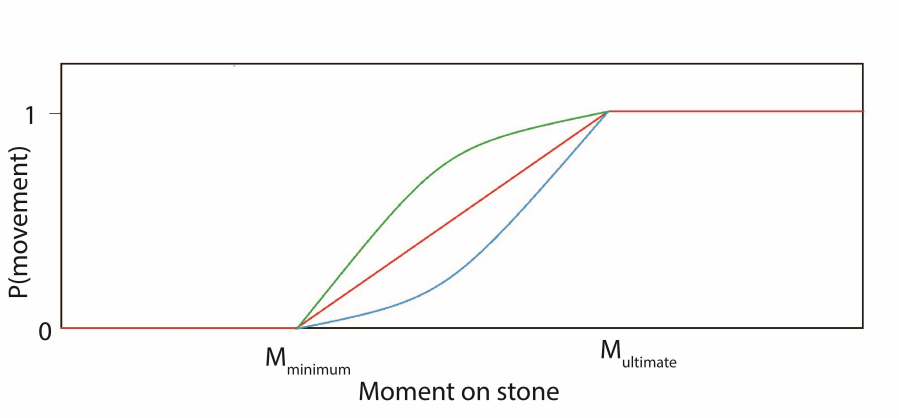

Figure 5.32: Probability of movement based on the moment of force on a stone for three different stones

Chapter 6

Application of the moment criterion

In section 5.4.2 it was found that the moment criterion could predict the movement of individual stones reasonably well. The most important factor was found to be the pressure difference over the stones, followed by the flow velocity. It is therefore of interest to find out how this criterion can be applied in the future for the design of breakwater toes. The biggest challenge is to determine what the pressure difference characteristics in a certain situation will be, since this information is not readily available like, for example, the wave climate at a location. Two possible solutions will be discussed here: determining the local hydraulic conditions at the toe by means of a numerical model and finding a relation between the wave height and the local hydraulic conditions at the toe.

6.1 Numerical modelling

Over the last decades, more and more computer models are used to simulate water behaviour and the field of wave-structure interaction is no exception. Although some models focus more on the larger scale, like wave reflection, diffraction etc. there are also models that can be focussed on the small scale of local hydraulic conditions. An example of such a model is the IH2VOF model, which is developed by IH Cantabria. This model can be used to simulate a numerical wave flume, in which coastal structures can be placed. These structures can very detailed, with different hydraulic flow properties for different layers. In Peters (2014), as part of an additional thesis, the application for this model to determine local hydraulic properties was performed. It was concluded that the model performed reasonably well in computing the local hydraulic conditions, although for some parameters the results were less reliable. The model cannot be readily applied to determine the pressures and flow velocities near toe structures, but it can give an initial indication for these properties. Further verification of the model therefore needs to be performed.

6.2 Estimation of local hydraulic conditions based on the wave conditions

The second option is to find a way to estimate the pressure differences based on the wave conditions. Although this is not the focus of this study, a small analysis is performed to check if this is a viable option. First the correlation between the pressure and the wave height will be determined.

6.2.1 Correlation of the wave height with the local hydraulic parameters

The correlation between the wave height and the local hydraulic parameters will be determined by using the characteristic root-mean-square values for Δp and u_i. These rms-values represent the characteristic peak values for the two parameters, i.e. the maximum pressure difference and maximum incoming flow velocity

For the determination of Δp the correlation with the incoming wave height, as computed by `Refreg`, will be used. Figure 6.1 shows the scatter plot for the observed pressure differences and wave heights. It is found that the correlation between the two parameters is 0.59, which verifies that there certainly is a connection between the two parameters. A linear trendline is plotted through the points in the figure of H_i and Δp that intersects with the origin, leading to a relation of $H_i = 0.0004 \cdot \Delta p$. As can be seen in figure 6.1, there are still a lot of deviations from this trendline and it is very uncertain if this relation can be used for wave conditions that were not tested in this study, let alone irregular waves. If in the future a good relationship between the (irregular) wave height and the pressure difference can be found, it is interesting to check the performance of the moment criterion again.

For the local flow velocity a more established approximation is used, since more research has been performed in this area. In the study of Nammuni-Krohn (2009) an approximation for the maximum flow velocity was developed. During this study the velocity just above the toe surface was measured and equation 6.1 was developed.

$$U_{max} = U_0 \cdot (m\xi \frac{h_t}{h_m} + a), \tag{6.1}$$

where m and a are linear fit coefficients. h_t represents the height of the toe. In her study she determined that for $D_{n,50} = 0.025$, $m = 0.015$ and $a = 1.034$. U_0 is defined as:

$$U_0 = \frac{\pi H}{T} \frac{1}{\sinh(k(h_m - h_t))}. \tag{6.2}$$

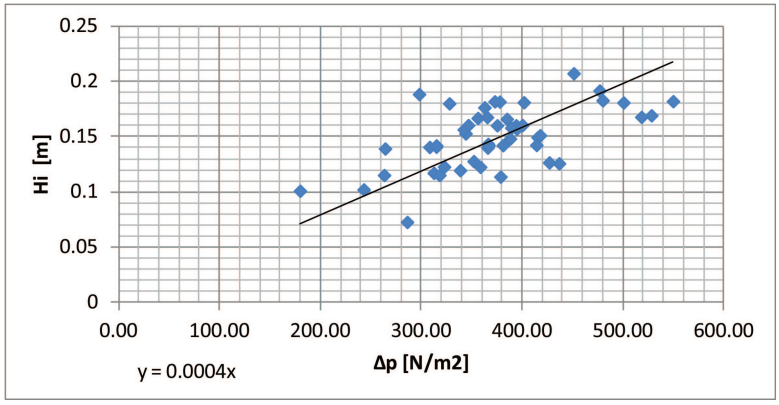

Figure 6.1: Correlation between the incoming wave height and the pressure difference over the stone

6.2.2 Computation of D_{n50}

With an approximation of the local hydraulic parameters, an example calculation for the required stone size for a case can be performed. To compare the results of the moment criterion, the D_{n50} is also computed with the Van der Meer design formula for breakwater toes (equation 6.3)

$$\frac{H_s}{\Delta D_{n50}} = \left(2 + 6.2(h_t/h_m)^{2.7}\right) N_{od}^{0.15}. \tag{6.3}$$

For the moment criterion a few adaptations need to be made, since the arms of the forces are not known as was the case during the experiments. The arm of the lift and weight forces are approximated by $0.5D_{n50}$ (half the nominal stone diameter) and the arm for the drag force by $0.7D_{n50}$. The moment equation then reads:

$$M_{stone} = (F_L - F_W) \cdot 0.5D_{n50} + F_D \cdot 0.7D_{n50}, \tag{6.4}$$

which can be written out using the information provided in section 5.1 as:

$$M_{stone} = 0.5D_{n50} \cdot [\Delta p \cdot D_{n50}^2 - (\rho_s - \rho_w)g \cdot D_{n50}^3] + 0.7D_{n50} \cdot [C_D \cdot \rho_w \cdot 0.4D_{n50}^2 \cdot u \cdot |u|]. \tag{6.5}$$

If the pressure difference and the flow velocity are known, this equation can be solved for $M_{stone} = 0$, which is the critical value. Note that in this equation Δp indicates the pressure difference over a stone, whereas Δ in equation 6.3 is the relative density.

The breakwater dimensions of the current study are used. Furthermore, a damage number of $N_{od} = 0.5$ is used, indicating the start of damage (Verhagen et al., 2009). The hydraulic conditions of R015-R063 are used for the wave characteristics, which can be found in table 3.3. Since this study has only used regular waves and the Van der Meer formula is designed for irregular waves, the wave heights mentioned in table 3.3 need to adapted. Therefore the wave heights meniontedin tabel 3.3 are considered to be the highest 2% waves of an irregular wave spectrum or $H_{2\%}$. If Rayleigh distributed waves are considered, a conversion of $H_{2\%} = 1.4 \cdot H_s$ can be assumed.

With the estimation for the relation between the wave height and the pressure difference ($\Delta p = H_{2\%}/0.0004$) and an estimation for the flow velocity (equation 6.1), both design formulas can be used to determine the required stone size D_{n50} for the breakwater toe.

Figure 6.2 shows the computed required stone sizes as a function of $H_{2\%}$. It can be seen that the moment criterion, in its current form, gives a more conservative stone size. A possible explanation for this phenommenon is that the Van der Meer formula uses the damage parameter $N_{od} = 0.5$, so some movement of stones is allowed. The moment criterion is designed for the movement of a single stone and is therefore prone to give a more conservative stone size. For future purposes it is therefore useful to incorporate some kind of damage parameter into the moment criterion. If this has been achieved, it is very useful to do a similar comparison and compare the required stone sizes of both methods. Since a design formula based on local hydraulic parameters is more theoretically correct, it should be able to determine the required stone size more accurately.

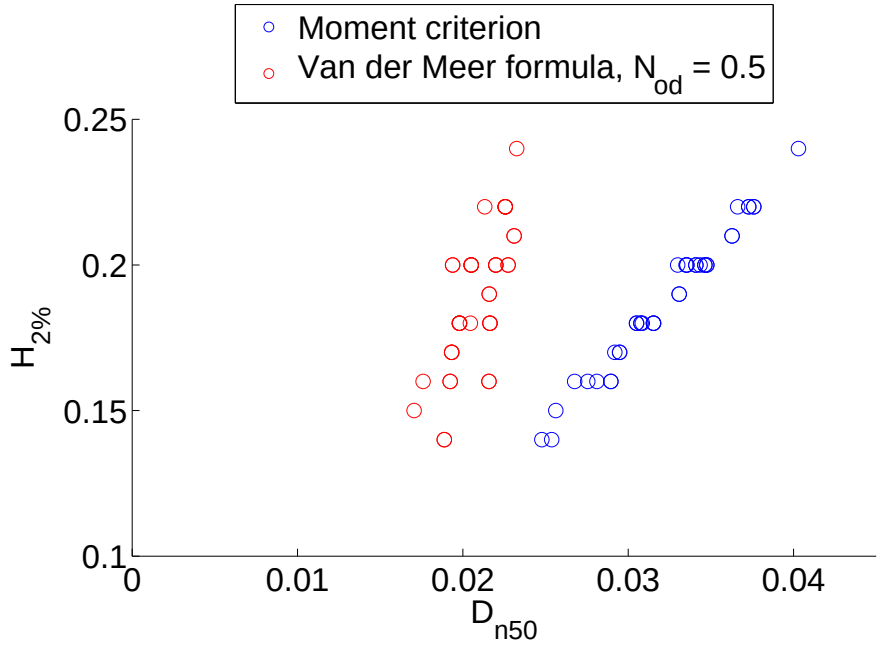

Figure 6.2: Computed stone sizes with the Moment criterion and the Van der Meer design formula

Chapter 7

Conclusions and recommendations

7.1 Conclusions

The goal of this study was stated in section 1.2 as:

To determine the point of incipient motion of stones in breakwater toes based on the local hydraulic conditions

This research objective was subsequently divided into two subquestions.

Which local hydraulic parameters influence the stability of a stone?

It was found that the most important hydraulic parameter to determine the point of incipient motion is the pressure difference over a stone, followed by the flow velocity. It was observed that stones start rocking and moving when the pressure differences become bigger. The point of incipient motion was usually preceded by a pressure difference peak or a period of increased pressure differences. The same holds more or less for the flow velocity, but here the pattern is less recognisable. The flow velocities did not vary much within an experiment run and less peaks were present when compared to the pressure data.

Can a relation be found which determines the point of incipient motion based on local hydraulic parameters?

In this thesis a criterion was proposed, which should be able to determine the point of incipient motion of a single stone. The pressure difference and the flow velocity have been translated into a lift force F_L and a drag force F_D on the stones. Using these two forces and the stabilising weight force F_W, the moment of force about the rotating point of the stone is computed. If this moment becomes positive, it is predicted that the stone will start to move.

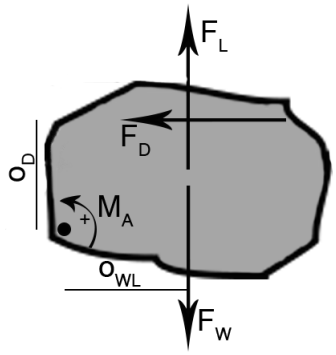

Figure 7.1: Moment of force on a stone in a breakwater toe

This moment criterion was tested by evaluating the experiment data and it was found that the moment criterion performs reasonably well. In 32% of the times a single stone moved, this was predicted by the criterion. The criterion, however, also gives False Positives, meaning that the criterion is surpassed but the stone did not move. It was found that 10% of the times that the criterion was surpassed, the stone actually moved. These values indicate that the moment criterion does have predictive capacities, but it cannot reliably pinpoint the point of incipient motion.

Previous research in stone stability indicates that turbulence induced forces may also play an important role in stone stability. In this study, however, the turbulence could not be determined from the measurement data and was therefore not used in the analysis. This means that the forces and moments computed in this thesis may be too low. With the turbulent forces included, the moment criterion would therefore be surpassed more often, leading to a higher sensitivity and possibly a higher precision for the criterion.

Another important factor that is not accounted for in the moment criterion is the damage to the toe. This

study was focussed on singular stones with all the other stones glued together, so no realistic damage value could be determined. Another restraint is that the moment criterion is verified for regular waves and it would be interesting to know how it can be applied for irregular waves. This makes practical application for the moment criterion, in its current form, hard.

This study does, however, give more insight in the mechanisms that cause stones in breakwaters to move. As was to be expected, the incoming wave has the biggest influence on the stone stability. The incoming wave causes a pressure difference over the stone, which destabilises it. Shortly thereafter the velocity peak follows, which pushes the stone out. It seems that this two-step mechanism causes the stone to move out towards the breakwater. Some stones went out towards the seaside and do not follow the two-step mechanism. From the videos of the measurements, however, it can be seen that these stones are almost always destabilised in landwards direction before the return flow drags them towards the sea.

In conclusion it can be said that this study has shown that it is possible to develop a design formula for breakwater toes that is based on the local hydraulic conditions. The first step was made in this study, by developing the moment criterion. However, more research is required to adapt this criterion for usage with irregular waves and incorporate damage numbers in the criterion. If this can be achieved, a more theoretically correct design formula can be developed, which may lead to a more accurate determination of the required stone size for breakwater toes.

7.2 Recommendations

A lot more insight in the processes governing the stability of stones in breakwater toes was gained during this study and a stability criterion based on local hydraulic parameters was developed. This criterion is, however, not ready to be used as design formula. A few recommendations for future research work are therefore given.

At this moment it is hard to determine the occurring pressure difference over a stone if no measurement data is available. It is very useful if a reliable relation between the external wave parameters and the pressure difference at the toe can be found. The current study has only used regular waves and was therefore not able to couple irregular wave parameters ,like H_s or $H_{2\%}$, to the pressure difference over a stone Δp.

Determining the local hydraulic properties experimentally, as was done in this study, can also be improved. The pressures above the toe are computed in this study, but if pressure meters could be incorporated in the stones this may give more reliable information.

For practical purposes it is also useful to incorporate the damage parameter N_{od} into the criterion. This could be done by using the dataset of a previous research in which the damage was determined, like Gerding (1993), and apply and adapt the moment criterion for its dataset. Alternatively, this could be achieved by using a numerical model.

Current study did not cover the subject of turbulence induced forces. In research of non-uniform bed flow it was shown that these forces may have a significant influence on the stability of a stone, especially on stones with low protrusion. It would be interesting to investigate the effect of these turbulent forces in the field of breakwater toes.

Appendix A

Stone properties

A.1 Nominal stone diameter

The nominal stone diameter D_{n50} has been determined by weighing a sample of the stones (100-200 stones) and determining the sieve curves for the different stone classes. For each individual stone the diameter is determined with $D_n = \sqrt[3]{\frac{m}{\rho}}$. The sieve curve can then be created when the stones are ranked from lightest to heaviest and the cumulative weight percentage is plotted against the stone diameter. This results in the sieve curves that are presented in figure A.1. From these curves the D_{n50} can be determined by finding the diameter that corresponds with a cumulative weight percentage of 50%. The stone grading $\frac{D_{n85}}{D_{n15}}$ can also be determined by dividing the diameter corresponding to cumulative weight percentage 85% by the diameter corresponding with 15%. The results are summarised in table A.1.

Table A.1: Nominal stone diameters and grading of the stones

Stone class	$D_{n50}[m]$	$\frac{D_{n85}}{D_{n15}}$
Armour	0.044	1.39
Core	0.022	1.26
Toe	0.025	1.36

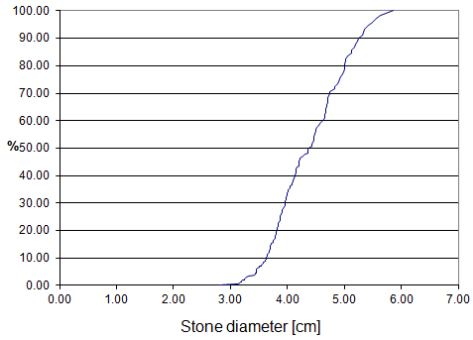

(a) Armour stones

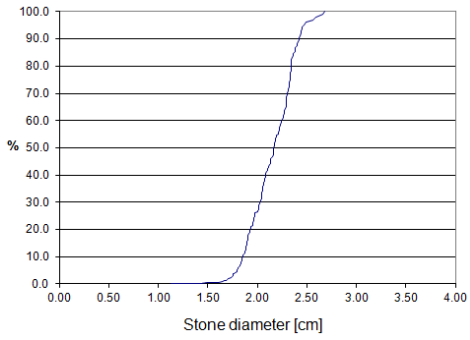

(b) Core stones

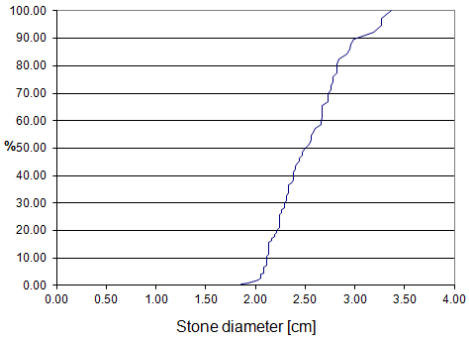

(c) Toe stones

Figure A.1: Sieve curves for the three stone classes

A.2 Target stones

Since the focus of this study is the movement of individual stones, it is important to know the properties of these stones. A total of 7 targets stones are used, which were painted to enhance their visibility and to distinguish them from each other. In table A.2 the relevant properties of the target stones are presented.

Table A.2: Target stones

Stone	**Colour**	$m_{stone}[g]$	$o_{wl}[m]$	$o_d[m]$	$A_f[m^2]$
A	Red	34.0	0.015	0.016	$0.4 \cdot D_{n50}^2$
B	Blue	35.0	0.019	0.015	$0.5 \cdot D_{n50}^2$
C	Yellow	33.8	0.010	0.018	$0.3 \cdot D_{n50}^2$
D	Black	33.4	0.018	0.019	$0.3 \cdot D_{n50}^2$
E	Blue	31.3	0.020	0.020	$0.4 \cdot D_{n50}^2$
F	Red	34.6	0.021	0.008	$0.5 \cdot D_{n50}^2$
G	Yellow	31.7	0.011	0.018	$0.3 \cdot D_{n50}^2$

Appendix B

Characteristic hydraulic conditions during the experiments

This appendix presents the hydraulic conditions as measured during the experiments.

Table B.1 shows the wave heights that were asked from the wave generator together with the analysis of `Refreg` (to determine the incoming wave) and the peak-trough analysis. The wave height for the `Refreg` analysis is determined by multiplying the incoming wave amplitude a_i by 2. For the peak-trough analysis the wave height is determined by adding the amplitude of the peak to the amplitude of the trough $H = a_{peak} + a_{trough}$. The incoming wave height is computed as 70% of that value, meaning that the reflection is 30%

Table B.2 also shows the peak-trough analysis for the other parameters. For some parameters the troughs are not of interest and are therefore omitted from the table. All values in this table are in SI units.

B.1 Peak-trough analysis

The peak-trough analysis identifies the highest and lowest values for a parameter during a wave period. Using this method the maximum incoming and returning flow speed, wave peaks and troughs an maximum pressure differences can be determined. The peaks and troughs during a 'stable' period are determined by using the `findpeaks` function of MATLAB. After all the peak and trough values are determined the root-mean-square (rms) value for each parameter is computed. This rms-value represents the characteristic value for a parameter during that experiment run and is computed by:

$$\Delta p_{rms} = \sqrt{\frac{1}{N}\sum_{i=1}^{N} \Delta p_i^2} \tag{B.1}$$

It should be noted that measurements R001-R014 showed some trouble with the velocity sensors, therefore the data of these measurements are not used in the analyses. They are not necessarily wrong but they are a bit more unreliable, still the characteristic values are shown for completeness sake.

Table B.1: Wave height analysis (all values in [m])

	Wave input	Refreg		Peak and trough analysis					Wave input	Refreg		Peak-trough analysis			
	H	a_i	H_i	a_{peak}	a_{trough}	H	H_i		H	a_i	H_i	a_{peak}	a_{trough}	H	H_i
R001	0.12	0.05	0.10	0.09	0.05	0.13	0.09	R033	0.2	0.08	0.17	0.16	0.09	0.26	0.18
R002	0.14	0.06	0.11	0.08	0.05	0.14	0.10	R034	0.22	0.09	0.18	0.19	0.09	0.28	0.20
R003	0.12	0.05	0.10	0.09	0.05	0.15	0.10	R035	0.2	0.09	0.18	0.12	0.08	0.21	0.14
R004	0.14	0.05	0.10	0.09	0.05	0.14	0.09	R036	0.22	0.09	0.18	0.19	0.11	0.30	0.21
R005	0.16	0.06	0.12	0.10	0.05	0.15	0.10	R037	0.22	0.09	0.18	0.20	0.11	0.31	0.22
R006	0.16	0.06	0.13	0.10	0.06	0.15	0.11	R038	0.22	0.09	0.18	0.19	0.09	0.28	0.19
R007	0.16	0.06	0.12	0.15	0.07	0.21	0.15	R039	0.18	0.07	0.14	0.14	0.08	0.22	0.15
R008	0.18	0.07	0.14	0.14	0.08	0.22	0.15	R040	0.16	0.06	0.13	0.10	0.06	0.15	0.11
R009	0.14	0.06	0.11	0.08	0.05	0.14	0.10	R041	0.16	0.06	0.12	0.14	0.07	0.21	0.15
R010	0.12	0.05	0.10	0.09	0.05	0.14	0.10	R042	0.18	0.07	0.14	0.13	0.08	0.21	0.15
R011	0.12	0.05	0.10	0.09	0.05	0.15	0.10	R043	0.14	0.06	0.11	0.09	0.06	0.14	0.10
R012	0.12	0.05	0.10	0.09	0.05	0.15	0.10	R044	0.14	0.05	0.10	0.09	0.05	0.13	0.09
R013	0.14	0.05	0.10	0.09	0.05	0.13	0.09	R045	0.16	0.06	0.12	0.10	0.04	0.15	0.10
R014	0.16	0.06	0.12	0.10	0.05	0.15	0.10	R046	0.16	0.06	0.12	0.11	0.04	0.15	0.10
R015	0.14	0.05	0.10	0.09	0.05	0.14	0.10	R047	0.17	0.04	0.07	0.19	0.08	0.27	0.19
R016	0.16	0.06	0.13	0.10	0.06	0.16	0.11	R048	0.19	0.08	0.16	0.14	0.07	0.21	0.15
R017	0.16	0.06	0.12	0.14	0.07	0.21	0.14	R049	0.18	0.08	0.15	0.11	0.07	0.18	0.13
R018	0.18	0.07	0.14	0.14	0.08	0.22	0.15	R050	0.2	0.08	0.16	0.12	0.07	0.19	0.14
R019	0.18	0.07	0.14	0.14	0.08	0.22	0.15	R051	0.18	0.08	0.17	0.14	0.08	0.22	0.15
R020	0.15	0.06	0.13	0.12	0.08	0.20	0.14	R052	0.2	0.08	0.17	0.14	0.07	0.21	0.15
R021	0.17	0.06	0.12	0.20	0.07	0.27	0.19	R053	0.21	0.08	0.16	0.15	0.09	0.24	0.17
R022	0.17	0.07	0.14	0.17	0.07	0.24	0.17	R054	0.18	0.07	0.14	0.16	0.07	0.23	0.16
R023	0.19	0.08	0.15	0.15	0.07	0.22	0.15	R055	0.2	0.07	0.14	0.16	0.07	0.23	0.16
R024	0.18	0.07	0.15	0.12	0.07	0.19	0.13	R056	0.2	0.08	0.17	0.17	0.09	0.26	0.18
R025	0.2	0.08	0.16	0.13	0.07	0.20	0.14	R057	0.22	0.09	0.18	0.19	0.09	0.28	0.20
R026	0.16	0.07	0.14	0.11	0.07	0.18	0.13	R058	0.2	0.06	0.12	0.12	0.08	0.20	0.14
R027	0.18	0.08	0.16	0.10	0.06	0.17	0.12	R059	0.22	0.09	0.18	0.19	0.11	0.30	0.21
R028	0.18	0.08	0.16	0.10	0.06	0.16	0.12	R060	0.2	0.09	0.18	0.13	0.11	0.24	0.17
R029	0.2	0.08	0.17	0.14	0.08	0.21	0.15	R061	0.2	0.09	0.19	0.13	0.10	0.23	0.16
R030	0.21	0.08	0.16	0.16	0.09	0.25	0.17	R062	0.22	0.10	0.19	0.11	0.08	0.19	0.14
R031	0.18	0.07	0.14	0.16	0.07	0.23	0.16	R063	0.24	0.10	0.21	0.16	0.08	0.24	0.17
R032	0.2	0.07	0.15	0.11	0.06	0.17	0.12								

Table B.2: rms-values for the different parameters (in SI $[m/s]$,$[N/m^2]$,$[m]$)

	u_{in}	u_{return}	p_{front}	p_{back}	p_{above}	$h_{toe,peak}$	$h_{toe,trough}$	H_{toe}	Δp_{front}	Δp_{back}
R001	0.43	0.34	2033.80	1989.40	2391.70	0.06	0.05	0.10	375.18	281.08
R002	0.65	0.42	2131.20	2041.00	2537.00	0.06	0.07	0.13	427.35	284.24
R003	0.63	0.36	2196.90	2171.90	2656.50	0.08	0.06	0.14	244.33	183.95
R004	0.72	0.47	2291.00	2327.00	2951.30	0.10	0.07	0.17	188.42	148.48
R005	0.73	0.50	2138.10	2140.00	2693.90	0.07	0.07	0.14	346.44	255.32
R006	0.60	0.38	2631.40	2613.60	3232.80	0.08	0.07	0.15	456.27	327.34
R007	0.80	0.39	2870.40	2913.30	3636.60	0.11	0.09	0.20	368.04	293.15
R008	0.73	0.49	2655.70	2693.50	3339.20	0.09	0.08	0.17	334.88	235.87
R009	0.73	0.38	2100.10	2150.70	2615.20	0.06	0.07	0.13	378.00	272.74
R010	0.67	0.35	2192.20	2236.70	2662.90	0.07	0.06	0.13	263.28	151.19
R011	0.67	0.34	2250.00	2241.40	2663.50	0.07	0.06	0.14	260.87	159.81
R012	0.67	0.34	2243.00	2246.50	2669.70	0.07	0.06	0.14	243.65	150.67
R013	0.66	0.42	2381.00	2403.20	2943.70	0.10	0.07	0.17	210.13	123.41
R014	0.82	0.44	2180.10	2214.90	2792.20	0.07	0.07	0.15	315.66	240.84
R015	0.72	0.47	2347.50	2390.60	2952.90	0.10	0.07	0.17	179.26	125.25
R016	0.60	0.38	2682.10	2693.70	3187.80	0.08	0.07	0.15	426.29	287.82
R017	0.77	0.41	2933.70	2949.90	3546.90	0.11	0.08	0.19	337.96	221.70
R018	0.72	0.50	2743.80	2760.40	3314.00	0.09	0.08	0.17	307.62	181.65
R019	0.74	0.49	2734.60	2758.60	3354.60	0.09	0.08	0.17	365.17	183.40
R020	0.65	0.40	3100.70	3108.30	3576.30	0.09	0.08	0.17	351.38	284.31
R021	0.75	0.45	3246.80	3296.40	3832.10	0.11	0.09	0.20	262.61	233.49
R022	0.67	0.46	3016.30	3027.80	3560.50	0.09	0.08	0.16	263.58	196.81
R023	0.79	0.47	3094.70	3110.30	3847.00	0.12	0.09	0.21	343.39	272.83
R024	0.69	0.42	3031.80	3005.90	3585.60	0.09	0.08	0.16	414.80	274.63
R025	0.80	0.48	3128.70	3109.90	3705.00	0.09	0.09	0.18	393.98	283.13
R026	0.49	0.37	3189.70	3145.00	3394.40	0.05	0.05	0.11	365.58	225.90
R027	0.63	0.38	3223.40	3232.80	3803.20	0.09	0.06	0.16	393.38	269.52
R028	0.61	0.38	3227.30	3230.50	3811.20	0.09	0.06	0.16	374.59	271.22

Continued on next page

Table B.2 – continued from previous page

	u_{in}	u_{return}	p_{front}	p_{back}	p_{above}	$h_{toe,peak}$	$h_{toe,trough}$	H_{toe}	Δp_{front}	Δp_{back}
R029	0.76	0.48	3285.00	3279.40	3928.30	0.09	0.09	0.18	364.70	234.93
R030	0.75	0.46	3322.30	3336.70	4044.40	0.11	0.09	0.19	399.69	290.56
R031	0.69	0.40	3259.00	3268.90	3875.30	0.10	0.08	0.17	413.59	354.28
R032	0.77	0.46	3375.80	3378.50	4263.10	0.13	0.10	0.23	387.47	302.64
R033	0.66	0.43	3785.30	3757.90	4092.90	0.07	0.08	0.15	527.53	336.50
R034	0.74	0.49	3826.60	3829.00	4365.40	0.09	0.10	0.20	549.05	338.45
R035	0.79	0.42	4099.20	4120.10	5060.10	0.15	0.11	0.27	327.21	235.23
R036	0.80	0.49	3920.70	3916.60	4783.20	0.13	0.12	0.25	377.17	286.94
R037	0.83	0.50	3886.60	3886.70	4719.50	0.12	0.12	0.24	372.21	264.52
R038	0.77	0.49	3862.90	3837.10	4415.20	0.09	0.10	0.20	479.26	327.07
R039	0.72	0.48	2701.20	2752.90	3322.40	0.09	0.08	0.17	314.30	182.54
R040	0.61	0.39	2649.90	2679.90	3191.00	0.08	0.07	0.15	436.05	285.09
R041	0.79	0.40	2914.20	2918.30	3542.80	0.11	0.09	0.20	311.88	230.37
R042	0.74	0.47	2706.70	2756.20	3378.00	0.09	0.08	0.17	314.32	200.65
R043	0.61	0.42	2129.70	2146.50	2549.30	0.06	0.07	0.13	378.00	295.16
R044	0.70	0.50	2419.80	2407.80	3018.90	0.11	0.07	0.17	242.33	134.53
R045	0.71	0.50	2196.30	2221.90	2739.50	0.07	0.07	0.15	357.90	259.39
R046	0.75	0.50	2178.10	2224.50	2732.40	0.08	0.07	0.15	322.11	269.15
R047	0.73	0.46	3195.10	3224.90	3737.20	0.11	0.09	0.20	285.42	258.87
R048	0.79	0.47	3125.70	3139.00	3882.20	0.11	0.09	0.21	341.62	275.66
R049	0.71	0.40	3042.70	3038.80	3608.10	0.09	0.08	0.16	417.21	284.48
R050	0.78	0.49	3058.60	3084.90	3640.80	0.09	0.09	0.18	346.01	257.85
R051	0.74	0.50	3295.40	3267.70	3913.30	0.09	0.09	0.18	355.45	229.09
R052	0.75	0.50	3286.60	3292.80	3896.90	0.09	0.09	0.18	384.30	242.92
R053	0.78	0.46	3334.10	3336.70	4006.70	0.11	0.09	0.19	388.78	274.52
R054	0.69	0.40	3281.00	3296.00	3975.30	0.10	0.08	0.18	366.09	305.46
R055	0.70	0.39	3270.80	3295.90	3921.70	0.10	0.08	0.18	380.38	335.81
R056	0.71	0.44	3776.80	3754.80	4094.10	0.07	0.08	0.14	517.63	372.41

Continued on next page

Table B.2 – continued from previous page

	u_{in}	u_{return}	p_{front}	p_{back}	p_{above}	$h_{toe,peak}$	$h_{toe,trough}$	H_{toe}	Δp_{front}	Δp_{back}
R057	0.75	0.49	3805.80	3813.10	4421.70	0.10	0.10	0.21	499.91	348.07
R058	0.77	0.43	4025.80	3944.10	4861.70	0.15	0.11	0.26	317.45	225.92
R059	0.80	0.50	3887.30	3917.10	4781.10	0.13	0.12	0.25	401.16	279.71
R060	0.54	0.35	4268.10	4251.60	4447.40	0.06	0.06	0.12	362.13	255.49
R061	0.74	0.43	4097.10	4435.80	5329.70	0.15	0.11	0.26	297.32	196.66
R062	0.68	0.40	4356.20	4354.20	4870.70	0.09	0.08	0.17	476.21	332.34
R063	0.75	0.47	4354.80	4361.70	5131.50	0.12	0.10	0.22	450.54	246.07

Appendix C

Binary classification test

This appendix presents the complete results of the binary classification test. In tables C.1 and C.2 the results for the moment and Baart criterion are shown respectively. Since only stone B and F have shown movement during the measurements, they are also evaluated separately.

In short the meaning of the columns are:

- **Measurement**: The name of the measurement
- **TPR**: True Positive Rate = total number of True Positives divided by the number of movements. If there was no movement during a test, this value can not be computed which is shown as NaN in the tables
- **FNR**: False Negative Rate = total number of False Positives divided by the number of movements If there was no movement during a test, this value can not be computed which is shown as NaN in the tables
- **TP B,F**: Number of True Positives
- **FN B,F**: Number of False Negatives
- **nr. movements**: Total number of stone movements observed during a measurement
- **nr. movements B,F**: Total number of stone movements observed during a measurement for stones B and F separately
- **Test positive B,F**: Number of times the critical value for M or u was exceeded during a measurement for B and F separately
- **FP A-G**: Total number of False Positives for all the stones separately. For stone B and F the counting of FP's stops if that stone is out of its cavity, since no movement could occur again
- **FP B,F total**: Total number of False Positives for B and F, where the counting continued even after the stones were out of their cavity. This is done to give an indication of the amount of times the critical value is exceed and makes the value for FP comparable to the other stones

Table C.1: Results of the binary classification test for the moment criterion

Measurement	TPR	FNR	TP B	TP F	FN B	FN F	nr. movements	nr. movements B	nr. movements F	Test positive B	Test positive F	FP A	FP B	FP C	FP D	FP E	FP F	FP G	FP B total	FP F total
R019	0.33	0.67	0	1	2	0	3	2	1	6	1	2	6	0	98	3	0	3	6	8
R020	NaN	NaN	0	0	0	0	0	0	0	3	0	0	3	0	21	1	0	3	3	3
R021	0.00	1.00	0	0	1	1	2	1	1	0	0	0	0	0	2	0	0	0	0	0
R022	0.00	1.00	0	0	1	1	2	1	1	0	0	0	0	0	5	0	0	0	0	0
R023	0.00	1.00	0	0	1	1	2	1	1	5	0	10	5	3	55	22	0	34	23	17
R025	1.00	0.00	1	0	0	0	1	1	0	10	0	0	9	0	93	13	0	14	9	19
R026	NaN	NaN	0	0	0	0	0	0	0	2	0	1	2	0	123	0	0	0	2	10
R028	0.00	1.00	0	0	0	1	1	0	1	4	4	0	4	0	121	6	4	3	4	41
R030	0.00	1.00	0	0	1	1	2	1	1	0	3	0	0	0	106	3	3	12	16	18
R031	0.00	1.00	0	0	0	1	1	0	1	12	0	4	12	1	88	44	0	64	12	58
R032	0.00	1.00	0	0	1	0	1	1	0	1	0	28	1	1	83	22	0	45	23	48
R033	1.00	0.00	1	2	0	0	3	1	2	5	5	6	4	0	125	59	3	47	109	107
R034	0.00	1.00	0	0	1	1	2	1	1	8	2	6	8	0	120	53	2	49	105	100
R035	0.00	1.00	0	0	1	0	1	1	0	1	0	0	1	0	25	0	0	3	3	4
R036	0.00	1.00	0	0	0	2	2	0	2	46	2	23	46	2	79	24	2	44	46	26
R039	1.00	0.00	0	1	0	0	1	0	1	1	1	0	1	0	91	2	0	3	1	0
R040	1.00	0.00	0	2	0	0	2	0	2	8	6	11	8	0	135	9	4	5	8	5
R041	0.00	1.00	0	0	0	1	1	0	1	2	4	0	2	0	52	0	4	0	2	4
R042	0.25	0.75	0	1	1	2	4	1	3	0	5	1	0	0	81	1	4	5	0	5
R043	NaN	NaN	0	0	0	0	0	0	0	2	0	0	2	0	122	30	0	0	2	11
R044	NaN	NaN	0	0	0	0	0	0	0	0	0	0	0	0	69	0	0	0	0	12
R045	0.50	0.50	2	0	0	2	4	2	2	5	4	0	3	0	82	0	4	1	3	4
R046	0.50	0.50	0	1	0	1	2	0	2	1	7	0	1	0	78	0	6	1	1	7
R047	0.00	1.00	0	0	0	1	1	0	1	0	0	0	0	0	2	0	0	1	0	0
R048	0.00	1.00	0	0	0	1	1	0	1	5	1	12	5	3	78	14	1	46	5	25
R049	0.50	0.50	0	1	1	0	2	1	1	0	1	0	0	0	119	11	0	0	16	21
R050	0.00	1.00	0	0	1	1	2	1	1	0	6	2	0	0	104	11	6	14	4	25
R051	0.33	0.67	1	0	0	2	3	1	2	1	3	0	0	0	113	1	3	3	0	9
R052	0.00	1.00	0	0	1	1	2	1	1	4	0	0	4	0	110	17	0	2	15	9
R053	0.00	1.00	0	0	0	1	1	0	1	7	0	0	7	0	107	4	0	12	7	10
R054	0.00	1.00	0	0	0	1	1	0	1	2	0	1	2	0	81	28	0	39	2	32

Continued on next page

Table C.1 – continued from previous page

Measurement	TPR	FNR	TP B	TP F	FN B	FN F	nr. movements	nr. movements B	nr. movements F	Test positive B	Test positive F	FP A	FP B	FP C	FP D	FP E	FP F	FP G	FP B total	FP F total
R055	1.00	0.00	0	1	0	0	1	0	1	3	8	10	3	1	84	32	7	40	3	37
R056	NaN	NaN	0	0	0	0	0	0	0	99	0	59	99	0	125	77	0	57	99	107
R057	1.00	0.00	2	1	0	0	3	2	1	21	4	38	19	0	110	75	3	52	95	99
R058	0.00	1.00	0	0	2	1	3	2	1	1	8	1	1	0	30	4	8	5	2	9
R059	0.00	1.00	0	0	1	1	2	1	1	0	0	21	0	3	94	16	0	41	18	16
R060	1.00	0.00	0	1	0	0	1	0	1	20	5	0	20	0	89	5	4	9	20	30
R061	NaN	NaN	0	0	0	0	0	0	0	0	0	0	0	0	44	0	0	1	0	2
R062	1.00	0.00	2	1	0	0	3	2	1	24	3	2	22	0	118	34	2	43	69	91
R063	0.50	0.50	0	1	1	0	2	1	1	3	2	11	3	1	118	7	1	27	65	78
Total			**9**	**14**	**17**	**25**	**65**	**26**	**39**	**312**	**85**	**249**	**303**	**15**	**3380**	**628**	**71**	**728**	**798**	**1107**
Average	**0.32**	**0.68**	**0.23**	**0.35**	**0.43**	**0.63**	**1.63**	**0.65**	**0.98**	**7.80**	**2.13**	**6.23**	**7.58**	**0.38**	**84.50**	**15.70**	**1.78**	**18.20**	**19.95**	**27.68**

Table C.2: Results of the binary classification test for the Baart criterion

Measurement	TPR	FNR	TP B	TP F	FN B	FN F	nr. movements	nr. movements B	nr. movements F	Test positive B	Test positive F	FP A	FP B	FP C	FP D	FP E	FP F	FP G	FP B total	FP F total
R019	0	1	0	0	2	1	3	2	1	0	0	0	0	0	0	21	0	21	0	21
R020	NaN	NaN	0	0	0	0	0	0	0	0	0	0	0	0	0	0	0	0	0	0
R021	0	1	0	0	1	1	2	1	1	0	0	0	0	0	0	0	0	0	0	0
R022	0	1	0	0	1	1	2	1	1	0	0	0	0	0	0	0	0	0	0	0
R023	0	1	0	0	1	1	2	1	1	0	0	0	0	0	0	14	0	14	0	14
R025	0	1	0	0	1	0	1	1	0	0	0	0	0	0	0	34	0	34	0	34
R026	NaN	NaN	0	0	0	0	0	0	0	0	0	0	0	0	0	0	0	0	0	0
R028	0	1	0	0	0	1	1	0	1	0	0	0	0	0	0	0	0	0	0	0
R030	0	1	0	0	1	1	2	1	1	0	2	0	0	0	0	5	2	5	0	5
R031	0	1	0	0	0	1	1	0	1	0	0	0	0	0	0	0	0	0	0	0
R032	0	1	0	0	1	0	1	1	0	0	0	0	0	0	0	24	0	24	0	24
R033	0	1	0	0	1	2	3	1	2	0	0	0	0	0	0	0	0	0	0	0
R034	0	1	0	0	1	1	2	1	1	0	0	0	0	0	0	1	0	1	0	1
R035	0	1	0	0	1	0	1	1	0	0	0	0	0	0	0	0	0	0	0	0
R036	0.5	0.5	0	1	0	1	2	0	2	1	2	1	1	1	1	7	1	7	1	6
R039	0	1	0	0	0	1	1	0	1	0	0	0	0	0	0	35	0	35	0	35
R040	0	1	0	0	0	2	2	0	2	0	0	0	0	0	0	0	0	0	0	0
R041	0	1	0	0	0	1	1	0	1	0	0	0	0	0	0	2	0	2	0	2
R042	0	1	0	0	1	3	4	1	3	0	9	0	0	0	0	26	9	26	0	26
R043	NaN	NaN	0	0	0	0	0	0	0	0	0	0	0	0	0	0	0	0	0	0
R044	NaN	NaN	0	0	0	0	0	0	0	0	0	0	0	0	0	2	0	2	0	2
R045	0.25	0.75	0	1	2	1	4	2	2	0	5	0	0	0	0	18	4	18	0	17
R046	0	1	0	0	0	2	2	0	2	0	2	0	0	0	0	38	2	38	0	38
R047	0	1	0	0	0	1	1	0	1	0	0	0	0	0	0	0	0	0	0	0
R048	0	1	0	0	0	1	1	0	1	0	0	0	0	0	0	28	0	28	0	28
R049	0	1	0	0	1	1	2	1	1	0	0	0	0	0	0	0	0	0	0	0
R050	0	1	0	0	1	1	2	1	1	0	0	0	0	0	0	5	0	5	0	5
R051	0	1	0	0	1	2	3	1	2	0	1	0	0	0	0	6	1	6	0	6
R052	0	1	0	0	1	1	2	1	1	0	0	0	0	0	0	11	0	11	0	11
R053	0	1	0	0	0	1	1	0	1	0	0	0	0	0	0	7	0	7	0	7
R054	0	1	0	0	0	1	1	0	1	0	0	0	0	0	0	0	0	0	0	0

Continued on next page

Table C.2 – continued from previous page

Measurement	TPR	FNR	TP B	TP F	FN B	FN F	nr. movements	nr. movements B	nr. movements F	Test positive B	Test positive F	FP A	FP B	FP C	FP D	FP E	FP F	FP G	FP B total	FP F total
R055	0	1	0	0	0	1	1	0	1	0	0	0	0	0	0	0	0	0	0	0
R056	NaN	NaN	0	0	0	0	0	0	0	0	0	0	0	0	0	0	0	0	0	0
R057	0	1	0	0	2	1	3	2	1	0	0	0	0	0	0	7	0	7	0	7
R058	0	1	0	0	2	1	3	2	1	0	1	0	0	0	0	1	1	1	0	1
R059	0	1	0	0	1	1	2	1	1	0	0	0	0	0	0	17	0	17	0	17
R060	0	1	0	0	0	1	1	0	1	0	0	0	0	0	0	0	0	0	0	0
R061	NaN	NaN	0	0	0	0	0	0	0	0	0	0	0	0	0	0	0	0	0	0
R062	0	1	0	0	2	1	3	2	1	0	0	0	0	0	0	0	0	0	0	0
R063	0	1	0	0	1	1	2	1	1	0	0	0	0	0	0	10	0	10	0	10
Total			**0**	**2**	**26**	**37**	**65**	**26**	**39**	**1**	**22**	**1**	**1**	**1**	**1**	**319**	**20**	**319**	**1**	**317**
Average	**0.02**	**0.98**	**0.00**	**0.05**	**0.65**	**0.93**	**1.63**	**0.65**	**0.98**	**0.03**	**0.55**	**0.03**	**0.03**	**0.03**	**0.03**	**7.98**	**0.50**	**7.98**	**0.03**	**7.93**

Appendix D

Experiment logs

This appendix shows the logbook that was kept during the experiments. For each experiment the relevant parameters and observations that were made are stated. Furthermore the moment of incipient motion and the direction of the movement are noted (lw stands for landwards and sw for seawards).

The measurements can be subdivided in the following parts.

- **R001-R019** These measurements were performed with the two EMS velocity sensors and were not videoed.
- **R020-R028** These measurements were performed with the two EMS velocity sensors and were videoed.
- **R039-R063** These measurements were performed with the two EMS velocity sensors and were videoed. Moreover a stopwatch was started at the beginning of the measurement which is used to 'synchronise' the videos with the measurement data. The moment of incipient motion can therefore be determined more accurately.
- **R063-R076** These measurements were performed with a EMS and an ADV velocity sensor and were videoed. Because the ADV required sediment to be added to the flow, the movement of stones was hard to observe.

Some of the measurements are not used in (part of) the analysis of the results for various reasons:

- **R001-R014** During these first experiments some trouble with the velocity sensors was encountered. Therefore it was chosen not to use this data in the analysis.
- **R015-R018** During these experiments the direction of the moving stones was not noted, moreover the moment of movement was sometimes determined incorrectly.
- **R024** The button, which is used to mark the moment of incipient motion, was pressed twice for one movement. Since it was not possible to determine the correct marker, this data is not used
- **R027** No visual observations were made during this measurement.
- **R029** The button was pressed too late, so the marker does not indicate the right time.
- **R037-R038** These measurements were performed with stones of $D_{n,50} = 0.025m$, but showed no movement. The different diameter would unnecessarily complicate the analysis of the results and therefore these measurements were not used.

TESTNAME: R001_D23_h30_H12_T139	
Date: 27-03-2014 9:55 TESTRUN: R001 Dn50 = 0.023 hm =0.3 H =0.12 s =0.04 T =1.39	Comments: • C rocks softly • B, D are rocking • Rest of the stones are laying still

Stone	A	B	C	D	E	F	G
Movement							

Additional comments:

- EMS at 5 cm

TESTNAME: R002_D23_h30_H14_T150	
Date:27-03-2014 10:10 TESTRUN: Dn50 = 0.023 hm =0.3 H =0.14 s =0.04 T =1.50	Comments: • F jumps out of its cavity and rolls back in. Counted as movement • B,D,E are heavily rocking

Stone	A	B	C	D	E	F	G
Movement						1	

Additional comments:

- This test is worth repeating since a lot of stones were close to the moment of incipient motion
- EMS at 5 cm

TESTNAME:R003_D23_h30_H12_T196	
Date:27-03-2014 10:30 TESTRUN: R003 Dn50 = 0.023 hm =0.3 H =0.12 s =0.02 T =1.96	Comments: • B,D,E are rocking • F is rocking heavily and shifted position within the cavity, not counted as movement

Stone	A	B	C	D	E	F	G
Movement							

Additional comments:

- EMS at 5 cm

TESTNAME: R004_D23_h30_H14_T212	
Date: 27-03-2014 10:50 TESTRUN: R004 Dn50 = 0.023 hm =0.3 H =0.14 s =0.02 T =2.12	Comments: • F is out • C,D rocking

Stone	A	B	C	D	E	F	G
Movement						1	

Additional comments:

- EMS at 5 cm

TESTNAME: R005_D23_h30_H16_T160	
Date: 27-03-2014 11:15 TESTRUN: Dn50 = 0.023 hm =0.3 H =0.16 s =0.04 T =1.60	Comments: • F jumps out and rolls back in (counted as movement) • F jumps out again, pushed the button a little too late (0.5 seconds or so) • B,D softly rocking

Stone	A	B	C	D	E	F	G
Movement						1,2	

Additional comments:

- After about two minutes into the test, the waves sometimes bended a little (right side of the wave was ahead of the left side)
- EMS at 5 cm

TESTNAME:R006_D23_h35_H16_T160	
Date:27-03-2014 11:55 TESTRUN: R006 Dn50 = 0.023 hm =0.35 H =0.16 s =0.04 T =1.60	Comments: • F out. At first F lay still, until the oblique waves were present. This resulted in heavy rocking and repositioning in the cavity. After the waves returned to normal, it jumped out of the cavity • D,E rocking • D,E rocking heavily under oblique wave attack

Stone	A	B	C	D	E	F	G
Movement						1	

Additional comments:

- The waves became very oblique two times in this run, resulting in heavy rocking. After about 20 seconds the waves returned to normal.
- EMS at 5 cm

TESTNAME: R007_D23_h35_H16_T226	
Date: 27-03-2014 12:15 TESTRUN: Dn50 = 0.023 hm =0.35 H =0.16 s = 0.02 T =2.26	Comments: • F out • B out a few seconds after the wave generator stopped, but the waves were the same as during the test, so counted as movement. • C rocking softly

Stone	A	B	C	D	E	F	G
Movement		2				1	

Additional comments:

- EMS at 5 cm

TESTNAME: R008_D23_h35_H18_T170	
Date: 27-03-2014 12:30 TESTRUN:R008 Dn50 = 0.023 hm =0.35 H =0.18 s =0.04 T =1.70	Comments: • B jumps out and rolls back in • F jumps out, button pressed too late (+-0.3 s) • B jumps out again • D rocking • C rocking softly

Stone	A	B	C	D	E	F	G
Movement		1,3				2	

Additional comments:

- Test is worth repeating, lots of movement. Also consider doing some tests with a slightly higher and lower wave height/steepness.
- EMS at 5 cm

TESTNAME: R009_D23_h30_H14_T150	
Date: 28-03-2014 10:50 TESTRUN: Dn50 = 0.023 hm =0.30 H =0.14 s =0.04 T =1.50	Comments: • F repositions in hole, not counted as movement • D,E rocking • It looked like an air bubble escaped from pressure meter F about 20-30 seconds into the test

Stone	A	B	C	D	E	F	G
Movement							

Additional comments:

- Measured with the velocity meters 3 cm above the toe. All the previous tests the velocity meters were 5 cm above the toe. This is done to check if there is a difference in results (magnitude of the velocity)
- EMS at 3 cm

TESTNAME:R010_D23_h30_H12_T196	
Date:28-03-2014 11:05 TESTRUN: R010 Dn50 = 0.023 hm =0.3 H =0.12 s =0.02 T =1.96	Comments: • D,F are rocking • G is rocking softy

Stone	A	B	C	D	E	F	G
Movement							

Additional comments:

- EMS at 3 cm

TESTNAME:R011_D23_h30_H12_T196	
Date:28-03-2014 11:40 TESTRUN: R011 Dn50 = 0.023 hm =0.3 H =0.12 s =0.02 T =1.96	Comments: • B,C,D,F rocking

Stone	A	B	C	D	E	F	G
Movement							

Additional comments :

- Changed the EMS at B (EMS 12 > EMS 13) as it shifted its equilibrium position with about .2 volts after each test. New test to check if this yields new results. Test started 15 minutes after installation. Still shift of equilibrium position, therefore for the next test the amplifier is changed (E9 > E8)
- EMS at 3 cm

TESTNAME:R012_D23_h30_H12_T196	
Date:28-03-2014 12:30 TESTRUN: R011 Dn50 = 0.023 hm =0.3 H =0.12 s =0.02 T =1.96	Comments: • B,D,F Rocking

Stone	A	B	C	D	E	F	G
Movement							

Additional comments:

- EMS at 3 cm

TESTNAME: R013_D23_h30_H14_T212	
Date: 28-03-2014 12:50 TESTRUN: R013 Dn50 = 0.023 hm =0.3 H =0.14 s =0.02 T =2.12	Comments: • F out • D rocking

Stone	A	B	C	D	E	F	G
Movement						1	

Additional comments:

- EMS at 3 cm

TESTNAME: R014_D23_h30_H16_T160	
Date: 28-03-2014 13:10 TESTRUN: Dn50 = 0.023 hm =0.3 H =0.16 s =0.04 T =1.60	Comments: • F,B out • D,E rocking heavily • G rocking

Stone	A	B	C	D	E	F	G
Movement		2				1	

Additional comments:

- EMS at 3 cm
- Near the end of the test the waves became distorted (oblique)

TESTNAME: R015_D23_h30_H14_T212	
Date: 28-03-2014 13:30 TESTRUN: R013 Dn50 = 0.023 hm =0.3 H =0.14 s =0.02 T =2.12	Comments: • F out •

Stone	A	B	C	D	E	F	G
Movement						1	

Additional comments:

- EMS at 5 cm

TESTNAME:R016_D23_h35_H16_T160	
Date:28-03-2014 14:25 TESTRUN: R016 Dn50 = 0.023 hm =0.35 H =0.16 s =0.04 T =1.60	Comments: • F out of the hole, rolls back in. Counted as movement • B,D rocking

Stone	A	B	C	D	E	F	G
Movement						1	

Additional comments

- EMS at 5 cm
- EMS Y2 reset to zero (the voltage kept on rising during previous tests.
- At about 30 seconds very oblique waves. At about 1 min waves back to normal. At about 1:30 again oblique until the end of the test
- After the test EMS Y2 is still near zero, so it appears to be working correctly now

TESTNAME: R017_D23_h35_H16_T226	
Date: 28-03-2014 14:45 TESTRUN: Dn50 = 0.023 hm =0.35 H =0.16 s = 0.02 T =2.26	Comments: • F repositions in its hole • D rocking

Stone	A	B	C	D	E	F	G
Movement							

Additional comments

- EMS at 5 cm

TESTNAME: R018_D23_h35_H18_T170	
Date: 28-03-2014 14:55 TESTRUN:R018 Dn50 = 0.023 hm =0.35 H =0.18 s =0.04 T =1.70	Comments: • F is turned upside down in its hole, not counted as movement • F is out of its hole, pressed the button about 1 sec too late

Stone	A	B	C	D	E	F	G
Movement						1	

Additional comments

- EMS at 5 cm
- Repeat the test since the button was pressed too late.

TESTNAME: R019_D23_h35_H18_T170	
Date: 28-03-2014 15:10 TESTRUN:R019 Dn50 = 0.023 hm =0.35 H =0.18 s =0.04 T =1.70	Comments: • F out landwards, ends up just under the EMS (visible in the data?) • B goes out (landwards), rolls back in • B goes out (landwards) rolls back in and immediately rolls out seawards. Only the first is counted as movement. • D rocking, E shifts position

Stone	A	B	C	D	E	F	G
Movement		2lw 82.680s 3lw 154.086s				1lw 42.110s	

Additional comments

- EMS at 5 cm

TESTNAME: R020_D23_h38_H15_T219	
Date: 03-04-2014 10:10 TESTRUN:R020 Dn50 = 0.023 hm =0.38 H =0.15 s =0.02 T =2.19	Comments: • B,D rocking • F rocking softly

Stone	A	B	C	D	E	F	G
Movement							

Additional comments

- EMS at 5 cm
- From here on the tests are videoed

TESTNAME: R021_D23_h38_H17_T233	
Date: 03-04-2014 10:30 TESTRUN:R021 Dn50 = 0.023 hm =0.38 H =0.17 s =0.02 T =2.33	Comments: • B out landwards (to breakwater) and back in hole • F out seawards (to generator) • All stones were rocking initially • B,D were rocking until the end

Stone	A	B	C	D	E	F	G
Movement		1lw 66.954s				2sw 69.670s	

Additional comments

- EMS at 5 cm
- Dasylab file is big, because I stopped recording too late (2 min after test)

TESTNAME: R022_D23_h38_H17_T191	
Date: 03-04-2014 10:45 TESTRUN:R022 Dn50 = 0.023 hm =0.38 H =0.17 s =0.03 T =1.91	Comments: • B out landwards (video 0:54) • F out seawards (video 1:40) • C,D Rocking • All stones rocking softly in the beginning

Stone	A	B	C	D	E	F	G
Movement		1lw 67.940s				2sw 114.818	

Additional comments

- EMS at 5 cm
- The video corresponding to this test shows R21 instead of R22 in the beginning

TESTNAME: R023_D23_h38_H19_T201	
Date: 03-04-2014 11:00 TESTRUN:R023 Dn50 = 0.023 hm =0.38 H =0.19 s =0.03 T =2.01	Comments: • F out seawards • B out landwards • All stones rocking, except stone D

Stone	A	B	C	D	E	F	G
Movement		2lw 133.826s				1sw 56.414s	

Additional comments

- EMS at 5 cm
- Around 2:30 the waves became oblique

TESTNAME: R024_D23_h38_H18_T170	
Date: 03-04-2014 11:15 TESTRUN:R024 Dn50 = 0.023 hm =0.38 H =0.18 s =0.04 T =1.70	Comments: • F out landwards • E Spins in its hole, not counted as movement • A lot of movement in the beginning • Button pressed multiple times, while only one movement was notated, therefore this test will not be used

Stone	A	B	C	D	E	F	G
Movement						1lw	

Additional comments

- EMS at 5 cm
- Test is worth repeating

TESTNAME: R025_D23_h38_H20_T179	
Date: 03-04-2014 11:30 TESTRUN:R025 Dn50 = 0.023 hm =0.38 H =0.20 s =0.04 T =1.79	Comments: • B out landwards • F turns in hole @ about 50 secs • E turns in hole @ 1 m • A rocking

Stone	A	B	C	D	E	F	G
Movement		1lw 126.066s					

Additional comments

- EMS at 5 cm
- Some whitecapping on the waves

TESTNAME: R026_D23_h40_H16_T160	
Date: 03-04-2014 12:15 TESTRUN:R026 Dn50 = 0.023 hm =0.40 H =0.16 s =0.04 T =1.60	Comments: •

Stone	A	B	C	D	E	F	G
Movement							

Additional comments

- EMS at 5 cm
- Stopped recording too late (2 minutes)

TESTNAME: R027_D23_h40_H18_T170	
Date: 03-04-2014 12:30 TESTRUN:R027 Dn50 = 0.023 hm =0.40 H =0.18 s =0.04 T =1.70	Comments: • Prof Uijttewaal visited during this test, so there was no observation. Do not use this data set.

Stone	A	B	C	D	E	F	G
Movement							

Additional comments

- EMS at 5 cm

TESTNAME: R028_D23_h40_H18_T170	
Date: 03-04-2014 12:40 TESTRUN:R028 Dn50 = 0.023 hm =0.40 H =0.18 s =0.04 T =1.70	Comments: • F out seawards • E shifts in hole • A,B,D,E Rocking

Stone	A	B	C	D	E	F	G
Movement						1sw 48.072s	

Additional comments

- EMS at 5 cm

TESTNAME: R029_D23_h40_H20_T179	
Date: 03-04-2014 12:55 TESTRUN:R029 Dn50 = 0.023 hm =0.40 H =0.20 s =0.04 T =1.79	Comments: • F out seawards (pressed button too late +-1s), therefore data is not used • E shifts in hole • D Rocking

Stone	A	B	C	D	E	F	G
Movement						1sw	

Additional comments

- EMS at 5 cm

TESTNAME: R030_D23_h40_H21_T183	
Date: 03-04-2014 13:45 TESTRUN:R030 Dn50 = 0.023 hm =0.40 H =0.21 s =0.04 T =1.83	Comments: • B out seawards • F out (first almost out landwards and directly after completely out seawards) • A,D,E rocking

Stone	A	B	C	D	E	F	G
Movement		1sw 53.854s				2sw 77.060s	

Additional comments

- EMS at 5 cm

TESTNAME: R031_D23_h40_H18_T196	
Date: 03-04-2014 14:00 TESTRUN:R031 Dn50 = 0.023 hm =0.40 H =0.18 s =0.03 T =1.96	Comments: • F out seawards • A,B,D Rocking • C,E Rocking softly

Stone	A	B	C	D	E	F	G
Movement						1sw 40.786s	

Additional comments

- EMS at 5 cm

TESTNAME: R032_D23_h40_H20_T207	
Date: 03-04-2014 14:15 TESTRUN:R032 Dn50 = 0.023 hm =0.40 H =0.20 s =0.03 T =2.07	Comments: • B out seawards • D,F Rocking

Stone	A	B	C	D	E	F	G
Movement		1sw 65.008s					

Additional comments

- EMS at 5 cm
- At about 1:30 waves became oblique and did not recover.
- Stopped recording too late (10 min)

TESTNAME: R033_D23_h45_H20_T179	
Date: 03-04-2014 15:00 TESTRUN:R033 Dn50 = 0.023 hm =0.45 H =0.20 s =0.04 T =1.79	Comments: • F out landwards and rolls back in • F out seawards and simultaneously B goes out landwards and rolls back in •

Stone	A	B	C	D	E	F	G
Movement		2 lw 42.390s				1lw 36.808s 2sw 42.390s	

Additional comments

- EMS at 5 cm

TESTNAME: R034_D23_h45_H22_T188	
Date: 03-04-2014 15:15 TESTRUN:R034 Dn50 = 0.023 hm =0.45 H =0.22 s =0.04 T =1.88	Comments: • F out seawards • E flips in hole • B out landwards three times in successive waves. Only last time registered. • D rocking heavily • G rocking softly

Stone	A	B	C	D	E	F	G
Movement		2lw 53.816s				1sw 39.590s	

Additional comments

- EMS at 5 cm

TESTNAME: R035_D23_h45_H20_T253	
Date: 03-04-2014 15:30 TESTRUN:R035 Dn50 = 0.023 hm =0.45 H =0.20 s =0.02 T =2.53	Comments: • B out landwards • F shifts in hole and gets stuck • C, D Rocking

Stone	A	B	C	D	E	F	G
Movement		1lw 55.850s					

Additional comments

- EMS at 5 cm
- Powerful wave, lot of overtopping

TESTNAME: R036_D23_h45_H22_T217	
Date: 03-04-2014 15:50 TESTRUN:R036 Dn50 = 0.023 hm =0.45 H =0.22 s =0.03 T =2.17	Comments: • F out landwards • F out seawards • B shifts position • E shifts position • D rocks

Stone	A	B	C	D	E	F	G
Movement						1lw 40.202s 2sw 47.732s	

Additional comments

- EMS at 5 cm

TESTNAME: R037_D25_h45_H22_T217	
Date: 03-04-2014 16:05 TESTRUN:R037 Dn50 = 0.025 hm =0.45 H =0.22 s =0.03 T =2.17	Comments: • A is rocking • D is rocking softly

Stone	A	B	C	D	E	F	G
Movement							

Additional comments

- EMS at 5 cm

TESTNAME: R038_D25_h45_H22_T188	
Date: 03-04-2014 16:20 TESTRUN:R038 Dn50 = 0.025 hm =0.45 H =0.22 s =0.04 T =1.88	Comments: • A,D rocking

Stone	A	B	C	D	E	F	G
Movement							

Additional comments

- EMS at 5 cm

TESTNAME: R039_D23_h35_H18_T170	
Date: 10-04-2014 10:20 TESTRUN:R039 Dn50 = 0.023 hm =0.35 H =0.18 s =0.04 T =1.70	Comments: • F Out lw (42:200) • B,C,D,E rocking heavily • B,E shifted in hole.

Stone	A	B	C	D	E	F	G
Movement						1lw 42.200s	

Additional comments

- EMS at 5 cm
- Third time this setting is tested (R018, R019)

TESTNAME:R040_D23_h35_H16_T160	
Date:10-04-2014 10:40 TESTRUN: R040 Dn50 = 0.023 hm =0.35 H =0.16 s =0.04 T =1.60	Comments: • F out of the hole lw after about 10 sec. Not pressed since too late, watch the video (49:60) • E shifts in hole (1:00:640) • B shifts in hole • F out seawards (1:01:440) • C,D rocking

Stone	A	B	C	D	E	F	G
Movement						1lw 49.600s 2sw 31.440s	

Additional comments

- EMS at 5 cm
- Waves were very oblique from 0:53-1:35 and from 2:12 on (video times)
- Video shows R41 but this is wrong

TESTNAME: R041_D23_h35_H16_T226	
Date: 10-04-2014 10:55 TESTRUN:R041 Dn50 = 0.023 hm =0.35 H =0.16 s = 0.02 T =2.26	Comments: • F out sw (1:06:300)after being destabilized lw (1:05:00) • B rocking

Stone	A	B	C	D	E	F	G
Movement						1sw 66.300s	

Additional comments

- EMS at 5 cm
- Video shows R42 but this is wrong

TESTNAME: R042_D23_h35_H18_T170	
Date: 10-04-2014 11:10 TESTRUN:R042 Dn50 = 0.023 hm =0.35 H =0.18 s =0.04 T =1.70	Comments: • F out lw (38:080) • B,F Very heavy rocking • B,F out lw (40:00) • F out sw (59:50) • B,C,D Rocking

Stone	A	B	C	D	E	F	G
Movement		2 lw 40.00s				1lw 38.080s 2lw 40.000s 3lw 59.500s	

Additional comments

- EMS at 5 cm
- Fourth time this setting is tested (R018, R019 R039)

TESTNAME: R043_D23_h30_H14_T150							
Date:10-04-2014 11:40 TESTRUN:R043 Dn50 = 0.023 hm =0.3 H =0.14 s =0.04 T =1.50	Comments: • F, E spin in their holes in the beginning (50:00-1:04:00) • D Rocking • B rocking in beginning then gets stuck • F rocking softly						
Stone	A	B	C	D	E	F	G
Movement							

TESTNAME: R044_D23_h30_H14_T212							
Date: 10-04-2014 12:00 TESTRUN: R044 Dn50 = 0.023 hm =0.3 H =0.14 s =0.02 T =2.12	Comments: • B,F Rocking heavily • D,E,G rocking						
Stone	A	B	C	D	E	F	G
Movement							

TESTNAME: R045_D23_h30_H16_T160							
Date: 10-04-2014 12:55 TESTRUN: R045 Dn50 = 0.023 hm =0.3 H =0.16 s =0.04 T =1.60	Comments: • F out lw (pressed burst instead of single pulse) (42:840) • B out lw (1:12:800) • F out sw(1:21:600) • B out lw(1:32:000) • A rocking slightly in the beginning • D rocking throughout the test						
Stone	A	B	C	D	E	F	G
Movement		2lw 72.800s 4lw 92.000s				1lw 42.840s 3sw 81.600s	

Additional comments

- Waves sometimes become oblique
- Much movement so the test will be repeated

TESTNAME: R046_D23_h30_H16_T160	
Date: 10-04-2014 13:05 TESTRUN: R046 Dn50 = 0.023 hm =0.3 H =0.16 s =0.04 T =1.60	Comments: • F out lw 42:040 • F out sw 1:24:080 • B rocking • D Rocking

Stone	A	B	C	D	E	F	G
Movement						1lw 42.040s 2 sw 84.080s	

TESTNAME: R047_D23_h38_H17_T233	
Date: 10-04-2014 13:40 TESTRUN: R047 Dn50 = 0.023 hm =0.38 H =0.17 s =0.02 T =2.33	Comments: • F out seawards 46:880 • B out lw, but not entirely. Pressed a little optimistic

Stone	A	B	C	D	E	F	G
Movement						1sw 46.880s	

Additional comments

- Stopwatch pressed a second too late

TESTNAME: R048_D23_h38_H19_T201	
Date: 10-04-2014 13:55 TESTRUN: R048 Dn50 = 0.023 hm =0.38 H =0.19 s =0.03 T =2.01	Comments: • F out seawards 52:520

Stone	A	B	C	D	E	F	G
Movement						1sw 52.520s	

Additional comments

- Oblique waves near the end of the test

TESTNAME: R049_D23_h38_H18_T170	
Date: 10-04-2014 14:10 TESTRUN: R049 Dn50 = 0.023 hm =0.38 H =0.18 s =0.04 T =1.70	Comments: • F out landwards 41:120 • B out landwards 44:640 • C,D,E Rocking

Stone	A	B	C	D	E	F	G
Movement		2lw 44.640s				1lw 41.120s	

Additional comment

- After the test I found out that EMS F had dropped 0.5 cm (4.5 cm above the bed) So keep this in mind during the analysis of today's tests. After this test I fixed the EMS with a tie rap.

TESTNAME: R050_D23_h38_H20_T179	
Date: 10-04-2014 14:25 TESTRUN: R050 Dn50 = 0.023 hm =0.38 H =0.20 s =0.04 T =1.79	Comments: • F out seawards 1:02:960 • B out landwards and back in 1:03:720

Stone	A	B	C	D	E	F	G
Movement		2lw 63.720s				1sw 62.960s	

TESTNAME: R051_D23_h40_H18_T170	
Date: 10-04-2014 15:20 TESTRUN:R051 Dn50 = 0.023 hm =0.40 H =0.18 s =0.04 T =1.70	Comments: • F out lw 38:780 • F out lw 49:200 • B out lw (clicked two times, only second should be counted) 1:03:640 • B,D,E rocking • G rocking softly

Stone	A	B	C	D	E	F	G
Movement		3lw 63.640s				1lw 38.780s 2lw 49.200s	

Additional comments

- EMS at 5 cm

TESTNAME: R052_D23_h40_H20_T179	
Date: 10-04-2014 15:35 TESTRUN:R052 Dn50 = 0.023 hm =0.40 H =0.20 s =0.04 T =1.79	Comments: • F out lw 40:080 • B out lw 52:720 • E,D rocking heavily • E shifted in hole

Stone	A	B	C	D	E	F	G
Movement		2lw 52.720s				1lw 40.080s	

Additional comments

- EMS at 5 cm

TESTNAME: R053_D23_h40_H21_T183	
Date: 10-04-2014 15:50 TESTRUN:R053 Dn50 = 0.023 hm =0.40 H =0.21 s =0.04 T =1.83	Comments: • F out sw 54:840 • D,E Rocking • E shifts between 2:00-2:20

Stone	A	B	C	D	E	F	G
Movement						1sw 54.840s	

Additional comments

- EMS at 5 cm
- Waves are breaking

TESTNAME: R054_D23_h40_H18_T196	
Date: 10-04-2014 16:05 TESTRUN:R054 Dn50 = 0.023 hm =0.40 H =0.18 s =0.03 T =1.96	Comments: • F out sw 47:000 • B shifts and locks in hole • D rocking

Stone	A	B	C	D	E	F	G
Movement						1sw 47.000s	

Additional comments

- EMS at 5 cm

TESTNAME: R055_D23_h40_H20_T207	
Date: 10-04-2014 16:20 TESTRUN:R055 Dn50 = 0.023 hm =0.40 H =0.20 s =0.03 T =2.07	Comments: • F out sw 1:03:400 • A,D,E rock • B shifts in hole and gets stuck • E keeps shifting in hole about 2:50 in video

Stone	A	B	C	D	E	F	G
Movement						1sw 63.400s	

Additional comments

- EMS at 5 cm

TESTNAME: R056_D23_h45_H20_T179	
Date: 11-04-2014 10:10 TESTRUN:R056 Dn50 = 0.023 hm =0.45 H =0.20 s =0.04 T =1.79	Comments: • B and F shift in hole and get stuck • A,D,E are rocking

Stone	A	B	C	D	E	F	G
Movement							

Additional comments

- EMS at 5 cm

TESTNAME: R057_D23_h45_H22_T188	
Date: 11-04-2014 10:30 TESTRUN:R057 Dn50 = 0.023 hm =0.45 H =0.22 s =0.04 T =1.88	Comments: • B,F out simultaneously landwards. B rolls back in 40:440 • F lies on the toe and keeps moving in and out hole and finally goes seawards (not counted as movement) • B out seawards 1:37:760 • E keeps shifting in its hole • A,D,E are rocking

Stone	A	B	C	D	E	F	G
Movement		1lw 40.440s 2sw 97.760s				1lw 40.440s	

Additional comments

- EMS at 5 cm
- IN THE VIDEO I SHOW THE WRONG LOG FORM (R058 instead of R057)

TESTNAME: R058_D23_h45_H20_T253	
Date: 11-04-2014 11:15 TESTRUN:R058 Dn50 = 0.023 hm =0.45 H =0.20 s =0.02 T =2.53	Comments: • B out landwards 36:400 • B out seawards 1:12:880 • F out landwards 2:37:920 • A,D,E rock

Stone	A	B	C	D	E	F	G
Movement		1lw 36.400s 2sw 72.880s				3lw 157.920s	

Additional comments

- EMS at 5 cm
- From this test on the backside of the breakwater has armourstones on it, because the overtopping wave was eroding the core stones.

TESTNAME: R059_D23_h45_H22_T217	
Date: 11-04-2014 11:35 TESTRUN:R059 Dn50 = 0.023 hm =0.45 H =0.22 s =0.03 T =2.17	Comments: • F out lw (37:800) • B out lw (42.300) • A,D Rocking

Stone	A	B	C	D	E	F	G
Movement		2lw 42.300s				1lw 37.800s	

Additional comments

- EMS at 5 cm
- Overtopping during the tests

TESTNAME: R060_D23_h50_H20_T179	
Date: 11-04-2014 12:50 TESTRUN: R060 Dn50 = 0.023 hm =0.50 H =0.20 s =0.04 T =1.79	Comments: • F out seawards 43:920 • E shifts in its hole near the end of the test • D rocking

Stone	A	B	C	D	E	F	G
Movement						1sw 43.920s	

Additional comments

- Overtopping during the tests

TESTNAME: R061_D23_h50_H20_T253	
Date: 11-04-2014 13:05 TESTRUN: R061 Dn50 = 0.023 hm = 0.5 H =0.2 s =0.02 T =2.53	Comments: • B,D,F, rocking

Stone	A	B	C	D	E	F	G
Movement							

Additional comments

- Overtopping during the tests

TESTNAME: R062_D23_h50_H22_T188	
Date: 11-04-2014 13:20 TESTRUN: R062 Dn50 = 0.023 hm =0.50 H =0.22 s =0.04 T = 1.88	Comments: • F out lw (42:00) • B out lw and back in (1:04:600) • B out lw (1:27:200) • C,D,G rocking • Stone from armour layer rolled down near stone G

Stone	A	B	C	D	E	F	G
Movement		2lw 64.600s 3lw 87.200s				1lw 42.000s	

Additional comments:

- Overtopping during the tests

TESTNAME: R063_D23_h50_H24_T196	
Date: 11-04-2014 13:35 TESTRUN: R063 Dn50 = 0.023 hm =0.50 H =0.24 s =0.04 T = 1.96	Comments: • F out landwards 40:000 • B out landwards 43:880

Stone	A	B	C	D	E	F	G
Movement		2lw 43.880s				1lw 40.000s	

Additional comments

- Prof Uijttewaal visited during test and pointed out that the water level behind the breakwater became higher due to the overtopping. (water flowed over the breakwater and returns slower) Therefore the rushdown is different from the cases where there was no overflow.

FROM TEST R064 ON THE ADV IS USED AT STONE F. STONE B STILL HAS THE EMS. SINCE A LOT OF CLAY IS ADDED TO THE WATER VISUAL CONFIRMATION OF THE MOMENT OF INCIPIENT MOTION IS NOT POSSIBLE. AFTER THE TESTS IT IS CHECKED IF AND WHERE THE STONES HAVE MOVED

TESTNAME: R064_D23_h40_H18_T170	
Date: 17-04-2014 10:10 TESTRUN: R064 Dn50 = 0.023 hm =0.40 H =0.18 s =0.04 T = 1.70	Comments: • F out lw within the minute

Stone	A	B	C	D	E	F	G
Movement						1lw	

Additional comments

- Wave gauged started with an offset (about 0.04 volts)

THE VIDEO OF THE TEST MAY BE USED TO DETERMINE THE POINT OF INCIPIENT MOTION. FROM TEST R065 ON THE VIDEO IS TAKEN FROM ABOVE THE WATER, SUCH THAT ALL STONES ARE (VAGUELY) VISIBLE.

TESTNAME: R065_D23_h40_H18_T196	
Date: 17-04-2014 10:25 TESTRUN: R065 Dn50 = 0.023 hm =0.40 H =0.18 s =0.03 T = 1.96	Comments: • F out sw

Stone	A	B	C	D	E	F	G
Movement						1 sw	

TESTNAME: R066_D23_h40_H20_T179	
Date: 17-04-2014 10:40 TESTRUN: R066 Dn50 = 0.023 hm =0.40 H =0.20 s =0.04 T = 1.79	Comments: • F out sw

Stone	A	B	C	D	E	F	G
Movement						1 sw	

TESTNAME: R067_D23_h40_H20_T207	
Date: 17-04-2014 10:55 TESTRUN: R067 Dn50 = 0.023 hm =0.40 H =0.20 s =0.03 T = 2.07	Comments: • F out sw • B out lw (for this one the button is pressed) • E shifted in its hole

Stone	A	B	C	D	E	F	G
Movement		2lw				1sw	

TESTNAME: R068_D23_h40_H20_T207	
Date: 17-04-2014 11:15 TESTRUN: R068 Dn50 = 0.023 hm =0.40 H =0.20 s =0.03 T = 2.07	Comments: • B out sw • F out sw

Stone	A	B	C	D	E	F	G
Movement		1sw				2sw	

Additional comments

- Velocity measured at 3 cm from bottom

TESTNAME: R069_D23_h38_H17_T233	
Date: 17-04-2014 11:40 TESTRUN: R069 Dn50 = 0.023 hm =0.38 H =0.17 s =0.02 T = 2.33	Comments: • F out sw •

Stone	A	B	C	D	E	F	G
Movement						1sw	

TESTNAME: R070_D23_h38_H18_T170	
Date: 17-04-2014 11:55 TESTRUN: R070 Dn50 = 0.023 hm =0.38 H =0.18 s =0.04 T = 1.70	Comments: • F out lw

Stone	A	B	C	D	E	F	G
Movement						1lw	

TESTNAME: R071_D23_h38_H19_T201	
Date: 17-04-2014 12:10 TESTRUN: R071 Dn50 = 0.023 hm =0.38 H =0.19 s =0.03 T = 2.01	Comments: • F out sw • B out lw and back in (pressed the button) (1:07:320)

Stone	A	B	C	D	E	F	G
Movement		2lw				1sw	

TESTNAME: R072_D23_h38_H20_T179	
Date: 17-04-2014 12:25 TESTRUN: R072 Dn50 = 0.023 hm =0.38 H =0.20 s =0.04 T = 1.79	Comments: • F out sw (1:00:00) • B out lw twice (1:51:16 and 1:52:88)

Stone	A	B	C	D	E	F	G
Movement		2lw 3lw				1sw	

TESTNAME: R073_D23_h35_H16_T160	
Date: 17-04-2014 12:50 TESTRUN: R073 Dn50 = 0.023 hm =0.35 H =0.16 s =0.04 T = 1.60	Comments: • F shifts in hole

Stone	A	B	C	D	E	F	G
Movement							

TESTNAME: R074_D23_h35_H16_T226	
Date: 17-04-2014 13:10 TESTRUN: R074 Dn50 = 0.023 hm =0.35 H =0.16 s =0.02 T = 2.26	Comments: •

Stone	A	B	C	D	E	F	G
Movement							

Additional comments:

- Henk-Jan visited during this test.

TESTNAME: R075_D23_h35_H18_T170	
Date: 17-04-2014 14:00 TESTRUN: R075 Dn50 = 0.023 hm =0.35 H =0.18 s =0.04 T = 1.70	Comments: • F out sw • B out lw (pressed the button)

Stone	A	B	C	D	E	F	G
Movement		2lw				1sw	

TESTNAME: R076_D23_h30_H14_T150	
Date: 17-04-2014 14:30 TESTRUN: R076 Dn50 = 0.023 hm =0.30 H =0.14 s =0.04 T = 1.50	Comments: • F spins in hole

Stone	A	B	C	D	E	F	G
Movement							

Additional comments

- Because of the low water depth the ADV is just underwater at the lowest point in the wave. It may be possible that the ADV is not always submerged. Further tests at this water height are therefore not performed, as it would not yield reliable data from the ADV.

Appendix E

Measurement equipment

During the experiments the water heights, flow velocities above the toe and the pressures under the stones of the toe were measured. This appendix gives further information on the equipment that was used to measure these parameters.

E.1 Wave gauges

The wave gauges used during this study are the standard wave gauges of the Fluid Mechanics Laboratory of Delft University of Technology (DUT). The wave gauge consists of two metal rods that are connected to a control unit. The metal rods are placed underwater and a current is sent trough them which travels trough the water to the other rod at the water surface. The higher the water level the lower the resistance that is measured by the control unit. Unfortunately no further technical information of this equipment is available.

E.2 Pressure sensors

The pressure sensors located under the stones of the breakwater toe are Honeywell pressure sensors. These pressure sensors were adapted for use under water by placing them in a tube with a diameter of 20 mm which are thereafter filled with an epoxy resin. One side of the pressure sensor is open to the water and the other side of the pressure sensor is connected to the atmospheric pressure by means of a tube. In between these two openings there is a small diaphragm which is bend by the difference in pressure, which changes the electrical resistance of the diaphragm. This change in resistance can be used to determine the difference in pressure. A static calibration was performed for each pressure sensor to determine how the translate the measured voltage to a water pressure. In figure E.1 the adapted pressure sensor is depicted. At the back of the tube the instrument cable and a tube were present.

Figure E.1: Adapted pressure sensor as used in this study

E.3 Velocity sensors

Two types of velocity sensors were used during the experiments. The majority of the measurements were performed with two EMS-velocity sensors. These sensors are widely used in the Fluid Mechanics Laboratory of DUT and have been developed by Delft Hydraulics (now Deltares). Technical information of this sensor can be found on the following pages.

During the last part of the measurements one EMS was replaced by a more accurate Acoustic Doppler Velocimeter (ADV) developed by Nortek. This sensor requires particles in the water to be able to acoustically determine the flow velocities. During the experiments it was found that the amount of sediment that needed to be added to the water was too much to be able to reliably determine the moment of incipient motion by observation. More technical information of this sensor is added after the information of the EMS sensor.

3. Specifications.

Unless specified, otherwise the data apply to:
- X- and Y-axis
- reference conditions
  (medium : water, 20° C.
  Conductivity 0.5 mS/cm
  ambient temp. 20° C.).

3.1 Probes. (Figure 9)

Sensors
- electromagnetic, bi-directional, 4-quadrants
- "E" type 30 mm diam.:
  ellipsoid, 11 x 33 mm
  rod 10 mm diam.
  max. immersion length 850 mm
  electronics unit 65 x 150 x 35 mm
  total probe length 1090 mm
  max. pressure 3 Bar
  cable length to control-unit
  100 m max. (std. 10 m.)

- "E" type 40 mm diam.:
  ellipsoid, 11 x 43 mm
  rod 10 mm diam.
  conn. box 35 mm diam., 1 = 160 mm
  fully immersible
  max. pressure 3 Bar
  connector: waterproof or cable-gland
  cable length to control-unit or if applied, field-box 100 m max.
  (std. 25 m.)
  cable length field-box to control-unit 1000 m max. (std. 25 m)
  Conditioning-unit 12 x 22 x 9 cm

- "S" type : sphere, diam. 40 mm
  rod 10 mm diam.
  conn. box 35 mm diam., 1 = 160 mm
  fully immersible
  max. pressure 3 Bar
  connector: waterproof or cable-gland
  cable length to control-unit or if applied, field-box 100 m max.
  (std. 25 m.)
  cable length field-box to control-unit 1000 m max. (std. 25 m)
  Conditioning-unit 12 x 22 x 9 cm

Materials - materials exposed to the medium:
- Stainless steel 316
- Ampco 45
- Platinum
- p.v.c.

Medium		- clean and dirty liquids, including slurries - minimum conductivity 0.2 mS/cm - max. temperature 50° C. (water)
Range	-"E"-30 type	0 to +/- 100 cm/s
	-"E"-40 type	0 to +/- 250 cm/s
	-"S" type	0 to +/- 250 cm/s

3.2 Control-unit (Figure 2)

Output	- 0 to +/- 10 V for range selected, min. load 2 kΩ
Dynamic responce	- 1 Hz (70 %); (5 Hz selectable)
Range	- 0 to +/- 100 or 250 cm/s, switch selectable
Range-shift	- ± 20 % of range selected
Display	- analog meter, X or Y selectable, scale length +/- 16 mm
Dimensions (cassette)	- 106 x 127 x 210 mm (w x h x d)
Weight	- 1 kg
(complete control-unit)	- 300 x 170 x 380 cm (w x h x d)
Weight	- 2 kg

3.3 System

Accuracy	-"E" types :	± 1 % of f.s. ± 0.5 cm/s for tilt angles between + and - 10° and V<= 20 cm/s
	-"S" type :	± 4 % of f.s. ± 0.5 cm/s + tilt response error

Specified accuracy applies to reference conditions and includes non-linearity and zero-stability.

Tilt response	-"S" type :	max. error ± 5% of reading for angles between + and - 30 degrees and V<= 30 cm/s

Zero-stability		- < 1 cm/s/24 hours.
Temperature influence		- medium : 0.1 cm/s/°C - ambient : 0.03 cm/s/°C
Conductivity influence		- 0.02 % of reading per mS/cm
Cables	-"E30"type :	Probe - Control-unit 10 m (Optional upto 100 m)
	-"E40 and S" type :	Probe-Control-unit 25m (std). OR: Probe - Fieldbox 25 meter (optional upto 100 m) and between Fieldbox and Control-unit std. 25 m (optional upto 1000 m).
Power	- 220 VAC ± 10 %, 50-60 Hz, 5 VA. - optional:	- 110 VAC or - 12 -30 VDC (max 400 mA dep. voltage supplied)

3.4 Mounting hardware.

- As mounting hardware strongly depends on the specific application, the E.M.S. is normally supplied without mounting hardware.
- Contact DELFT HYDRAULICS for advice or installation instructions and hardware proposed.

4. Assembly.

4.1. General.

In general, the instrument consists of the following basic parts:
a. the probe, with pre-amplifier
b. the Control-unit in U.C.C. (Universal Carrying Case) and
c. connection-cable(s).

When the probe has to be installed at greater distance (> 100 mtr) from the Control-unit, part of the processing-electronics (item b.) will be mounted in a "Field-box". Connection-cables between this box and the Control-unit may then reach up to a 1000 meter.

4.2 Set-up.

Two types of set-up exist. (Figures 3 and 4).

a. for laboratory use:

- a disc type probe ("E"-type 30 mm) and a Control-unit in a portable housing, with 10 m connec- tion-cable.

- the ellipsoidal sensor has been designed specifically for high spatial resolution velocity profiling, velocity-area flow metering and other applications that are characterized by a main stream direction in one plane.

  The small dimensions, streamlined body and small sensing area enable its use in pipes as small as 2" diameter. In open channel applications the profile can be measured up to a distance of 0.5 cm from the bottom and side-walls.

OR

b. for field use:

- an ellipsoidal type "E"-probe (fully watertight) with a 40 mm diameter sensor and a Control-unit in a portable housing, with 25 m connection-cable.

- a sphere type "S"-probe (fully watertight) and a signal-processor-unit in a portable housing, with 25 m connection-cable.

  The spherical sensor has been designed for applications where it is necessary to take the influence of vertical velocity components in account.
  This means that the X and Y signals shall represent the cosine vector of the instantaneous velocity for flow from all directions.

4.3 Cables.

Standard supplied connection cables for the "E30" probe will be 10 meters long. For the "E40" and "S"-probes, standard length is 25 m. The connection-cable between probe and Control-unit can be ordered (against cost) up to 100 meter length.
If greater length is necessary, a connection-cable (10 or 25 meter) between probe and additional Field-box can be supplied together with a connection-cable of any length up to 1000 meter.

4.4 Probe mounting.

As the EMS probe has to detect microvolt level signals, certain precautions have to be taken with respect to the installation.

- the probe has to be fitted as sturdy as possible
- electrical current(s) should not be allowed close to the probe
- electrical ground loops have to be avoided close or along the probe.

4.5 Velocity reference, direction.

The plane with the serial number is in parallel with the Y-axis. Looking at the serial number, the Y current moves from left to right with a positive signal output and the X current is flowing perpendicular the y axis from back of the probe to the front with also a positive signal output.

The actual velocity can be calculated from the measured velocities Vx and Vy following:

$$Ve = \sqrt{Vx^2+Vy^2}$$

and the angle α by:

$$tg\ \alpha = Vy \div Vx$$

For the last calculation the sign-correction has to be taken in consideration as:

V-out X	V-out Y	α
+	+	0 - 90°
-	+	90 - 180°
-	-	180 - 270°
+	-	270 - 360°

5. To get started.

5.1 Connections

Check if the mains supply is in consonant with the supply required (standard 220 Vac).
Connect the unit with the supplied mains cord to the mains.

The probe connection-cable has to be connected to the input-connector #1 when the Control-unit is installed in the left hand section of the transport-case.
Socket #2 is for the right-hand cassette position

5.2. Zero-setting.

Before starting measurements, the zero-outputs have to be checked. Place the probe to be used in standing water and adjust the X and Y output for 0.00 Volt by means of the potentiometers on the front panel.

5.3 Outputs.

The signal of the X or Y axis can be displayed on the meter (selectable by switch).
At the BNC-connectors on the front of the cassette the X and Y output voltages are both continiously available.
* BNC-connectors at the rear of the unit are for synchronisation purposes only !

5.4 Interference.

The "E" and "S"-type probes are automatically synchronized at half the mains frequency.
This implies that each probe measures during the same period. It may cause some offset voltage at the output when the probes have been installed too close to each other.

There will be NO synchronisation when the Control-unit is powered from a DC voltage source.

5.5 Synchronisation.

If more EMS combinations (up till 4 units) have to be installed close to each other, synchronisation of these sets is necessary.
One unit is set for MASTER by switching the DIPswitch combination on PCB 1300 (inside the cassette) in the following pattern:

S1 off
S2 off
S3 off
S4 off
S5 ON
S6 ON

The other units (up till 3) have to be SLAVE´S by switching the DIPswitch combination on PCB 1300 (inside the cassette) in the following pattern:

S1 off
S2 off
S3 ON
S4 ON
S5 off
S6 off

The Nortek Vectrino II provides new and unique opportunities for high resolution profiling velocity measurements in the laboratory and in the field. With 1 mm vertical resolution over a range of 30 mm, the Vectrino II moves beyond the classical acoustic Doppler velocimeter and opens the door to new types of velocity measurements.

Vectrino II
3D Profiling Velocimeter

Vectrino II measuring the flow over an artificial seagrass during a demonstration experiment at MIT. The computer shows an image of data collected during the experiment.

The Vectrino II comes with enhanced data collection and display software

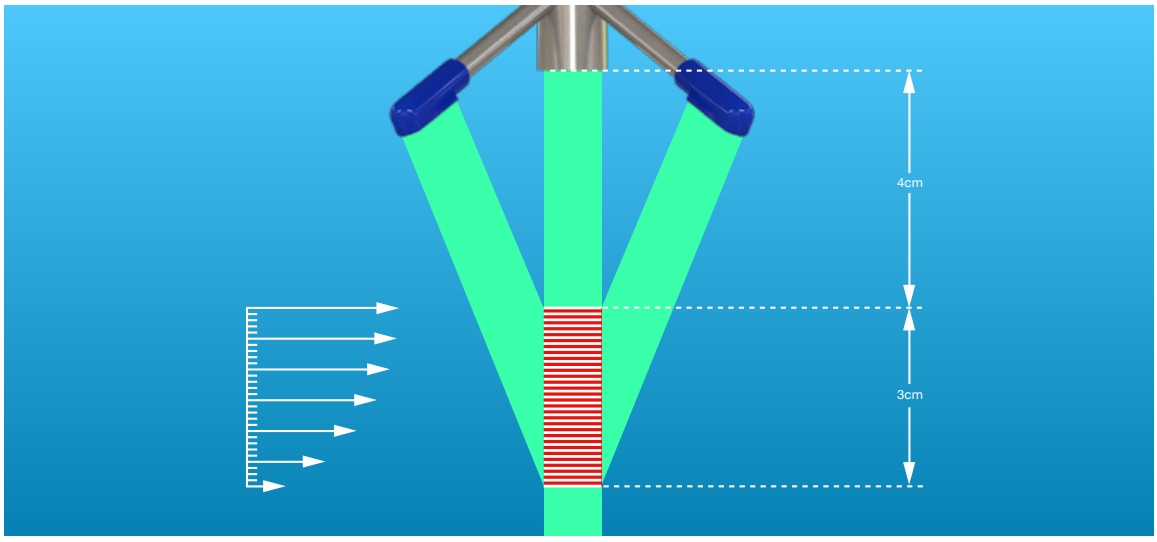

The Vectrino II profiles the water column over a 3 cm range and provides three-component velocity observations with a resolution as fine as 1 mm and sampling rate as fast as 100 Hz. The Vectrino II can measure the distance to the bottom at rates of up to 10 Hz by interleaving bottom detection pings and velocity profiling pings. New interface software provides enhanced capabilities such as real-time plots of velocity profiles, velocity standard deviation, energy spectra and color contour plots.

CURRENT AND WAVE MEASUREMENTS IN THE OCEAN, LAKE AND LABORATORY

NORTEK

Nortek AS
Vangkroken 2
1351 Rud, Norway
Tel: +47 6717 4500
Fax: +47 6713 6770
E-mail: inquiry@nortek.no

www.nortek-as.com
True innovation makes a difference

Vectrino II

The next level in acoustic Doppler velocimetry

With the Nortek Vectrino II we have added profiling capability (30 mm range) to classical acoustic Doppler velocimetry. Designed from the ground up to take advantage of advances in modern electronics hardware, we have also made a leap in temporal (100Hz) and spatial resolution (1 mm). Add to this the excellent performance of acoustics in sediment flows and the Vectrino II leaves you free to pursue data collection schemes that were previously reserved for more complex and expensive technologies.

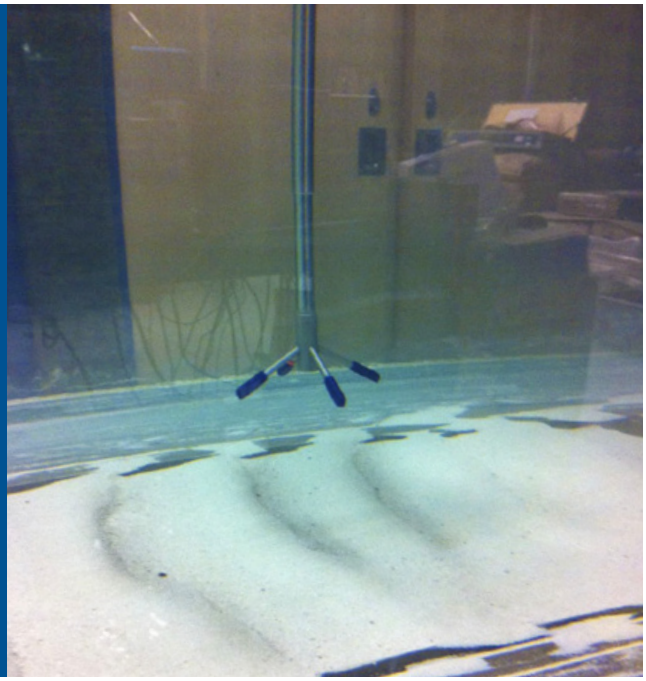

Boundary Layer Measurements
The Vectrino II is well suited for measuring near boundaries, able to capture a velocity profile at 1 mm resolution over a 30 mm profile. The 100 Hz sample rate allows visualization of structures within the flow providing a well resolved spatial and temporal data set for analysis. Coupled with the interleaved bottom distance measurements, the Vectrino II can be used to determine bed stress and boundary movement during erosion studies.

Adaptive Ping Interval
Pulse coherent profilers are susceptible to pulse interference when measuring near boundaries. The Vectrino II is able to dynamically configure the pulse intervals by examining acoustic returns and identifying interference regions. The Vectrino II can perform an adaptive check once at the start of data collection or continuously at intervals from 1 second to 1 hour. When measuring near dynamic boundaries which are eroding or accreting during data collection, or during the passage of bed forms, this is a valuable feature to improve data quality and reduce interference.

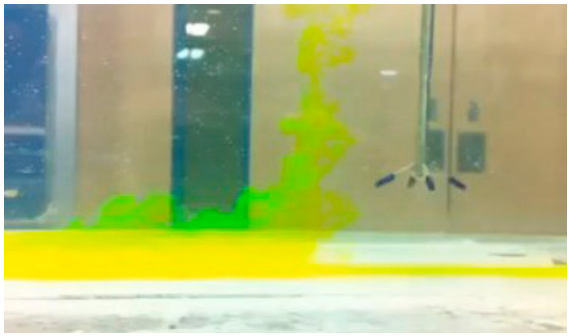

In this demostration experiment at Cornell University , yellow dye is used to illustrate the flow structure. The Vectrino II can measure the flow velocity as close as 3-4 mm from a solid boundary.

Interleaved Distance Measurements
The Vectrino II measures distance to a boundary using a special bottom ping interleaved at a sample rate up to 10 Hz with velocity measurements. Measurement range is user selectable, starting 20 mm from the central transducer while maximum range is limited by the boundary echo strength. Typically, a range is specified and divided into 1 mm range cells, resulting in an accuracy of 0.5 mm over a variety of surfaces. The ability to measure boundary distance on the same time scale as the velocity measurements allows the velocity measurements to be referenced to a coordinate system that moves as the bed geometry changes.

Estimation of bed shear stress (top) and measurement of boundary movement (bottom) during an erosion study at Cornell University.

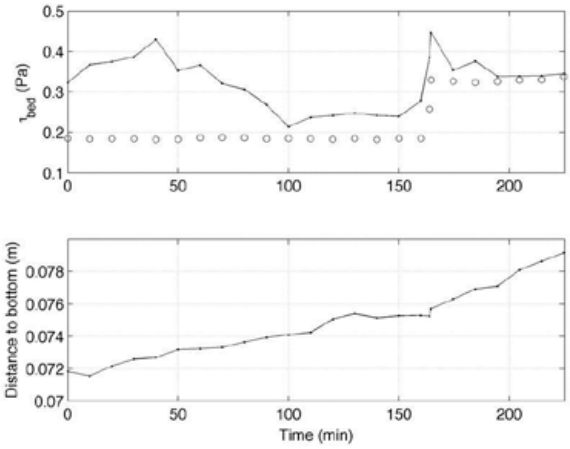

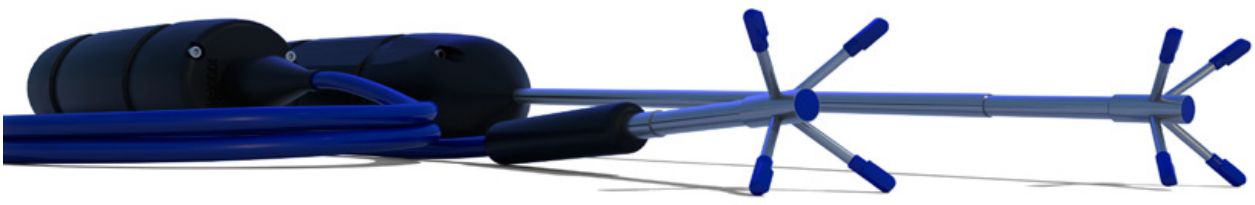


Field experiment with Vectrino II at UNC – Chapel Hill

Wave Flume
The Vectrino II is well suited for measurements in wave flumes. The profiling capability allows multiple instantaneous observations over the wave boundary layer for each wave passing by and reduces the need for multiple individual instruments or repetitive test runs. The profile of velocity will also help to characterize flow around or behind a structure such as scale piling or bulkhead. Finally, the real-time velocity energy spectra can be used to monitor wave energy in the frequency domain.

Field Experiments
The Vectrino II has many uses in outdoor field experiments. Outstanding measurements have been made in the shallow swash zone, in the bottom boundary layer above a muddy tidal channel, and over various substrates such as sand ripples, and sea grass and oyster beds. The distance measurement feature allows the Vectrino II to be positioned precisely above the bottom even in poor visibility conditions. High-speed communication and power supply are possible over cable lengths up to 100 m.


Demonstration experiment in wave flume at University of Quebec, INRS-ETE

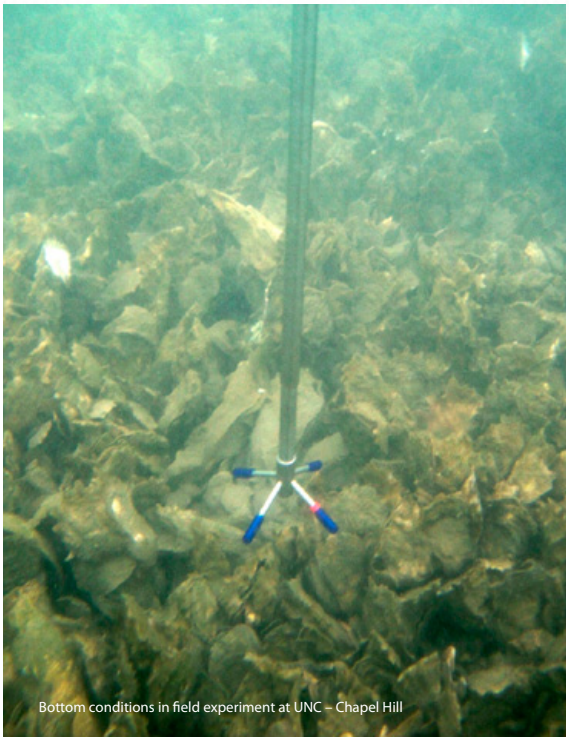
Bottom conditions in field experiment at UNC – Chapel Hill

Technical Specifications

Water Velocity Measurements	
Velocity Range:	Increments of 0.1 m/s to a maximum of 3.0 m/s
Adaptive ping interval:	Once, or at 1 second to 1 hour intervals
Accuracy:	±0.5% of measured value ±1 mm/s
Sampling rate (output):	1-100 Hz
Distance Measurements	
Minimum range:	20mm
Maximum range:	Up to 2 meters depending on signal strength
Cell Size:	1-4 mm (user selectable)
Accuracy:	0.5 mm at 1 mm cell size
Sampling rate:	1-10 Hz
Sampling Volume	
Profile Range:	Up to 30mm
Location:	45 – 75 mm from probe
Diameter:	6 mm
Cell size:	1-4 mm (user selectable)
Echo Intensity	
Acoustic frequency:	10 MHz
Resolution:	Linear & log scale
Dynamic range:	60 dB
Sensors	
Temperature:	Thermistor embedded in probe
Range:	–4°C to 40°C
Accuracy/Resolution:	1°C/0.1°C
Time response:	5 min
Data Communication	
I/O:	RS-485 (high speed RS-485-to-USB converter)
Communication Baud rate:	Up to 1.25 Mbps
User control:	Handled via Vectrino II configuration and collection software
Analog outputs:	None
Synchronization:	SynchIn and SyncOut

Software ("Vectrino II")	
I/O:	RS 485–USB support for devices with 1, 2, 4, and 8 serial ports.
Operating system:	Windows XP, Vista and 7 (32 and 64 bit)
Functions:	Instrument configuration, data collection, data storage. Probe test modes. Data file playback. Data export to MATLAB* .mat binary format.
Multi Unit Operation	Vectrino II software allows multiple Vectrino II to be run within a single instance of the program.
Power	
DC Input:	12–48 VDC
Peak current:	2.5 A at 12 VDC
Max. consumption:	4 W at 100 Hz
Connectors	
Bulkhead:	Splash proof connector or MCBH-12-FS, bronze (Impulse) – see also options below.
Cable:	Splash proof or PMCIL-12-MP – see also options below.
Materials	
Standard model:	Delrin® housing. Stainless steel (316) probe and screws.
Environmental	
Operating temperature:	–4°C to 40°C
Storage temperature:	–15°C to 60°C
Shock and vibration:	IEC 721-3-2
Dimensions	
See below for main dimensions	
Weight in air:	1.2 kg
Weight in water:	Neutral

Options

- 4-beam down-looking probe. Fixed stem or 1m flexible cable
- 10, 20, 30 50 or 100 m cable with choice of splashproof or Impulse underwater connector
- RS 485–USB converter (one-to-one, four-to-one or eight-to-one)

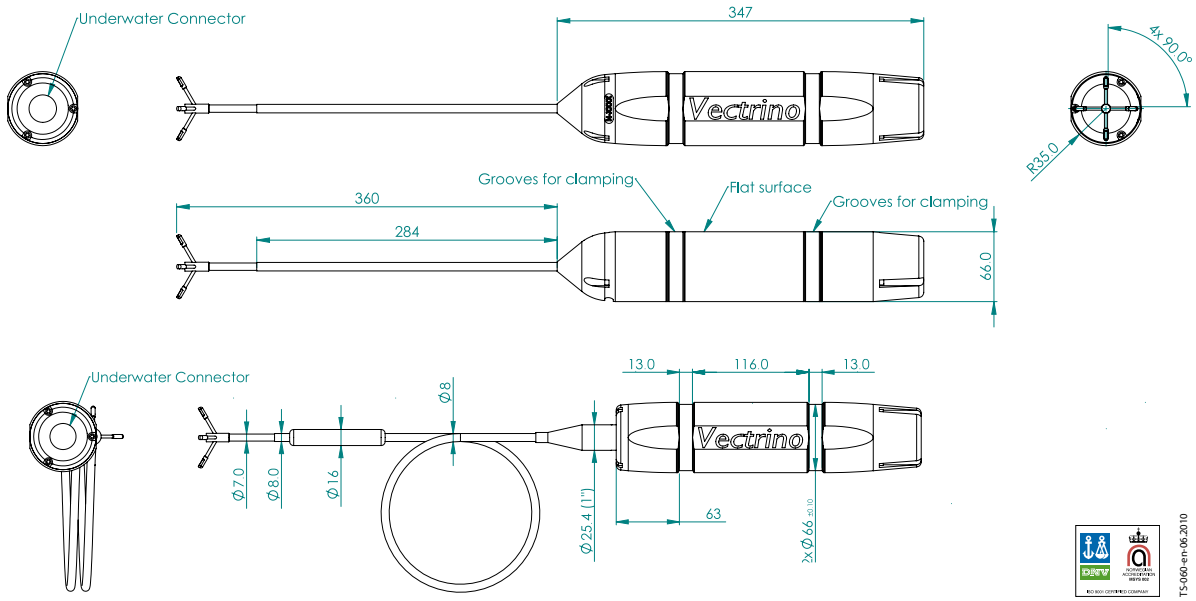

T5-060-en-06.2010

TRUE INNOVATION MAKES A DIFFERENCE

NortekMed S.A.S.
Z.I. Toulon Est
BP 520
83 078 TOULON cedex 09
FRANCE
Tel: +33 (0) 4 94 31 70 30
Fax: +33 (0) 4 94 31 25 49
E-mail: info@nortekmed.com

NortekUK
Mildmay House, High St.
Hartley Wintney
Hants. RG27 8NY
Tel: +44- 1428 751 953
E-mail: inquiry@nortekuk.co.uk

NortekUSA
27 Drydock Avenue
Boston, MA 02210
Tel: 617-206-5750
Fax: 617-275-8955
E-mail: inquiry@nortekusa.com

青岛诺泰克测量设备有限公司
地址：中国青岛香港西路65号
汇融广场1302
邮编：266071
Tel: 0532-85017570, 85017270
Fax: 0532-85017570
E-mail: inquiry@nortek.com.cn

Nortek B.V.
Schipholweg 333a
1171PL Badhoevedorp
Nederland
Tel: +31 20 6543600
Fax: +31 20 6599830
email: info@nortek-bv.nl

Bibliography

James E Allison, Lori C Sakoda, Theodore R Levin, Jo P Tucker, Irene S Tekawa, Thomas Cuff, Mary Pat Pauly, Lyle Shlager, Albert M Palitz, Wei K Zhao, J Sanford Schwartz, David F Ransohoff, and Joseph V Selby. Screening for colorectal neoplasms with new fecal occult blood tests: update on performance characteristics. *Journal of the National Cancer Institute*, 99(19):1462–70, October 2007. ISSN 1460-2105. doi: 10.1093/jnci/djm150. URL http://www.ncbi.nlm.nih.gov/pubmed/17895475.

John D. Anderson, Jr. *Fundamentals of Aerodynamics, Fourth Edition*. McGraw-Hill, 2007. ISBN 007-125408-0.

S. A. Baart. Toe structures for rubble mound breakwaters, 2008. URL http://dx.doi.org/10.4121/uuid:4d63df11-914d-430f-989b-16c09e0bd743.

R. E. Ebbens. Toe structures of rubble mound breakwaters: Stability in depth limited conditions, 2009. URL http://dx.doi.org/10.4121/uuid:2e453b6d-71dd-44a5-a76e-f7b95a875fe7.

E. Gerding. Toe structure stability of rubble mound breakwaters, 1993. URL http://repository.tudelft.nl/view/ir/uuid:51af1788-de9f-4ef3-8115-ffefb2e26f76/.

Yoshimi Goda and Yasumasa Suzuki. Estimation of incident and reflected waves in random wave experiments. 1976. URL https://icce-ojs-tamu.tdl.org/icce/index.php/icce/article/view/3096/2761.

Bastiaan Hofland. *Rock 'n' Roll: Turbulence-induced damage to granular bed protections*. PhD thesis, March 2005. URL http://repository.tudelft.nl/view/ir/uuid:90796c07-7666-4550-b73b-2b8f70057768/.

Ivar G Jonsson. A new approach to oscillatory rough turbulent boundary layers. *Ocean Engineering*, 7(1): 109–152, January 1980. ISSN 00298018. doi: 10.1016/0029-8018(80)90034-7. URL http://linkinghub.elsevier.com/retrieve/pii/0029801880900347.

Julia Nammuni-Krohn. Flow velocity at rubble mound breakwater toes, 2009. URL http://dx.doi.org/10.4121/uuid:91312903-7701-406e-a1b0-2d7bc456155c.

Ruben Peters. Evaluation of the IH2VOF model for modelling of hydraulic properties near breakwater toes, 2014.

Jentsje W Van der Meer. Geometrical design of coastal structures. 1998. URL http://www.vandermeerconsulting.nl/downloads/stability_b/1998_vandermeer_ch9.pdf.

Constant Van Heemst. Stability of a Crown Wall on a Breakwater, 2014. URL http://repository.tudelft.nl/view/ir/uuid:1c7957a1-d28b-4ebc-8c97-37542c447d6a/.

Henk Jan Verhagen, Kees d'Angremond, and Ferd Van Roode. *Breakwaters and Closure dams, 2nd edition*. VSSD, 2009. ISBN 978-90-6562-173-3.

Barbara Zanuttigh and Jentsje W. Van der Meer. Wave reflection from coastal structures. 2006. URL http://www.vandermeerconsulting.nl/downloads/functional_c/2006_zanuttigh_vandermeer.pdf.